Department of Mathematics and Statistics

Mathematical Modelling Of Cancer Growth

Tiffany Jones

This thesis is presented for the Degree of
Doctor of Philosophy
of
Curtin University

April 2014

Declaration

To the best of my knowledge and belief this thesis contains no material previously published by any other person except where due acknowledgement has been made. This thesis contains no material which has been accepted for the award of any other degree or diploma in any university.

Dedication

This research was initially started with Associate Professor Peg-Foo Siew from the Department of Mathematics and Statistics, Curtin University of Technology, Perth, Western Australia.

Under Associate Professor Siew's guidance I completed an Honours degree in Mathematics on the topic of Mathematical Modelling of Cancer Growth. If it wasn't for his enthusiasm and dedication as a teacher and researcher this research would have been finished before it even started.

Associate Professor Peg-Foo Siew passed away in September 2005 from an incurable cancerous growth.

Acknowledgements

There are many people to acknowledge and thank for there continuing support and guidance in completing this work, in particular in an area that required external knowledge of something that was quite foreign to me.

I would firstly like to thank all the administration staff in the Department of Mathematics and Statistics for support throughout the completion of this research.

Many thanks go to my fellow postgraduate students, past and present, whose encouragement I found enormously helpful and am eternally grateful for.

My supervisor, Professor Lou Caccetta, I know without his words of wisdom and guidance this project would not of been possible. I know that I haven't always been the best student but you have shown me that no matter what, I can achieve and I can do what I thought was impossible.

My co-supervisor, Associate Professor Volker Rehbock, for the time spent sitting and explaining concepts to me in an area that was not my strength. His patience, tolerance and continuing support will never be forgotten.

There are some special acknowledgements I would like to mention here. Special thank you's go to Dr Ryan Loxton for his discussions on optimal control and editing much of my thesis. Dr Chris Hines from iVEC at the Australian Resources Research Centre, Technology Park, for much needed computer programming help and assistance using the supercomputer Cognac. Professor Yong Hong Wu for discussions relating to numerical analysis and machine accuracy. Dr Greg Gamble for his invaluable help with LaTeX, my typesetting

and programming skills have excelled as a result. Dr Rima Caccetta for discussions on biochemistry and kinetics, I now have a new found interest and passion for this field. Dr Ian van Loosen for words of encouragement and simply just putting up with me.

If it wasn't for the support of my friends, my family and everyone else in between, I would not have completed this research.

Special thanks go to both my mother-in-laws, Jan and Robin, for babysitting so I could get this done. Your ongoing support and help will never be forgotten. Thank you so much to both of you.

I would also like to acknowledge my father-in-law for his constant encouragement and support throughout completing my PhD. Thank you so much Russ.

I would like to acknowledge my closest and dearest friend Krista. Thank you for all the talks, all the advice, all the support and never ending friendship you have given me throughout the completion of this thesis.

To my siblings, Jackie, Tara and Christopher, thank you for your words of encouragement and for your constant imploring to never give up.

A special thank you to my parents who have supported me from the very moment I told them I wanted to study at university. Thank you so very much Mum and Dad! Your ongoing support is something that I will always hold very dear to me and I just hope that I have made you both very proud.

My two little angels Sophie and Holly, both of whom I have done this for. On day Mummy will explain to you both why I wasn't always able to spend time with you.

Last, but certainly not the least, my wonderful fiancé Shane. I know while completing this research I have not been the easiest person to get along with, I just hope that you are proud of me and what I have achieved. Thank you for allowing me to be me.

Abstract

Mathematical medical sciences is a growing area of interest, particularly with many diseases, such as diabetes, cancer and heart disease reaching epidemic levels. The associated rising costs to society are also a major concern.

Cancer is becoming more prevalent in modern society and there is a large body of research concerned with its treatment and prevention. Some of the key issues relating to cancer growth and its treatment can be addressed through the use of mathematical modelling.

In this thesis, we analyse existing methodologies and techniques associated with mathematical modelling of cancer and non-cancer cell cycle modelling. We apply Optimal Parameter Selection techniques to two existing cell cycle models published in literature.

We develop a mathematical model to describe cell cycle growth of melanoma. The model is unique as it specifically describes the activities relating to the Braf protein which are often mutated in melanoma growths.

We firstly review current literature relating to cell cycle modelling both for cancer and non-cancer cell division cycles. We discuss the methodologies that have been used and duplicate results from a well known paper in the

literature. We then apply kinetic principles to this model and discuss how small changes in the kinetic dynamics can lead to significant changes in the simulation results.

We then apply optimal parameter selection techniques to both cancer and non-cancerous cell cycle models. The cancer cell cycle model is based on a mammalian cell cycle while the non-cancerous model is based on a yeast cell cycle. Specifically, we use multiple characteristic time points on each of the cancer and non-cancerous models to solve the problem computationally using the software package MISER3.3. The results returned by MISER3.3 show that published parameter values are not optimal for the cancerous cell model. More precisely, MISER3.3 returned optimal parameter values for the cancer cell cycle model that were considerably different to the previously published values. In contrast, the optimal parameter values returned by MISER3.3 for the non-cancer model were very close to those published, showing that the published parameters are indeed optimal. This result highlights the ability of our formulation and MISER3.3 to determine optimal model parameters for complex cell cycle models.

We also present a new mathematical model for melanoma growth as there is very little literature published in this area. We develop the melanoma model using existing kinetic modelling principles and we incorporate the activities of the mutated Braf protein. The model is based on a mammalian cell cycle and we work at the subcellular level where we examine activities occurring inside the cell. We use a set of ordinary differential equations to model the cell cycle for melanoma growth over a given time horizon.

In summary, we are essentially proposing a new framework for cancerous cell cycle models, where uncertain model parameters can now be readily optimised so that the model output resembles the desired behaviour, itself based on experimental results, as closely as possible.

Contents

List of Figures

List of Tables

Chapter 1

Introduction

In society today mathematical medical research is a vital part of diagnosis, treatment and prevention. The top three deadly illnesses, according to the World Health Organisation Statistics Report, 2013, (World Health Organization, 2013), were cardiovascular diseases and diabetes, cancer and chronic respiratory conditions. Data published by Globocan in 2008 reported that cancer was responsible for approximately 7.564 million (or 13%) deaths worldwide (Globocan, 2010). In Australia alone, cancer was reported as one of the main causes of death in 2011, with almost 44,000 deaths in total (Cancer Council Australia, 2013).

Australia has one of the highest rates of skin cancer in western society. Skin cancer accounts for approximately 80% of all newly diagnosed cancers (Cancer Council Australia, 2012). With alarming figures like these it is vital that research continues in this area. Mathematical modelling and optimisation techniques are able to significantly aid research in this area. Optimisation techniques can be used to accurately match models to real-life data

through the use of parameter optimisation and simulation.

This research aims to present work using optimal parameter selection techniques applied to cancerous and non-cancerous cell cycle models. We also present a new mathematical model for melanoma growth using existing kinetic principles. Our mathematical model for melanoma growth will be the first to describe the activity of the Braf protein that is often mutated in melanoma cancers.

We present here our motivation for using optimal parameter selection techniques and developing a model for melanoma growth with an accompanying brief overview into some of the mathematical models for cancer growth in this field of research. We will then give a detailed discussion on the theory involved in our research. This mainly revolves around optimal parameter selection methodologies involving multiple characteristic time points. We state the general formulation of our objective function and highlight some alternative formulations. We also give an overview of some models in optimal control and cancer therapies.

1.1 Motivation

Research into the mathematical modelling of cancer growth has exploded in the last decade or so (Araujo and McElwain, 2004; Alarcón et al., 2004a,b, 2005; Betteridge et al., 2006; Alarcón et al., 2006; Anderson, 2005; Ayati et al., 2006; Jiang et al., 2005; Lachowicz, 2005). As a result there has been considerable collaboration on growth modelling as well as treatment modelling and scheduling. The mathematical models in this area vary in complexity and generality.

We give a brief overview here of some of these models which are well cited in literature.

Alarcón et al (Alarcón et al., 2003, 2004a, 2005) published a series of papers that mathematically describe cancer growth. The initial paper of interest by Alarcón et al, describes a cancerous growth using cellular automaton modelling techniques (Alarcón et al., 2003). The authors describe the model as being hybrid, since there are elements to the model that are discrete while others are continuous. The cells are considered discrete entities while the elements, such as oxygen and protein concentrations, are considered continuous over a particular time horizon. These concentrations are modelled by a set of partial differential equations.

The next paper of particular interest by Alarcón et al uses a set of ordinary differential equations to describe the cell cycle of both normal and cancerous cells. It shows the effects that oxygen starvation (hypoxia) has on cancerous cells, specifically, how hypoxia doesn't stop cancer cells from proliferating. The Alarcón et al model is based on a yeast cell cycle model of Tyson and Novak (Tyson and Novak, 2001). We review both the Alarcón et al and Tyson and Novak models in Chapter 3. Here we will, however, briefly point out the difficulties with duplicating the Alarcón et al (Alarcón et al., 2004a) model.

We attempted to duplicate the results published by Alarcón et al (Alarcón et al., 2004a) but we encountered problems with matching the time horizon and deciphering correct parameter values. This led us to use Optimal Parameter Selection techniques to see if we could determine parameter values that

would give a clearer sense of a real-life setting and a closer match to the results published. We give further discussion of our duplication attempts and the results we obtained using optimal parameter selection techniques on this model in Chapter 4.

Another model by Alarcón et al which needs mentioning is a multiple scale model published in 2005 that describes a cancer cell cycle at differing levels of growth (Alarcón et al., 2005). There are 3 distinct levels of growth, macroscopic, cellular and subcellular.

The vascular or macroscopic level describes events occurring outside of the cell, such as blood flow and developing vasculature. Alarcón et al (Alarcón et al., 2005) use Poiseulle's Law to model the blood flow in each vessel and Kirchoff's Laws to model the other activities relating to blood flow, such as pressure and flow rates. The cellular layer looks at the activities occurring between the cells and in the Alarcón et al model they have incorporated the competition between cancer and non-cancer cells by defining mathematical rules governed by probabilities.

There are many activities occurring inside a cell, be it cancerous or non-cancerous. These include protein interactions, check point control and protein under or over-expression. Protein under and over-expression is commonly related to mutated cells that have become cancerous (Weinberg, 2007). Alarcón et al (Alarcón et al., 2005) use a set of ordinary differential equations to describe the dynamics occuring at the subcellular level of cell growth.

Other models worth mentioning are those developed by Anderson (Anderson, 2005) and in collaboration with Ayati and Webb (Ayati et al., 2006).

Similar to the hybrid cellular automaton model proposed by Alarcón et al (Alarcón et al., 2003) the model by Anderson (Anderson, 2005) is also hybrid. The cells themselves are considered as individual entities and therefore, discrete, whereas the interactions occurring outside of a cell are on a continuous time horizon. Partial differential equations are used to describe the interactions occurring amongst cells and activities occurring outside of the cell.

Ayati et al (Ayati et al., 2006) extend Anderson's previous work (Anderson, 2005) by considering multiple time and length scales as independent variables. Independent physiological variables are introduced, such as age and size, with the standard space and time variables also included. Partial differential equations are once again used to model the dynamics of the system. Computations are performed on a simplified version of the model that excludes the independent size variable. Data for the computations is estimated and results show the accuracy of their computational methodology is superior to traditional methods. Ayati et al use a step-doubling alternating direction implicit method (ADI) instead of a backward Euler ADI.

There are still areas of mathematical modelling in cancer growth that need to be examined. There is limited focus on the use of mathematical optimisation methods in the modelling process for cancer growth. In particular, the model we choose to examine by Alarcón et al (Alarcón et al., 2004a) has no mention of any parameter optimisation techniques. Model duplication as mentioned previously was met with great difficulty which leads us to examine the parameters and apply optimal parameter selection techniques.

The mathematical models analysed in this thesis are of a generic form

and not specific to any particular type of cancer. There are mathematical models that relate to particular cancer types, however, these are limiting and generally only involve breast and glioma cancer growths (Franks et al., 2005; Swanson et al., 2003). Melanoma is one of the most common cancers in Australia (Cancer Council Australia, 2012) and very little mathematical modelling is present in current literature. This presents another area for investigation and, as another major contribution, in this thesis we will present a new mathematical model for a different cancer, melanoma growth.

1.2 Optimal Parameter Selection Problems

Optimal parameter selection problems form a subclass of more general optimal control problems. Both types of problems incorporate a dynamical system which is defined in terms of a set of differential equations, a set of initial conditions and, in some cases, constraints. Optimal Parameter Selection problems also involve a set of parameters that need to be chosen to optimise a given objective. In contrast, Optimal Control problems require us to determine a set of functions (control functions), possibly in addition to scalar parameters, that will optimise a given objective. We note here that pure optimal parameter selection problems do not contain control functions.

We give below a description, in general terms, of a standard optimal parameter selection problem, with accompanying canonical constraints. The general form encapsulates different constraints to allow for varying situations, particularly in real-life scenarios, see (Teo et al., 1991).

The dynamical system is a set of non-linear ordinary differential equa-

tions that evolve over a given time horizon, namely $(0,T]$. The dynamical system for such a problem is given below,

$$\dot{\boldsymbol{x}}(t) = \mathbf{f}\big(t, \boldsymbol{x}(t), \boldsymbol{\zeta}\big) \tag{1.1}$$

$$\boldsymbol{x}(0) = \mathbf{x}_0(\boldsymbol{\zeta}). \tag{1.2}$$

where $\boldsymbol{x} = [x_1, x_2, \ldots, x_n]^\top \in \mathbb{R}^n$, is the state and $\boldsymbol{\zeta} = [\zeta_1, \zeta_2, \ldots, \zeta_s]^\top \in \mathbb{R}^s$, is the system parameter vector, $\boldsymbol{x}_0(\boldsymbol{\zeta})$ is the vector of initial conditions for the state which could be defined as a set of functions dependent on the system parameter, $\boldsymbol{\zeta}$, as a set of constant terms or as a combination of both and is defined as $\mathbf{x}_0 : \mathbb{R}^s \to \mathbb{R}^n$. $\dot{\boldsymbol{x}}$ is the vector representing the first derivatives of the states and $\mathbf{f}$ describes the dynamics of the problem in terms of the states and system parameters.

We also need to define the notation that we will be using throughout this section, where $\boldsymbol{x}(\cdot|\boldsymbol{\zeta})$ represents the solution of (1.1) to (1.2) with respect to the system parameter, $\boldsymbol{\zeta}$.

Before we can state the full problem we also need to define the equality and inequality constraints in canonical form.

$$g_i(\boldsymbol{\zeta}) = \Phi_i\big(\boldsymbol{x}(\tau_i|\boldsymbol{\zeta}), \boldsymbol{\zeta}\big) + \int_0^{\tau_i} \mathcal{L}_i\big(t, \boldsymbol{x}(t|\boldsymbol{\zeta}), \boldsymbol{\zeta}\big)\mathrm{d}t \begin{cases} = 0, & i = 1, \ldots, N_e\,, \\ \leq 0, & i = N_e + 1, \ldots, N\,, \end{cases} \tag{1.3}$$

where $\Phi_i : \mathbb{R}^n \times \mathbb{R}^s \longrightarrow \mathbb{R}$, $i = 0, \ldots, N$ and $\mathcal{L}_i : [0,T] \times \mathbb{R}^n \times \mathbb{R}^s \longrightarrow \mathbb{R}$, $i = 0, \ldots, N$ are both continuous and differentiable real valued functions with respect to $\boldsymbol{x}$ and $\boldsymbol{\zeta}$. g_i is also assumed to be a differentiable function on $\mathbb{R}$

and τ_i is the characteristic time of the i^{th} constraint. Furthermore, N_e denotes the number of equality constraints while N is the total number of constraints.

The aim is to minimise an objective functional subject to the dynamical system given by equations (1.1) and (1.2) and subject to the constraints (1.3). The objective functional is expressed in the form,

$$\min_{\boldsymbol{\zeta}\in\mathcal{Z}} g_0(\boldsymbol{\zeta}) = \Phi_0(\boldsymbol{x}(T \mid \boldsymbol{\zeta})) + \int_0^T \mathcal{L}_0(t, \boldsymbol{x}(t \mid \boldsymbol{\zeta}), \boldsymbol{\zeta})\, \mathrm{d}t\,, \tag{1.4}$$

where $\mathcal{Z} = \{\boldsymbol{\zeta} = [\zeta_1, \ldots, \zeta s]\epsilon\mathbb{R}^s : a_i \leq \zeta_i \leq b_i\,,\ i = 1, \ldots, s\}$ is a compact and convex subset of $\mathbb{R}^s$. Here, a_i and b_i are real numbers for each $i = 1, \ldots, s$ (Teo et al., 1991). The above problem essentially constitutes a mathematical programming problem and can, in principle, be solved using non-linear programming techniques such as sequential quadratic programming (SQP). However, the presence of the dynamic constraints (1.1) means that the required gradients of the objective and constraint functionals need to be calculated in a round about manner.

For each $i = 0, \ldots, N$ define the Hamiltonian by,

$$H_i(t, \boldsymbol{x}, \boldsymbol{\zeta}, \boldsymbol{\lambda}) = \mathcal{L}_i(t, \boldsymbol{x}, \boldsymbol{\zeta}) + \boldsymbol{\lambda}^i \boldsymbol{f}(t, \boldsymbol{x}, \boldsymbol{\zeta})\,. \tag{1.5}$$

We then define the costate systems as follows,

$$\frac{d\boldsymbol{\lambda}^i(t)}{dt} = -\Big[\frac{\partial H_i(t, \boldsymbol{x}(t|\boldsymbol{\zeta}), \boldsymbol{\zeta}, \boldsymbol{\lambda}^i(t|\boldsymbol{\zeta}))}{\partial \boldsymbol{x}}\Big]^\top, \qquad i = 0, \ldots, N, \tag{1.6}$$

with

$$\boldsymbol{\lambda}^i(\tau_i) = \frac{\partial \Phi_i(\boldsymbol{x}(\tau_i|\boldsymbol{\zeta}), \boldsymbol{\zeta})}{\partial \boldsymbol{x}}, \qquad i = 0, \ldots, N, \tag{1.7}$$

where $\tau_0 \equiv T$. The solution to the costate system for $\boldsymbol{\zeta} \in \mathbb{R}^s$ is denoted by $\boldsymbol{\lambda}(\cdot|\boldsymbol{\zeta})$. We can now state Theorem 1 as follows,

Theorem 1. *(Teo et al., 1991) Consider the problem defined by equations (1.1) to (1.3) and (1.4). For each $i = 0, 1, \ldots, N$, the gradient of the functional g_i is given as follows:-*

$$\begin{aligned}\frac{\partial g_i(\boldsymbol{\zeta})}{\partial \boldsymbol{\zeta}} = \frac{\partial \Phi_i(\boldsymbol{x}(t|\boldsymbol{\zeta}), \boldsymbol{\zeta})}{\partial \boldsymbol{\zeta}} + (\boldsymbol{\lambda}^i(0, |\boldsymbol{\zeta}))^\top \frac{\partial \boldsymbol{x}^0(\boldsymbol{\zeta})}{\partial \boldsymbol{\zeta}} \\ + \int_0^{\tau_i} \frac{\partial H_i(t, \boldsymbol{x}(t|\boldsymbol{\zeta}), \boldsymbol{\zeta}, \boldsymbol{\lambda}^i(t, \boldsymbol{\zeta}))}{\partial \boldsymbol{\zeta}}\, dt\end{aligned}$$

where H_i is defined in equation (1.5) and $\boldsymbol{\lambda}^i(t|\boldsymbol{\zeta})$ is the solution of (1.6) and (1.7). Theorem 1 allows us to determine the gradients of the objective and constraint functionals with respect to the system parameter vector $\boldsymbol{\zeta}$. These gradients are required to the solve the problem using numerical optimisation techniques. Standard mathematical programming methods can now be applied to solve the optimal parameter selection problem. The optimal control software, MISER3.3 (Jennings et al., 2004), uses an SQP algorithm for this purpose along with a comprehensive numerical integration routine, LSODA (Jennings

et al., 2004). MISER3.3 is software that is specifically designed to both simulate and optimize dynamical systems. It is capable of incorporating a wide variety of dynamical systems, objectives and constraints. It also incorporates built in smoothing techniques to deal with non-differentiability in the objective or constraints. Gradient formulae must be determined for the objective function and the dynamics with respect to each of the states and each component in $\boldsymbol{\zeta}$. We note here that MISER3.3 is only capable of returning a locally optimal solution for general nonlinear problems. In this thesis, we use the terminology 'optimal solution' with the understanding that this may only represent a locally optimal solution.

In the context of cell cycle models, the dynamics represent the activities occurring inside a cell, while the system parameter vector can be used to describe model parameters whose values are not well defined. More specifically, the problem that we propose has a system parameter vector $\boldsymbol{\zeta}$, where the parameter values represent biological constants. These values can often not be estimated easily from experimental results and most publications in the literature merely contain guesses for many of their parameters. As shown below, the objective function can be cast in several different ways to measure the difference between the model outputs and data from a real cell cycle experiment. We detail several different objectives and constraints that can be used in various biological settings.

For our set of problems we firstly need to define $\boldsymbol{x}^*$(t) as the vector of observed outputs from an experiment which correspond to the state variables in our mathematical model. A first objective functional g_0 can be defined as follows,

$$\begin{aligned}\min_{\boldsymbol{\zeta}\in\mathcal{Z}} g_0(\boldsymbol{\zeta}) = (\boldsymbol{x}(T) - \boldsymbol{x}^*(T))^\top S(\boldsymbol{x}(T) - \boldsymbol{x}^*(T)) + \\ \int_0^T (\boldsymbol{x}(t) - \boldsymbol{x}^*(t))^T Q(\boldsymbol{x}(t) - \boldsymbol{x}^*(t)) dt\,,\end{aligned} \tag{1.8}$$

where S and Q are diagonal matrices and their positive entries represent the weights on matching different state components. This is a general quadratic form of the objective in model matching problems.

The objective function g_0 stated in equation (1.8) can be defined using absolute values of the differences between model and experimental states instead of the quadratic form which can yield very small values when a model is closely matched to real data. Some state values in our formulation have a unit value much less than one and need to be handled appropriately. The absolute value is much better suited for these smaller values over the least squares approximation as their value is not lost. In general, the absolute value function is non-smooth and is hence more difficult to handle computationally. However, MISER3.3 has a built in smoothing transformation, making it capable of solving such problems. Hence, we may pose an alternative objective function as

$$\min_{\boldsymbol{\zeta}\in\mathcal{Z}} g_0 = \int_0^T \sum_{i=1}^{n} \left| x_i(t) - x_i^*(t) \right| dt\,. \tag{1.9}$$

The form (1.9) still assumes that all states in the model have counterparts in the experimental results that can be observed over the entire time horizon. However, experimental data of this nature is not always available and alternative formulations will be presented to discuss how this maybe handled from a modelling perspective.

It may be the case that not all of the states are measurable in an experimental sense, so we must make do with observable functions of the states from the experiments. Thus, an objective may be formulated as

$$\min_{\boldsymbol{\zeta}\in\mathcal{Z}} g_0 \quad = \quad \int_0^T \sum_{j=1}^{m} \left| h_j(\boldsymbol{x}(t)) - h_j(\boldsymbol{x}^*(t)) \right| dt \,, \tag{1.10}$$

where each h_j, $j = 1, \ldots, m$ is some function of the model states that can be observed experimentally.

The formulation (1.10) still assumes that experimental outputs are available at all points in the time horizon $[0, T]$. More realistically, experimental data may only be available at a certain sequence of M observation times, τ_i for $i = 1, \ldots, M$. In this case, the objective should take the form

$$\min_{\boldsymbol{\zeta}\in\mathcal{Z}} g_0(\boldsymbol{\zeta}) = \sum_{i=1}^{M} \sum_{j=1}^{m} \left| h_j(x(\tau_i)) - h_j(x^*(\tau_i)) \right| , \tag{1.11}$$

The objective (1.11) does not fit into the general canonical form of (1.4) due to the presence of multiple characteristic times in the objective, τ_i, $i = 1, \ldots, M$. General forms of functionals of this type are first described in (Martin, 1992), (Martin and Teo, 1994) and (Loxton et al., 2008). Rory Martin (Martin, 1992) introduced the concept of Multiple Characteristic Time points to model

treatment scheduling for cancer chemotherapy. Martin (Martin, 1992) was able to show that by using multiple characteristic time constraints for treatment scheduling it is beneficial to offer a low dose initially then switch to a high dose after a fixed point in time. The results published by Martin (Martin, 1992) were also shown to be inline with published clinical studies. Patients were studied with small cell lung cancers who had been treated with chemotherapy with successful treatment scheduling following a similar regime to that suggested by Martin (Martin, 1992).

Martin and Teo (Martin and Teo, 1994) presented a theoretical approach for dealing with multiple characteristic time points in objective and constraint functionals. The notation used by Martin and Teo is similar to what we have used above. In particular, they derived the gradients of such functionals and these were later incorporated into the optimal control software MISER3.3. They also derived convergence results for solving control problems of this type by a sequence of numerical approximations. We refer the interested reader to the published work by Martin and Teo.

These alternative formulations highlight the versatility of using optimal parameter selection techniques in a biological setting. In such an environment we can match experimental observations at particular time points during the experiment. In this environment it is often reasonable to use the formulation involving multiple characteristic times. This technique, when applied to a biological setting, allows for observed experimental data to be taken at particular points throughout the experiment while matching a theoretical value at the same time point. This allows us to optimise parameters in order to achieve the

best possible match between experimental observations and the corresponding model predictions.

1.3 Optimal Control and Modelling of Cancer Therapies

We include in this section reviews on several applications of optimisation methods in cancer treatment as this is related to the main focus of our research which concentrates on optimal parameter selection and how it is applied to cancer growth modelling.

We firstly define a general class of Optimal Control Problems with cost functional $g_0(\boldsymbol{u}, \boldsymbol{\zeta})$, as follows,

$$\min_{(\boldsymbol{u},\boldsymbol{\zeta})\in\mathcal{U}\times\mathcal{Z}} g_0(\boldsymbol{u},\boldsymbol{\zeta}) = \Phi_0\big(\boldsymbol{x}(T),\boldsymbol{\zeta}\big) + \int_0^T \mathcal{L}_0\big(t,\boldsymbol{x},\boldsymbol{u},\boldsymbol{\zeta}\big)\mathrm{d}t\,, \tag{1.12}$$

subject to,

$$\dot{\boldsymbol{x}} = \mathbf{f}\big(t,\boldsymbol{x},\boldsymbol{u},\boldsymbol{\zeta}\big)\,, \tag{1.13}$$

$$\boldsymbol{x}(0) = \boldsymbol{x}_0(\boldsymbol{\zeta})\,, \tag{1.14}$$

$$g_i(\boldsymbol{u},\boldsymbol{\zeta}) = \Phi_i\big(\boldsymbol{x}(T),\boldsymbol{\zeta}\big) + \int_0^T \mathcal{L}_i\big(t,\boldsymbol{x},\boldsymbol{u},\boldsymbol{\zeta}\big)\mathrm{d}t \begin{cases} = 0, & i = 1,\ldots,N_e\,, \\ \leq 0, & i = N_e+1,\ldots,N\,, \end{cases} \tag{1.15}$$

where $\boldsymbol{u}(t) = [u_1(t),\ldots,u_r(t)]^\top$ is the control function mapping from $(0,T]$ into $\mathbb{R}^r$, U is defined as a compact and convex subset of $\mathbb{R}^r$, a function $\mathbf{u}(t)$ is

said to be an admissable control if $\mathbf{u}(t) \in U$ for almost all $t \in [0, T]$ and $\mathcal{U}$ is defined as the class of all such admissable controls.

A background into Optimal Control Theory will be not be given here, but the interested reader is referred to (Teo et al., 1991).

1.3.1 Optimal Control and Cancer Chemotherapy

A good starting point for optimal control and cancer chemotherapies is the work done by Kok Lay Teo and Rory Martin (Martin and Teo, 1994). Teo and Martin use optimal control techniques to design a treatment schedule that will benefit patients using, at the time, current cancer treatments but yet incorporating bounds on toxicity levels so the patient will still have a reasonable quality of life.

The problem is defined as minimising the final tumour size for a particular patient with drug toxicity levels kept in mind. Teo and Martin formulate the problem as an optimal parameter selection problem, where the objective is to minimise the following objective,

$$J_1(\boldsymbol{u}) = N(T)\,, \tag{1.16}$$

where $\boldsymbol{u} = [u_1, \ldots, u_n]\top \in \mathbb{R}^n$ is the dose vector, N is the tumour cell population and T is the terminal time. The minimisation of 1.16 is subject to the following,

$$\dot{N}(t) = \lambda N(t) \ln[\theta/N(t)] - k\big(v(t) - v_{th}\big) H\big(v(t) - v_{th}\big) N(t)\,, \tag{1.17}$$

$$N(0) = N_0\,, \tag{1.18}$$

$$v(t) = \sum_{i=1}^{n} u_i \exp\big(-\gamma(t-t_i)\big) H(t-t_i)\,, \tag{1.19}$$

with the constraints,

$$0 \leq v(t) \leq v_{max} \quad \forall \quad t \in [0,T]\,, \tag{1.20}$$

$$N(t) \leq N_{max} \quad \forall \quad t \in [0,T]\,, \tag{1.21}$$

$$\int_0^T v(s)\mathrm{d}s \leq v_{cum}\,, \tag{1.22}$$

where,

$v(t)$: drug concentration at time t,

v_{max} : maximum bound on drug concentration (constant),

N_{max} : maximum bound on tumour cell population,

$v(s)$: concentration of the anti-cancer drug at the cancer site at time t,

v_{cum} : maximum bound on $\int_0^T v(s)\mathrm{d}s$,

k : constant parameter representing proportion of tumour cells killed for each drug concentration per unit of time t,

λ : growth rate parameter,

v_{th} : threshold value where drug administration stops being effective.

The heaviside step function $H(\cdot)$ is defined as,

$$H(t-t_i) = \begin{cases} 0\,, & \text{if} \quad t < t_i\,, \\ 1\,, & \text{if} \quad t \geq t_i \end{cases}$$

Teo and Martin (Martin and Teo, 1994) solve the optimal parameter selection problem presented with objective (1.16) using appropriate computational methods. They use non-clinical data to generate solutions to the stated objective, where 3 differing drug types are used. The drug types are categorised as highly effective, moderately effective and low effectiveness. They are able to effectively show that using the optimal treatment schedule they propose, the final size of the tumour is reduced in all 3 drug type cases.

1.3.2 Combination Therapy

The team d'Onofrio, Ledzewicz, Maurer and Schättler have modelled combination therapy treatments for tumour growth using optimal control techniques (d'Onofrio et al., 2009; Ledzewicz et al., 2009, 2011).

They firstly describe a simplistic model for tumour growth that models the tumour at a vascular level and incorporates the tumour using its own nutrient supply, in other words, creating its own vasculature (angiogenesis).

They formulate the problem as an optimal control problem for both the primary tumour and vasculature populations. The optimal control problem is given as,

$$\min J(u) = p(T)\,, \tag{1.23}$$

subject to the following dynamics,

$$\dot{p} = \xi p F\left(\frac{p}{q}\right) - \varphi p v\,, \qquad p(0) = p_0\,, \tag{1.24}$$

$$\dot{q} = bp - I(p)q - \mu q - \gamma q u - \eta q v\,, \qquad q(0) = q_0\,, \tag{1.25}$$

$$\dot{y} = u\,, \qquad y(0) = 0\,, \tag{1.26}$$

$$\dot{z} = v\,, \qquad z(0) = 0\,, \tag{1.27}$$

where,

$$F\left(\frac{p}{q}\right) = -\ln\left(\frac{p}{q}\right)\,, \tag{1.28}$$

$$I(p) = dp^{2/3}\,. \tag{1.29}$$

We list the associated terms below,

$p(t)$: primary tumour volume,

$q(t)$: maximum size the tumour can reach by its vasculature,

$v(t)$: concentration of the cytotoxic agent,

$u(t)$: concentration of anti-angiogenic agent,

γ : anti-angiogenic elimination parameter,

μ : baseline loss of vascular support through natural causes,

b : birth rate parameter,

d : death rate parameter,

ξ : tumour growth parameter,

φ : cytotoxic killing parameter for tumour,

η : cytotoxic killing parameter for vasculature,

t : time, in days,

F : function describing growth,

I : function that represents the inhibitor.

Optimal results are obtained for the combination treatments for 2 cases of differing initial conditions for the tumour volume p_0 and carrying capacity q_0. The results published by (d'Onofrio et al., 2009) highlight the need for further investigation into optimal treatment scheduling and the need for more realistic biological data. More importantly the results that the authors were able to produce showed a significant trend towards combination therapy being a worthwhile treatment with reductions in both tumour volume and the carrying capacity of the vasculature.

A second paper published by Ledzewicz, Maurer and Schättler (Ledzewicz et al., 2009) extended from their original optimal control problem (above) to analyse bang-bang and singular controls. They present a similar system to the one mentioned above with the same objective. There is a detailed description dealing with singular controls and mathematical formulae are given for calculating singular control regimes for variable $u(t)$, the concentration of anti-angiogenic agent.

The final paper under consideration for optimal control of combination therapy is by Ledzewicz, Maurer and Schättler, see (Ledzewicz et al., 2011). The same model describing the tumour growth rate and the rate of formation of the vasculature is used as in the previous papers detailed above. However, in the current model there are some key features added such as a pharmacokinetic expression which describes the treatment drugs' concentration.

A Gompertz model is still used to describe the tumour growth rate and the carrying capacity is modelled by the similar function described in previous papers, see (Ledzewicz et al., 2008, 2009, 2010).

The optimal control problem is stated as,

$$\min J(u) = p(T)\,, \tag{1.30}$$

subject to the following dynamics,

$$\dot{p} = -\xi p \ln \frac{p}{q} - \omega p v\,, \qquad p(0) = p_0\,, \tag{1.31}$$

$$\dot{q} = bq^{2/3} - dq^{4/3}\mu q - \gamma q u - \eta q v\,, \qquad q(0) = q_0\,, \tag{1.32}$$

$$\dot{y} = u\,, \qquad y(0) = y_0\,, \tag{1.33}$$

$$\dot{z} = v\,, \qquad z(0) = z_0\,. \tag{1.34}$$

This model shows significant advancements towards optimal treatment scheduling may be possible and it is an example of a growing trend in how mathematics can be used to optimise such scheduling. Ledzewicz, Maurer and Schättler (Ledzewicz et al., 2011) have described the treatment scheduling

in this paper by applying standard optimal control techniques but yet being able to incorporate a real-life perspective by adding limiting amounts for each treatment, in this case amounts of chemotherapy and anti-angiogenesis agents. They publish results for the theoretical model only but show how these results can be used in a treatment scheduling environment. The parameters used in the computational analysis are also chosen from a theoretical perspective and to show how optimal combination therapy could be used. The only downside to this paper is that there is no mention of future work towards gaining biological data to show their model working in a practical environment. However, the results published, as discussed above, highlight the importance of this type of mathematical modelling and how it can be harnessed to effectively reflect a real world situation.

1.4 Overview

The thesis is broken into 6 distinct chapters which we will outline here. Chapter 1 details the motivation behind our research into the mathematical modelling of the cell cycle and, in particular, the cancer cell cycle. We then give a background into the theory of Optimal Parameter Selection Problems. We present some alternative formulations in the objective for Optimal Parameter Selection problems and the need for Multiple Characteristic Time points. The remainder of the chapter is devoted to reviews of some treatment scheduling models employing optimal control methods. We include these reviews since Optimal Parameter Selection problems and their solution methods are closely related to Optimal Control problems.

Chapter 2 gives a detailed background into the cell biology that we have applied to our modelling process. Our research has a strong biological influence and hence, a background into the biological processes that occur in relation to our research is important. We describe cell cycle growth and the cell biology in relation to the normal cell cycle as well as the cancer cell cycle. Our work primarily deals with the mammalian cell cycle but there are comparisons to the yeast cell cycle due to similarities and the ease of collecting experimental data. We also give some brief summaries into certain proteins that often appear mutated in certain cancers, our main focus being melanoma. We discuss how widespread these mutations are and the significant role they play in cancer growth in general. A background into kinetics is also included here as this has a strong influence on the models we analyse as well as on the models that we develop.

A background into previous literature on cell cycle and cancer growth models is presented in Chapter 3. We start with an analysis of a yeast cell cycle model as this is the basis behind much of the modelling that we investigate and the cancer cell cycle model we base most of our research on stems from a yeast division cycle. We give an indepth analysis of a particular cancer cell model which we use in out computational work in Chapter 4.

In Chapter 4 we present our analysis of a cancer cell cycle model with Optimal Parameter Selection techniques applied and a discussion of our results. We show the effects of optimising parameters from a theoretical perspective with significant results. We also give a discussion on computer accuracy and precision and how this can play a significant role in numerical simulations. We

show that computer precision has a significant impact on the mathematical modelling of biological processes when running numerical simulations.

We present our own mathematical model for a particular type of cancer, melanoma growth, in Chapter 5. With little literature existing for the mathematical modelling of melanoma growth, we chose to develop a cell-based mathematical model for melanoma. We give a brief background into two current melanoma growth models that exist in literature. We review the biochemical kinetics that we presented earlier in Chapter 2, the basis for our own melanoma model. The model we present incorporates cell cycle growth and protein mutations relevant to melanoma growth.

In Chapter 6 we summarise what we were able to achieve and provide a discussion of future work. We also highlight the importance and significance that mathematical modelling, particularly optimisation techniques, can have on biological processes and in particular cancerous growths.

We have introduced the nature and motivation behind our research and background into the mathematical techniques we use throughout this thesis. We also proposed differing forms of objectives that could be used in similar scenarios depending on what experimental data is available and at what time points this can be measured. We have also provided a brief summary of how optimisation techniques can be used in a practical sense, by calculating optimal combination treatment schedules.

Chapter 2

Biological background

The main aim of this chapter is to describe the basic principles behind cell dynamics and how these dynamics relate to cancer growth. The mathematical modelling of cancer growth is a difficult task and requires many approximating assumptions. Consequently, a thorough understanding of the biology of cancer and how it grows is essential to any modelling attempt. The interactions that occur during the mammalian cell cycle are complex and require a high level of biochemistry and biological understanding. We explain some of these interactions in a simplified manner and show how we can describe them using mathematical processes.

The chapter is organised into three sections. Section 2.1 outlines the features of the cell cycle for both normal and cancerous cells. We will give a brief description relating to cancer development and how it spreads in Section 2.2. In this section we will also provide summaries of proteins relevant to our research and detail cancers that have been reported to display associated mutations. The final section, 2.3, will give a description of the Michaelis-

Menten kinetics which is used extensively in the models we analyse. We will also discuss an extension of the Michaelis-Menten kinetics by Goldbeter and Koshland (Goldbeter and Koshland, 1981), highlighting the significance in relation to our research.

2.1 The Cell Cycle

The biological aspects of this research are based around the eukaryotic cell cycle, in particular the phases of the cell cycle and the reactions occurring in these phases in association with mammals and cancer growth, melanoma growth specifically. Much mathematical modelling is now centred on interactions occurring inside the cell and the dynamics that these interactions follow are an important part of the modelling process. Hence, this is a logical place for us to start our discussion.

The eukaryotic cell cycle is broken into 4 distinct phases, see Figure 2.1. The first is a gap phase, G1, followed by Synthesis or 'S' phase, then followed by G2, a second gap phase and finally the division phase referred to as the Mitosis or 'M' phase. The G1 phase is the longest phase in the cell cycle during which the cell can decide its future. This is the only period in the cycle where a cell can decide its own fate. This may be to continue in the cycle, to rest and enter a quiescent state (often referred to as G0) or to commit to programmed cell death, known as apoptosis. There is a special point during this first phase known as the Restriction point or R point and it represents a point of no return. Once a cell reaches this point there is now a commitment to proceed further through the cycle and continue onto the transition phase

Figure 2.1: The four phases of the mammalian cell cycle

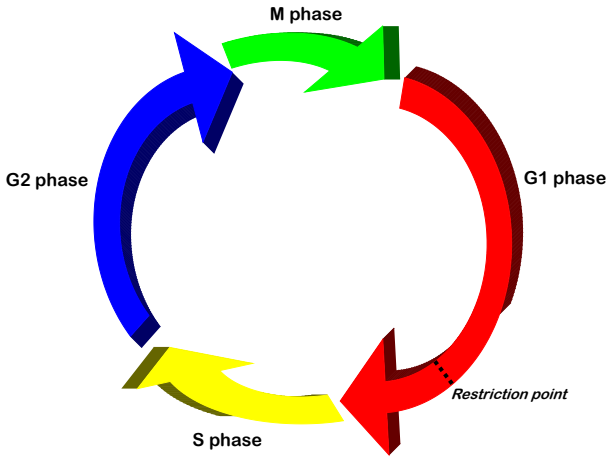

between G1 and S, however, this may not always occur in a straight forward manner due to a changing environment as is the case for cancerous cells.

In cancer cells the restriction point is often where things start to go wrong. The restriction point is often said to be the point where cancer cells are able to deregulate the transition process and hence increase their proliferation rate. The nature of the restriction point also characterizes the greatest difference between normal and cancer cells. Most other aspects of the cell division process of cancer cells are much the same as those of normal cells once the cell has passed the restriction point (Weinberg, 2007). This is particularly important to the mathematical modelling, since cancer can start with a single cell mutation and this is initiated at the restriction point. The restriction point is where a decision needs to be made about the future life of a cell. It is also a checking point in the cycle where information is gathered about the cell and

it is determined whether the cell can proceed further in the division process.

The main focus of our research is the G1/S transition phase of the cell cycle, so an in depth knowledge of the later phases, including the Mitosis phase, is not essential to this research. A brief description of the later phases, however, will be given below.

Synthesis, the second phase in the cell cycle, follows from G1 once the cell has passed through the R point. Synthesis or the 'S' phase is where the cell initiates DNA duplication and there is much activity occurring inside the cell throughout this entire phase. For a mammalian cell the S phase is typically between 10 to 12 hours of the cell cycle (Alberts et al., 2008).

Once passing through synthesis the cell can then proceed to the next gap phase, G2, where there is not much activity present as the cell is preparing itself for separation and the final phase of the cell cycle. This second gap phase is not as long as the first as there is no quiescence state to enter, where a cell could seek refuge for any amount of time.

Mitosis (M phase) is the shortest of the phases where the cell must go through a checkpoint similar to that of the R point in G1. Mitosis or M phase can be broken into 5 distinct subphases - prophase, prometaphase, metaphase, anaphase and telophase. Mitosis ends with cytokinesis where the separation of the cytoplasm occurs and the two daughter cells are finally separated, each having their own nucleus (Alberts et al., 2008).

A brief description of each of the subphases of mitosis will be given here, we refer the reader to (Alberts et al., 2008) for a more in depth explanation. The first phase of mitosis is prophase and is where the chromosomes

that were replicated during Synthesis to produce 2 sister chromatids condense. Prometaphase allows the chromosomes in prophase to attach to spindle microtubules (Alberts et al., 2008). During metaphase the chromosomes start to align themselves in the centre of the spindle and the sister chromatids can move to opposing ends. In the next subphase, anaphase, the sister chromatids become two daughter chromosomes and must be completed with great precision to ensure division occurs correctly. The final phase of mitosis is telophase where the two daughter chromosomes and two nuclei are formed. At the end of telophase the cell is now ready to enter cytokinesis the final step in the division cycle.

In normal cells mitosis is quite straight forward and is simply where chromosomes are formed and two identical nuclei are formed so that the cell can then divide into two identical new cells. In cancer cells this phase is somewhat different and it is when cancer cells are most active. There is another checkpoint similar to that of the Restriction point in the mammalian cell cycle that occurs during the mitosis phase. The second checkpoint is the G2/M transition phase where the cell is prepared for chromosome alignment through activating the early stages of mitosis. A third checkpoint that also occurs during the M phase is where the cell makes the transition from metaphase to anaphase. This checkpoint signifies the end of mitosis, the cell is now ready to divide and proceed with the final stage of mitosis and cell cycle-cytokinesis as detailed in the previous paragraph (Alberts et al., 2008).

We will give brief mention here to the work undertaken by Smith and Martin (Smith and Martin, 1973) and the model they proposed for cell cycle

division using transition probabilities. Smith and Martin re-interpret the traditional 4 phase cell division cycle described above, by stating there are 2 distinct time periods throughout the division cycle, A-state and B-phase. The authors were able to show variability in the length of A-state, traditionally G1 phase of the cell cycle, and postulate the activities in B-phase and when it begins. The authors were able to show the effectiveness of using transition probability between A-state and B-phase by successfully predicting experimental data and growth rates of cell population.

In the yeast cell cycle the restriction point is known as 'Start', it is the transition between phases G1 and S/M. The transition phase S/M to G1 is called 'Finish' (Nasmyth, 1995, 1996; Tyson and Novak, 2001). Authors Tyson and Novak refer to these 'Start' and 'Finish' phases throughout much of their work, see (Novak et al., 1998a,b; Tyson and Novak, 2001). Our research is based on the mathematical modelling of the cell cycle, which we discuss in Chapter 3, and we often refer and use the models developed by Tyson and Novak (Novak et al., 1998a,b; Tyson and Novak, 2001). These transition phases are significant in the cell cycle process as these are where particular cyclin/Cdk complexes and other regulatory protein complexes become active or inactive. Often when a cell becomes cancerous certain proteins or their forming complexes can be over or under-expressed impacting on their activity status during the cell cycle.

The yeast cell cycle is often used as a comparison to the mammalian cell cycle in experimental and modelling situations. The yeast cell cycle shares many similarities with the mammalian cell cycle with yeast being much easier

to study and consequently used much more vigorously in an experimental environment (Buschhorn and Peters, 2006). The yeast cell cycle is considerably shorter than a mammalian cell cycle hence, making it more attractive to use in experiments.

Depending on the type of cell the length of each phase in the cycle and the overall length of the cell cycle can vary remarkably. For instance, the cells lining the intestines divide every 3 days, however, cells in the liver only divide after approximately 1 year (Murray and Hunt, 1993). In general terms, the typical length of G1 for mammalian cells varies for different types of cells, but is the longest phase of the cell cycle regardless of the cell type. The length of this phase can vary significantly depending on the external conditions surrounding the cell and whether the cell will enter the G0 or rest phase. A cell can stay in this rest phase for any length of time and may even stay in a rest state until the cell dies. Obviously, this rest state can greatly influence the overall length of a cell cycle as seen in the above example.

An obvious question at this stage is: how does the molecular machinery, or in other words, *the cell cycle clock* implement decisions that are made regarding the future of a cell?

The answer is that there are groups of proteins and enzymes which act as chemical messengers and guide the cell through the division process. It is these proteins, enzymes and their complexes which we have chosen to model in this research.

The cyclins are groups of proteins that are active throughout the cell cycle and initiate DNA synthesis. Throughout the cell cycle different cyclins

become active at different stages. There are four main cyclin groups - A, B, D and E, each with their associated subgroups. Each cyclin has its own role to play in the division cycle of a cell. Cyclins bind with their associated kinases (enzymes that are responsible for covalently attaching phosphate groups to substrate molecules, mainly in the form of proteins) (Weinberg, 2007).

There are many enzymes and proteins that make up the machinery of the cell cycle. Protein kinases are special enzymes that are responsible for emitting signals to the responder molecules and phosphorylate distinct targets which we know as substrates. Cyclin-dependent kinases (Cdk's) are enzymes (kinases) that work with their associated cyclin subunits to help bind them together. It has been reported (Weinberg, 2007) that the levels of Cdk activity during the cell cycle itself does not change greatly. The complexes formed between cyclins and their associated Cdk's are what greatly influence the level of activity occurring at different stages of the cell cycle. In the budding yeast cell cycle, for instance, there is only one cyclin-dependent kinase, Cdc28, with 9 corresponding cyclins. The regulation of this cyclin-dependent kinase will activate or deactivate other proteins in the cell cycle and consequently aid with the progression of the cycle by forming active complexes (Tyson and Novak, 2001; Novak et al., 1998b).

Cancer cells in particular have a unique ability to shut down certain proteins which give them the ability to progress through the cell cycle without the cell recognising that something is not in balance. Cancer starts with a mutation in a single cell and when a cell divides the mutation is present in the daughter cells that form from the division process (Weinberg, 2007). The

tumour suppressor gene pRb can be inactivated by cancer mutated cells. The reason behind this is that cancer cells have the inept ability to shut down and suppress the inhibitor protein $p16^{INK4a}$. This leads to excessive amounts of the cyclinD/Cdk4,6 complex being produced and excessive kinase activity. This is the specific case of melanoma growth as it has been recognised that the inhibitor protein $p16^{INK4a}$ can be found to be altered in many melanoma cancers.

The restriction point in the later G1 phase of the cell cycle is where cancer cells seem to have an advantage over normal cells in their cell cycle. Cancer cells are able to bypass the restriction check point and continue in the cell cycle even though there is an over-expression of certain proteins or complexes.

The APC/C (see Table 2.1) is used extensively in the mathematical models that we analyse. Hence, a more in depth understanding of this complex is required. It is a protein complex that exists in both yeast and mammalian cell cycle dynamics. The APC/C is best described as a group of proteins that are active during the late Mitosis phase and G1 phases of the cell cycle (Buschhorn and Peters, 2006). It is required throughout the mitosis and G1 phases of the cell cycle for degrading substrates (Waŝch and Engelbert, 2005).

The APC/C works with 2 key proteins, Cdh1 and Cdc20 in yeast and p55cdc in humans, to regulate the mitosis and G1 phases of the cell cycle. These activities include activation and inactivation of cyclin/Cdk complexes (Novak and Tyson, 2004).

Figure 2.2: The Ras Signalling Pathways

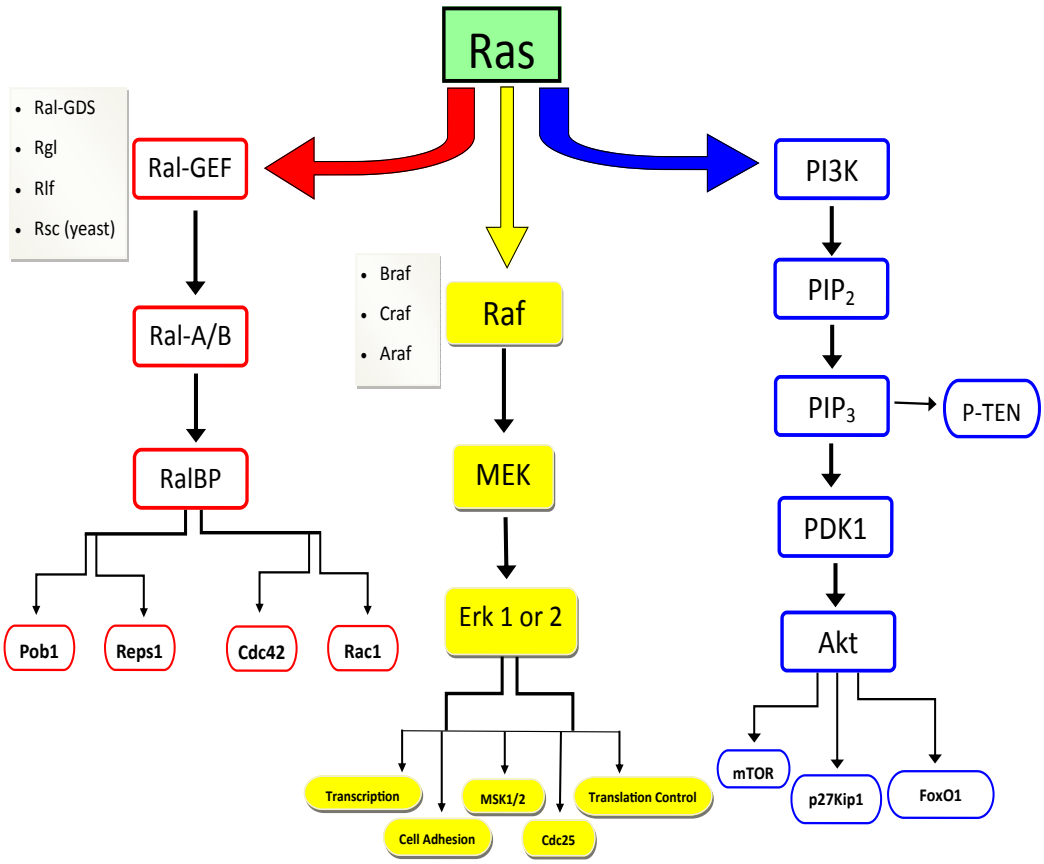

2.1.1 Terminology

Table 2.1 lists the key terms and terminology used.

2.1.2 Cell Cycle Signalling Pathways

There are also differing signalling pathways in the mammalian cell cycle and often disruptions in these pathways can lead to cancerous growth. Figure 2.2

Table 2.1: Biological definitions

Term	Definition
cyclin	Any of a group of proteins active in controlling the cell cycle and in initiating DNA synthesis.
kinase	Any of various enzymes that catalyse the transfer of phosphate groups from a high energy phosphate containing molecule (as ATP or ADP) to a substrate.
cyclin-dependent kinase	(Cdk's) Enzymes that do not act on their own; they depend on associated regulatory subunits – the cyclin proteins.
eukaryote	All other forms of life other than bacteria (Prokaryotes). They have a true membrane-bounded nucleus.
phosphorylation	Reaction in which a phosphate group is covalently coupled to another molecule.
hypo-phosphorylation	Weak state of phosphorylation of a protein.
hyper-phosphorylation	Elevated levels of phosphorylation of a protein.
Rb	Retinoblastoma.
mRNA	Messenger RNA.
RNA	Ribonucleic acid.
E2F	Transcription factor activating adenovirus E2 gene.
DNA	Deoxyribonucleic acid.
MAPK	Mitogen activated protein kinase pathway. We can also have MAP2K (kinase, kinase) and a MAP3K (kinase, kinase, kinase) pathways.
monomer	A molecule of low molecular weight capable of reacting with identical or different molecules of low molecular weight to form a polymer.
dimer	A compound formed by the union of 2 radicals or 2 molecules of a simpler compound.
melanocyte	An epidermal cell that produces melanin.
ERK	Extracellular signal-regulated kinase.
wildtype	The allele of a gene that is commonly present in the great majority of individuals in a species.
Cdh1	E-Cadherin or Cadherin 1 (protein).
APC/C	Anaphase-promoting complex/cyclosome.
hypoxia	A deficiency of oxygen reaching the tissue of the body.
GEF	Guanine nucleotide exchange factors.
angiogenesis	Growth of new blood vessels from existing vasculature.

represents the three pathways stemming from the Ras protein. The Ras protein pathway is significant due to the mutations that often occur along the three pathways that stream downward from this protein. Obviously, many different cancers arise from these mutations along these different pathways.

The Ras $\rightarrow$ Raf $\rightarrow$ MEK kinase pathway has been shown to inhibit mutations in a particular Raf gene, BRAF, which is evident in specific types of cancer, melanoma being the most common (Davies et al., 2002). This pathway is also known as the MAP3K pathway as it phosphorylates each kinase as they travel downstream of the signalling pathway. If there is a mutated oncoprotein along the Ras $\rightarrow$ Raf $\rightarrow$ MEK $\rightarrow$ Erk $\rightarrow$ pathway then cancer development is inevitable. In particular it has been shown in the past decade that the mutated B-raf gene can occur frequently, as mentioned above melanoma being a strong candidate along with cancers such as lung, thyroid, colorectal and ovarian (Weinberg, 2007). A more detailed discussion of the mutant Braf gene will follow in Section 2.2.2.

There are 2 other important kinase pathways stemming from the Ras protein which can affect cancer development. The Ras $\rightarrow$ PI3K $\rightarrow$ PIP3 or commonly referred to as the PI3K (phosphatidylinositol 3-kinase) pathway (Weinberg, 2007) is one of these pathways. It involves the attachment of phosphate to phospholipids.

The third kinase pathway involving the Ras protein for cancer development is the Ras $\rightarrow$ Ral $\rightarrow$-GEF $\rightarrow$ Ral A/B. Ral is short for Ras-like as the Ral group of GTPases closely relate to the Ras GTPases (Neel et al., 2011). The Ral protein is a member of the Ras family of proteins, this family of proteins

account for a large number of proteins that aid with the cell cycle process.

More recently, an intricate kinase pathway was published by Bandyopadhyay (Bandyopadhyay et al., 2010) that describes the complex MAPK pathways that can exist for humans. The pathway is based on a hybrid "yeast type" model but shows just how involved the human kinase pathway might be. Through the authors' experimentation they were able to show that the human MAPK pathway could have as many as 2,269 protein to protein interactions in total. These interactions would stem from a total of nearly 1,500 different proteins (Bandyopadhyay et al., 2010).

2.2 Cancer development

With cancer being one of the most deadly diseases in modern society one might be under the impression that there are significant and wide ranging differences between a cancer cell and a normal cell. The reality is somewhat less dramatic. As mentioned in Section 2.1 the cell cycle for both normal cells and cancerous cells is very similar and we now draw attention to what can happen once a cell has become cancerous.

There are three main forms of tumour development that we will briefly discuss. The first is the benign stage of tumour development, followed by in situ growth and then lastly the malignant stage of cancer development.

A tumour is said to be benign when it has arisen from any tissue and will grow locally. A benign tumour will also cause damage by local pressure or obstruction. At this stage a tumour is non-metastatic and does not have it's own vasculature (Weinberg, 1997). The next stage of tumour development

is the in situ stage and is where the tumour can develop in the epithelium (membranous cellular tissue). An in situ tumour is still small in size and is not capable of invading surrounding tissue such as the basement membrane or the supporting mesenchyme (Weinberg, 1997).

The third stage that we will mention and the most lethal, is when a tumour becomes malignant. Once a tumour has becomes malignant it can invade and destroy the surrounding mesenchyme, this can lead to metastatic activity. Metastasis can have devastating consequences as this is where a tumour has its own vascular network leading to cancers arising in any tissue and often destroying whole organs (Weinberg, 1997).

The development of cancer can be viewed on different time and length scales which we will briefly mention here. The first level of growth is the outer level which is commonly referred to as the macroscopic or tissue level of growth (Preziosi, 2003). The activities at this level of growth relate to the outer activities of the cell, such as oxygen and blood flow which are important for determining a vascular network, more specifically angiogenesis (Alarcón et al., 2005).

The second level of growth is the cellular level which relates to the activities that occur among differing cells, such as cell-cell interaction and distribution of nutrients (Betteridge et al., 2006). The final growth level is the microscopic or subcellular level which relates to the activities occurring inside the cell. Such activities include protein interactions, cell cycle progression and alterations, protein mutations, gene expression and pathway signalling. This final level of growth is the stage of growth that we will concentrate on in our

research and modelling process.

Cancers can arise from many varying influences including environmental factors, when there has been a pre-existing carcinogen whether it be physical or chemical e.g. such as the chemicals inhaled from smoking cigarettes. Even someone's age could contribute to a cancer growth or the cancer could be organ specific where it relates to a hormonal change, for example, breast or prostate cancer.

2.2.1 The spread of tumours

Cancer has the unique ability to spread anywhere in the body once it has established it's own vascular system. This is accomplished through a biological process known as angiogenesis. This is a process by which new blood vessels are formed. In a cancerous environment angiogenesis enables nutrients to be transported between a 'primary' tumour to secondary sites.

2.2.2 Cell Cycle Genes and Cancer

In this section we provide a summary of particular genes and their protein functions and in which cancers they most frequently occur. Prior to giving this summary we must first give some biological explanation for methylation and how DNA methylation can influence cancer development. Methylation can take on different meanings for different science-based disciplines. Since we are focussing on biochemical reactions we will define methylation as follows: a process by which an organism can take on an epigenetic structure where the structure can be formed when a substrate is added to a methyl group (Al-

berts et al., 2008). There are also different states of DNA methylation that can occur at different stages of tumour development. The stage of DNA *hyper*methylation is observed as a discrete targeted event within tumour cells, resulting in specific loss of gene expression and DNA *hypo*methylation is what usually occurs in advanced stages of tumour development (Weinberg, 2007).

We found while compiling this summary that many of the proteins we chose to summarise were frequent in many different types of cancers so some references may appear in more than one protein summary. Some proteins were also found to have more influence in certain types of cancers i.e. familial or hereditary cancers, while others were seen to play a minor role in many cancers.

One of the most influential genes in cancer progression is the retinoblastoma gene or *Rb*, a tumour suppressor gene. The retinoblastoma protein (pRb), isolated from the gene, is significant in the early stages of the cell cycle, particularly in the G1/S transition phase (Nelson and Cox, 2005). pRb is important to restriction point control as it aids the cell in its decision to continue along the cell cycle path (Weinberg, 2007).

The human tumour suppressor gene $p53$ influences cell death by means of apoptosis (programmed cell death) where the cell chooses to commit suicide. It has been shown that $p53$ is frequently mutated in many human cancers hence blocking the natural cell death that cells may go under if they are found to have a defect. This is part of the reason why cancer cells can spread so quickly and why it is even harder to kill them as they are able to avoid this programmed cell death and keep proliferating (Weinberg, 2007; Nelson and Cox, 2005).

The cell-cell adhesion receptor, Cdh1, can cause mutations that lead to a loss of expression of E-cadherin. The cancers where this is most common to occur are colon, breast, lung, bladder and gastric (Weinberg, 2007). Cdh1 also activates the APC/C towards the end of mitosis, in particular after anaphase, and during the G1 phase of the cell cycle (Weinberg, 2007).

The E2F transcription factor 1, or E2F1, is apart of a family of transcription factors that are active during the G1 phase of the cell cycle (Weinberg, 2007). In relation to cancer growth the over-expression of E2F1 is largely associated with melanoma growth (Bennett, 2007) and has also been linked to breast cancer (Sun et al., 2010). It also has been shown to have links to the activation of the tumour suppressor gene, p53 (Zhang et al., 2010), which is pivotal to tumour progression.

A mutated Raf gene, known as Braf, is found downstream along the Ras $\rightarrow$ Raf $\rightarrow$ MEK pathway. This gene has been discovered to be mutated mostly in malignant melanoma by several different research groups. Davies and colleagues were the first to show clear evidence that mutated Braf occurred most frequently in malignant melanoma (Davies et al., 2002). Weinberg also reported that of a class of melanoma's studied, 60 - 70% of them were found to have the mutated Braf gene (Weinberg, 2007).

The mutated Braf gene is said to increase MAP kinase activity and together with a mutation found in p16 which is further downstream along this pathway, can lead to uncontrolled growth (Smalley, 2007).

The Braf mutation can also be found in human naevi (moles) that enter a phase of growth arrest due to senescence (the process of growing old) that leads

the naevi to not grow further and hence not employ oncogenic signalling. This can lead to naevi becoming a malignant melanoma. Senescence could lead to mutated Braf found in human naevi to discontinue signalling and cause rapid proliferation (Michaloglou et al., 2005).

There also exists a relationship between mutated Braf and the cyclin-dependent kinase inhibitor $p16^{INK4a}$, also known as CDKN2. More specifically, there exists a strong correlation between the two in relation to melanoma growth (Michaloglou et al., 2005).

$$\text{Ras} \rightarrow \text{Raf} \rightarrow \text{MEK}$$
$$\text{(Braf)}$$
$$\downarrow$$
$$\text{CycD/Cdk4,6}$$
$$\downarrow$$
$$\text{Rb (hypophosphorylated)}$$
$$\downarrow$$
$$\text{E2F}$$
$$\downarrow$$
$$\text{G1/S progression}$$

$p14^{ARF}$ is part of the p53 pathway and is often coupled with the $p16^{INK4a}$ protein (from the p16 gene) along this pathway. The $p14^{ARF}$ protein, in particular its methylation status, has been linked quite frequently with colon cancer as well as bladder and breast cancers. There is also evidence pointing towards the suppression of both $p14^{ARF}$ and $p16^{INK4a}$ in melanoma, see (Sharpless and Chin, 2003). More recently, a group of researchers were able to show the signif-

icant effect that $p14^{ARF}$ has on the development of malignant melanoma (Ha et al., 2007).

Apoptotic peptide activating factor 1, or abbreviated to $APAF-1$, is frequently associated with several different cancers, mostly malignant melanoma (Soengas et al., 2001; Jones, 2001; Cecconi and Gruss, 2001). There is, however, evidence of an association with leukaemia, neuroblastoma and glioblastomas (Watanabe et al., 2003; Grau et al., 2011; Fu et al., 2003). APAF-1 runs downstream of the $p53$ apoptotic pathway (Jones, 2001) where the $p53$ gene is the tumour suppressor gene which is often found to be mutant in many human cancers, as previously mentioned.

MGMT (O-6-methylguanine-DNA methyltransferase) is a DNA repair enzyme and has mostly been associated with colorectal (or bowel) cancer (Psofaki et al., 2010; Graham and Leedham, 2010) and glioma (Piperi et al., 2010; Suzuki et al., 2010). The experimental study carried out by Piperi and associates (Piperi et al., 2010) examined several different genes relating to glioblastomas (primary brain tumours) and their methylation. The four gene types that they investigated were 2 tumour suppressor genes, *RASSF1A* and $RAR\beta$, a cell adhesion gene *CDH13* and a DNA repair gene *MGMT*. The methylation status of each of these were examined in 23 patients of which 17 exhibited grade IV tumour and 6 were categorised as grade II. Those patients with a more aggressive grade tumour, glioblastoma, showed a lower mean survival time with a higher occurrence of methylation of the genes studied, in particular, the DNA repair gene *MGMT*.

CASP8 (caspase 8, apoptosis-related cysteine peptidase) or Caspase 8

is known for its role in apoptotic cell death and its ability to activate associated apoptotic pathways (Chaudhary et al., 2000). It has been shown to be prevalent in neuroblastomas and the corresponding gene hypermethylation status (Hoebeeck et al., 2009; Lázcoz et al., 2006). Research also indicates that a loss of CASP8 in neuroblastoma cells can promote metastasis, hence influencing the survival rate of patients (Lázcoz et al., 2006; McKee and c. J. Thiele, 2006).

Retinoic acid receptor $\beta 2$ (RAR$\beta 2$), a tumour suppressor gene, has been shown to be in association with several different tumours, in particular where a loss of this gene is prevalent. Olasz and associates were able to show the influence of loss of expression of RAR$\beta 2$ in head and neck squamous cell carcinoma (HNSCC) and the varying factors contributing to the grade of tumour growth and expression of RAR$\beta 2$ (Olasz et al., 2007).

p73 (tumour protein p73), often referred to as TP73, is a tumour suppressor gene that is a member of the p53 protein family. This particular tumour suppressor gene has been downregulated in several different cancers leading to over-expression or proliferation of cancer cells. The p73 protein has previously been examined in conjunction with the VEGF which plays an important role in angiogenesis and hence tumour progression (Salimath et al., 2000). The p73 protein and its isoforms have been linked with a diverse range of tumours including acute lymphoblastic leukemia (ALL), lymphoma, hepatocellular carcinoma, neuroblastoma, ovarian, breast, bladder, prostate and colon cancers. Rufini and associates were able to summarise the over expression or upregulation, and the downregulation of p73 isoforms on several different cancer types,

highlighting the widespread nature of this particular protein on cancer growth and progression (Rufini et al., 2011).

MLH1 (mutL homolog 1) has been shown to be associated with pancreatic cancers (Yamamoto et al., 2001), colon cancer (Ricciardiello et al., 2003; Niv, 2007; Drost et al., 2010; Arnold et al., 2003), gastric cancers (Ling et al., 2010) and endometrial cancers (Drost et al., 2010; Obermair et al., 2010). Colon and endometrial cancers belong to the hereditary Lynch Syndrome which make examining MLH1 an important element in prognostic and diagnostic analysis of these cancers. Especially since MLH1 is a DNA mismatch repair enzyme and mutations occurring in this protein will lead to a loss of expression of this protein, hence, leading to a cancerous growth.

Transforming Growth Factor-Beta receptor II (TGFBR2) is a member of a particular protein kinase family and is associated with several different cancers including colon, gastric and various lung cancers. A paper by Ilyas and associates highlighted that mutations in TGFBR2 may lead to a level of cell adhesion which can lead to growth inhibition in colorectal cancers (Ilyas et al., 1999). There is also evidence pointing towards the influence of TGFBR2 in large cell carcinomas (LCC) (Xu et al., 2007) and giant cell carcinomas (GCC) (Wang et al., 2007).

The APC (adenomatous polyposis coli) is a human tumour suppressor gene and has been found to be mutated in several different cancers. The current research is limited but so far there is evidence pointing towards mutations in urothelial cancer (Kastritis et al., 2009), colon cancer (Chen et al., 2009; Markowitz and Bertagnolli, 2009) and germ cell tumours (Okpanyi et al.,

2011). There is also evidence pointing towards a rare malignancy known as parathyroid cancer (Svedlund et al., 2010) and even some suggestion that mutations in the APC occur in prostate cancer (Gerstein et al., 2002). Mutations in the APC is synonymous with the activation of the Wnt/β-catenin pathway in most, if not all of the cancers mentioned above.

There are many more proteins we could list, but it is out of the scope of this research. The brief summaries we have provided highlight current research that exists and what research possibly lies ahead. There are potential proteins that may not have been discovered and mutations in existing proteins that have not been identified in particular cancers.

2.3 Molecular Dynamics and Enzyme Kinetics

There are numerous interactions that occur in the cell cycle. In particular, the mammalian cell cycle houses many complex and intricate interactions between proteins, enzymes and the complexes that form between them and each other. In this section we will describe several enzyme kinetic models that can be used to describe these interactions. These kinetic principles are incorporated into the models we examine in Chapters 3 and 4. We also use these principles in developing a mathematical model for melanoma growth.

2.3.1 Michaelis-Menten

The Michaelis-Menten kinetics is a fundamental part of biochemistry that describes the reactions taking place when an enzyme reacts with an associated

substrate. This reaction forms a temporary complex before a product and free enzyme is finalised. Leonor Michaelis and Maud Menten worked on modelling this biochemical reaction in the early 1900's, their work was later revised by Haldane and Briggs, see (Briggs and Haldane, 1925). The kinetic equation that describes the Michaelis-Menten kinetics is,

$$E + S \underset{k_{-1}}{\overset{k_1}{\rightleftharpoons}} ES \xrightarrow{k_{cat}} E + P, \tag{2.1}$$

where E is the free enzyme, S is the substrate, ES is the complex formed between the substrate and free enzyme and P is the product that results. The rate constants k_1 and k_{-1} represent rates of association and dissociation respectively, while k_{cat} is defined as the turnover number (or catalytic rate constant) which measures the number of substrate molecules processed per enzyme molecule each second, (Alberts et al., 2008). Michaelis-Menten kinetics are considered an important part of biochemical processes due to the Michaelis constant that is derived from the kinetic equation (2.1). The Michaelis constant, K_m, is defined as,

$$K_m = \frac{k_{-1} + k_{cat}}{k_1}. \tag{2.2}$$

Using this constant we can then write the kinetic equation in a mathematical form as follows,

$$V = \frac{k_{cat} E_t S}{K_m + S}, \tag{2.3}$$

where K_m is the Michaelis constant described by (2.2), the constant term E_t is the total enzyme concentration and V is the reaction velocity, both at time t.

Some examples where Michaelis constants are calculated for particular enzymes are given in (Alberts et al., 2008) and (Rawn, 1989). The Michaelis constant is measured universally in terms of molar solution, that is 1 mole of substance per 1 litre of solution. It is important to state this definition as throughout this work we will often refer to the Michaelis constant in the papers that we review and in our own mathematical modelling.

2.3.2 Briggs-Haldane

Other important contributors to kinetic theory in biochemistry are Briggs and Haldane and their enzymetic equations (Briggs and Haldane, 1925).

$$A + E \underset{k_2}{\overset{k_1}{\rightleftharpoons}} AE \xrightarrow{k_3} B + E \tag{2.4}$$

$$\tag{2.5}$$

where,

$$A = a - x\,,$$

$$E = e - p\,.$$

The definition of variables is listed below,

A : is the concentration of the substrate at time t,

E : is the concentration of the enzyme at time t,

AE : complex forming A and E at time t,

B : is the concentration of product after time t,

a : is the initial concentration of A at time t,

x : is the concentration of B produced after time t,

e : is the total concentration of enzyme E at time t,

p : is the concentration of the enzyme combined with the substrate at time t.

The rate constants are k_1, k_2 and k_3 which can be referred to the reaction rate constant, the dissociation constant and the catalytic rate constant respectively (Rawn, 1989; Holum, 1998). The magnitude of the catalytic rate constant, k_3, is important to the reaction as the complex formed is then turned into a product and free enzyme, likewise the concentration of the complex is also a key element to this reaction.

2.3.3 Goldbeter and Koshland

Albert Goldbeter and Daniel Koshland's model for modified and unmodified protein interactions offers an alternative and perhaps more detailed version of the kinetics described by Michaelis and Menten. The notion of modified and unmodified proteins can be defined as a protein being reacted upon, modified, versus a protein not being reacted upon, unmodified. We will briefly describe

the equations that Goldbeter and Koshland use to describe the biochemical reaction for protein interaction.

Firstly, the kinetics for modified and unmodified protein, similar to that of the interaction described by Michaelis and Menten, is below:

$$W + E_1 \underset{d_1}{\overset{a_1}{\rightleftharpoons}} WE_1 \xrightarrow{k_1} W^* + E_1 \tag{2.6}$$

$$W^* + E_2 \underset{d_2}{\overset{a_2}{\rightleftharpoons}} W^*E_2 \xrightarrow{k_2} W + E_2, \tag{2.7}$$

where W^* is the concentration of modified protein, W is the concentration of unmodified protein, E_1 and E_2 are the concentrations of free enzyme for equation (2.6) and (2.7) respectively, WE_1 and W^*E_2 are the products formed. The constant terms a_1, a_2, d_1, d_2, k_1 and k_2 are the association, dissociation and catalytic rate constants (Goldbeter and Koshland, 1981). The equation which is of most concern to our research is as follows and describes the rate of change of unmodified protein with respect to time:

$$\frac{dW^*}{dt} = \frac{V_2}{W_T}\left[\frac{(V_1/V_2)(1-W^*)}{K_1+1-W^*} - \frac{W^*}{K_2+W^*}\right] \tag{2.8}$$

where, W^* is the modified protein W as mentioned above, V_1 and V_2 are velocity terms (for the interested reader please refer to reference (Goldbeter and Koshland, 1981) for further details on velocity terms), K_1 and K_2 are Michaelis type terms which are defined using Michaelis constants, see equations

(2.9) and (2.10) below:

$$K_1 = \frac{K_{m_1}}{W_T} \tag{2.9}$$

$$K_2 = \frac{K_{m_2}}{W_T}, \tag{2.10}$$

$$W_T = W + W^* + [WE_1] + [W^*E], \tag{2.11}$$

where W_T is defined as the conservation equation (2.11) for modified and unmodified protein, K_{m_1} and K_{m_2} are Michaelis constants. For the interested reader we refer to (Goldbeter and Koshland, 1981) for a full description of the modelling and derivation.

2.4 Conclusion

There are many proteins, cyclins, kinases and biological phenomena in general that all contribute to the growth of cancer. In this chapter we have outlined the cell division cycle of a mammalian cell with comparisons to the yeast division cycle. We have also distinguished the differences between a cancer and normal cell cycle.

We have given brief summaries for particular proteins that influence the growth of certain cancer types, with the main attention being focused on melanoma growth.

Enzyme kinetics, in particular the Michaelis-Menten kinetics, play an important role in this research. Modelling biological growth often is coupled with enzymetic phenomenon due to the close relationship between biology and

biochemistry especially since this research is analysing growth that involves biochemical reactions between certain proteins and enzymes in the cell cycle of a cancer cell.

Chapter 3

Cell Cycle Modelling

This chapter will review articles that describe mathematical models for the yeast and mammalian cell cycle. We also discuss mathematical models for the division cycle of a cancerous cell.

There are three sections to this chapter. Section 3.1 will discuss mathematical models that describe the yeast cell cycle, mainly models proposed by Tyson and Novak (Novak et al., 1998b; Tyson and Novak, 2001). Following from this there will be a review on a mammalian cell cycle model by Tyson and Novak (Novak and Tyson, 2004) in Section 3.2.

A detailed review on a cancer cell cycle model proposed by Alarcón et al. (Alarcón et al., 2004a) will by discussed in Section 3.3, this model being the main focus of our research.

3.1 Models based on the yeast cell cycle

To our knowledge there are very few mathematical models on melanoma cancer growth. We will review models based on both cancerous and normal cell cycle division as both have been a major influence in this work and, in particular, help us to develop a mathematical model for melanoma growth.

To understand the human or mammalian cell cycle we must firstly understand how the cell cycle operates in yeast as this cycle is much less complicated, hence making it easier to acquire data and develop simplistic models to further our understanding of the cell cycle. The mammalian cell cycle is a complex and intricate pattern of interactions and signals between proteins and molecules that aid cells in their division process, making it difficult to model precisely. The modelling of the yeast division cycle is a logical and simple starting point.

The main models under consideration are by Tyson and Novak, with joint work and collaborations, (Tyson et al., 1995; Novak et al., 1998a,b; Tyson and Novak, 2001; Novak and Tyson, 2004). Tyson and Novak are able to model very accurately the yeast cell division cycle and, in part of the modelling process, they utilised the Michaelis-Menten kinetics.

3.1.1 Basic Yeast Cell Cycle Model

In 1995 a model developed by Tyson and colleagues (Tyson et al., 1995) was built from a theoretical perspective and applied to the cell cycle in frog embryos, fission yeast and budding yeast cell cycles. The model was very simplistic and based around two checkpoints that had been previously discovered

for yeast. In (Tyson et al., 1995), the authors do mention a third checkpoint. However, this checkpoint is not modelled in their published paper that we discuss here and is not relevant to our research. The two mentioned checkpoints occurred during the G1 and G2 gap phases of the cell cycle and are hence referred to as the G1 and G2 checkpoints.

The system of equations for the G2 checkpoint are presented below,

$$\frac{dm}{dt} = k_3 x(c_1 + x - y) - m f_1(m) + f_2(m)(y - x - m) - k_5 m\,, \tag{3.1}$$

$$\frac{dx}{dt} = k_4 - x f_1(m) - k_3 x(c_1 + x - y)\,, \tag{3.2}$$

$$\frac{dy}{dt} = k_4 - y f_1(m)\,, \tag{3.3}$$

and

$$f_1 = k_1 + k_1' m^2\,,$$

$$f_2 = k_2 + k_2' m^2\,,$$

where,

$m(t)$: average concentration of active Maturation Promoting Factor (MPF) at time t,

$x(t)$: average concentration of cyclin B monomer at time t,

$y(t)$: total concentration of cyclin B at time t,

k_i : rate constants, for $i = 1, \ldots, 5$,

k_i' : rate constants relating to respective k_i's, for $i = 1, 2$,

c_1 : total concentration Cdc2 (constant),

f_1 : function describing the feedback activity of MPF on the rate of cyclin degradation,

f_2 : function describing the feedback activity of MPF on the rate of tyrosine dephosphorylation,

t : time in minutes.

All concentrations in the above model are assumed to be average concentrations.

The system of equations (3.1) to (3.3), although simplistic, shows the relationship between maturation promoting factor (MPF) and cyclin B. More specifically, the equations represent a biochemical network that describes the kinetic reaction occurring between cyclin monomers, in this case cyclin B, and Cdc2 monomers to form active MPF. It also shows how the activities of these two together influence the G2 checkpoint in the yeast cell cycle. The relationship between MPF and Cyclin B can be seen in Figure 3.1, taken from the paper published by Tyson et al (Tyson et al., 1995). Recall, that G2 is the second gap phase in the cell cycle, this is for both yeast and mammalian cell cycles. The G2 phase of the cell cycle occurs just before the onset of Mitosis or M phase. There is a check point during this gap phase that the cell must go through before proceeding onto M phase.

The system is being solved over the time horizon depicted in Figure 3.1. At time $t = 40$ minutes a so-called superthreshold is imposed on the system. This essentially means that an instantaneous adjustment is made to the active

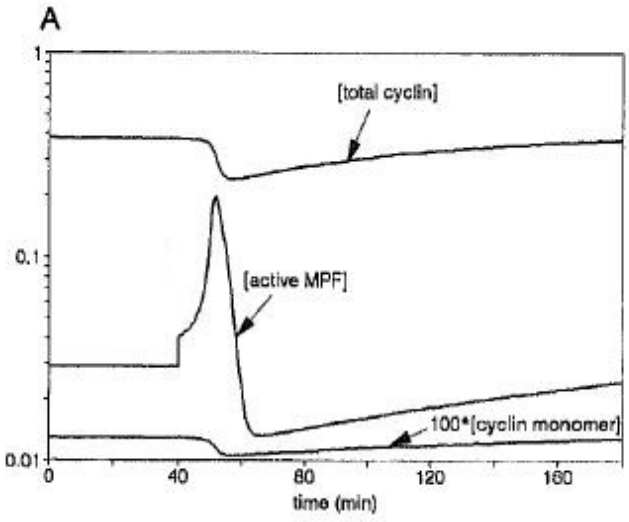

Figure 3.1: Figure from Tyson et al (Tyson et al., 1995) showing the relationship between cyclin B monomer, x, total cyclin, y, and active MPF, m, at the G2 check point. Time t is in minutes.

MPF. The system then continues along a different path. From a biological perspective, this is forcing the cell cycle to enter mitosis and reach the mitotic checkpoint so the cell can then divide. Equations (3.1) to (3.3), due to their simplicity, will not enter into mitosis without the imposition of this threshold value.

After solving the system of ordinary differential equations (3.1) to (3.3) for $m(t)$, $x(t)$ and $y(t)$ we can calculate the values for inactive MPF, $z(t)$, and concentration of Cdc2 monomer, c_2. In yeast MPF becomes inactive once active MPF is degraded by protein Wee1 and Cdc2 monomer exists when Cdc2 is synthesized. We can express $z(t)$ and c_2 as follows,

$$z(t) = y(t) - m(t) - x(t)\,,$$

$$c_2 = c_1 - m(t)z(t)\,.$$

Tyson and colleagues' go on to describe the G1 checkpoint in the yeast cell cycle. The system is presented below,

$$\frac{dz}{dt} = k_5' + wk_5 - zk_6\,, \tag{3.4}$$

$$\frac{dw}{dt} = \frac{k_7(a_1+z)(c_2-w)}{J_3+c_2-w} - \frac{k_8 a_2 w}{J_4+w}\,, \tag{3.5}$$

where,

$z(t)$: average concentration of cyclin-kinase at time t,

$w(t)$: average concentration of active transcription factor SBF at time t,

a_1 : constant term for the starter kinase,

a_2 : constant term for the amount of phosphatase,

c_2 : total of active SBF and inactive SBF added(constant),

k_i : rate constants, for $i = 5 \text{ to } 8$,

J_i : Michaelis constants which are determined experimentally, for $i = 3, 4$.

t : time in minutes.

The above system is the starting point for much of the work that Tyson and colleagues' publish relating to the modelling of the yeast cell cycle. We present

several of their extended models involving the G1 checkpoint. We also use Tyson and colleagues' modelling of the G1 checkpoint for the motivation behind our own cell cycle modelling presented in Chapter 5.

3.1.2 Extended Yeast like Model

Tyson and colleagues' advanced on their simple yeast like model by expanding it to incorporate steady states relating to the G1 and G2-S-M phases of the cell cycle, see (Novak et al., 1998b). The purpose of the model was to show the activity present between cyclins and their kinases and the active anaphase-promoting complex. The model is presented below,

$$\frac{d\,[\mathrm{CDK}]}{dt} = k_1 s - \left[k_2'(1-[\mathrm{APC}]) + k_2''\,[\mathrm{APC}]\,\right][\mathrm{CDK}] \tag{3.6}$$

$$\begin{aligned}\frac{[\mathrm{APC}]}{dt} &= \frac{(k_3' + k_3''\,[\mathrm{ACT}])(1-[\mathrm{APC}])}{J_3 + 1 - [\mathrm{APC}]} \\ &\quad - \frac{(k_4' + k_4''\,[\mathrm{CDK}])\,[\mathrm{APC}]}{J_4 + [\mathrm{APC}]}\,,\end{aligned} \tag{3.7}$$

where,

[CDK] : represents the concentration of cyclin-CDK dimers in the nucleus,

[APC] : represents the concentration of active [APC], which is a fraction of the total active [APC],

[ACT] : hypothetical activator of the [APC],

s : measure of the size of the cell such as the cell mass,

k_i : rate constants, for $i = 1, \ldots, 4$,

k_i' : rate constants relating to respective k_i's, for $i = 1, \ldots, 4$,

k_i'' : rate constants relating to k_i''s, for $i = 1, \ldots, 4$,

J_i : Michaelis constants, for $i = 3, 4$,

t : time in minutes.

Equations (3.6) and (3.7) are the foundations behind the models in cell cycle control that Tyson and Novak have developed, as can be seen throughout parts of this chapter.

We discuss in detail several extended models developed by Tyson and Novak below and in Section 3.2. The advantage to the modelling approach adopted by Tyson and Novak is that it links the protein complexes and their activation to either the G1 or G2-S-M phases of the cell cycle. The only disadvantage to this type of modelling is the one-dimensionality associated with the independent variable, here being time. The model could be expanded to include other independent variables such as size and weight or even age of a cell. However, this would drastically change the dynamics of the system. The model would then change from a set of ordinary differential equations to a set of partial differential equations. The simplicity of the model would also be lost due the addition of more dependent variables.

The model below describes the division of a cell influenced by particular proteins and their complexes and it is the next model in the Tyson-Novak series (Tyson and Novak, 2001). Even though this model is based on the division cycle of a budding yeast cell it still can give insights into how a mammalian cell

will grow and eventually divide over time. The system below represents the dynamics of the cell cycle for particular interactions occurring for a budding yeast cell cycle as described by Tyson and Novak (Tyson and Novak, 2001).

$$\frac{d\,[\text{Cdh1}]}{dt} = \frac{(k_3' + k_3'' A)(1 - [\text{Cdh1}])}{J_3 + 1 - [\text{Cdh1}]} - \frac{k_4 m\,[\text{Cdh1}]\,[\text{CycB}]}{J_4 + [\text{Cdh1}]}\,, \tag{3.8}$$

$$\frac{d\,[\text{CycB}]}{dt} = k_1 - (k_2' + k_2''\,[\text{Cdh1}])\,[\text{CycB}]\,, \tag{3.9}$$

$$\frac{dm}{dt} = \mu m\Big(1 - \frac{m}{m_*}\Big)\,. \tag{3.10}$$

The variables are defined as follows,

m : the mass of an adult cell,

[CycB] : average concentration of cyclinB/CDK dimers,

[Cdh1] : average concentration of active Cdh1/APC complexes,

A : generic activator (parameter),

k_i : rate constants for $i = 1, \ldots, 4$,

k_i' : rate constants relating to k_i's, for $i = 2, 3$,

k_i'' : rate constants relating to k_i', for $i = 2, 3$,

J_i : Michaelis constants, for $i = 3, 4$.

Equation (3.8) represents the activation and inactivation of a labelling protein, Cdh1. The APC is the anaphase-promoting complex which is a group of proteins that Cdh1 is a member of. Michaelis-Menten type modelling is used to describe the rates of activation and inactivation. Activation is modelled by

the first expression in equation (3.8) and the inactivation is modelled by the second expression in the same equation. The cyclin-dependent kinases (CDK) work with their cyclin partners to send out signals to responder molecules. The average concentration is measured as grams of protein per gram of total cell mass.

The authors have incorporated the use of work done by Goldbeter and Koshland (Goldbeter and Koshland, 1981), previously mentioned in Chapter 2, on protein complexes. The use of the Goldbeter-Koshland model ensures that the cyclins are still substrates but their complexes, which form with the corresponding Cdk's, are protein complexes. The basic principles behind the work done by Goldbeter and Koshland are the kinetics from Michaelis and Menten, or commonly referred to as Michaelis-Menten kinetics as detailed in Chapter 2.

The authors also define a function type which they label as the Goldbeter-Koshland function and which they use to calculate the nullclines for [Cdh1]. The nullcline is defined as the curve (in the [Cdh1], [CycB] plane) along which the first time derivative in each of [CycB] and [Cdh1] is equal to zero, respectively. The authors then interpret the steady-state solutions to be where the nullclines intersect for variables [Cdh1] and [CycB].

Synthesis and degradation of cyclin B are described by equation (3.9), where equation (3.10) represents the actual growth rate of the cell. The maximum mass of the cell is m_* and the rate constant to describe the rate of growth is μ. The authors also assume that cyclin B molecules rapidly combine with an excess of Cdk subunits. This allows them to disregard the interaction with

Cdk and only consider the complex forming with cyclin B.

For implementation purposes we also looked at the full system for the budding yeast cell cycle with the anaphase of mitosis being activated by protein Cdc20. The generic activator A in equation (3.8) can now be replaced by active Cdc20, denoted by $[\mathrm{Cdc20_A}]$.

$$\frac{d\,[\mathrm{Cdh1}]}{dt} = \frac{(k_3' + k_3''\,[\mathrm{Cdc20_A}])(1 - [\mathrm{Cdh1}])}{J_3 + 1 - [\mathrm{Cdh1}]} - \frac{k_4 m\,[\mathrm{Cdh1}]\,[\mathrm{CycB}]}{J_4 + [\mathrm{Cdh1}]}\,, \tag{3.11}$$

$$\frac{[\mathrm{CycB}]}{dt} = k_1 - (k_2' + k_2''\,[\mathrm{Cdh1}])\,[\mathrm{CycB}]\,, \tag{3.12}$$

$$\frac{dm}{dt} = \mu m\Big(1 - \frac{m}{m_*}\Big)\,, \tag{3.13}$$

$$\begin{aligned}\frac{d\,[\mathrm{Cdc20_A}]}{dt} = {} & \frac{k_7\,[\mathrm{IEP}]([\mathrm{Cdc20_T}] - [\mathrm{Cdc20_A}])}{J_7 + [\mathrm{Cdc20_T}] - [\mathrm{Cdc20_A}]} \\ & - \frac{k_8[\mathrm{MAD}]\,[\mathrm{Cdc20_A}]}{J_8 + [\mathrm{Cdc20_A}]} - k_6\,[\mathrm{Cdc20_A}]\end{aligned}\,, \tag{3.14}$$

$$\frac{d\,[\mathrm{Cdc20_T}]}{dt} = k_5' + \frac{k_5''([\mathrm{CycB}]\,m/J_5)^n}{1 + ([\mathrm{CycB}]\,m/J_5)^n} - k_6\,[\mathrm{Cdc20_T}]\,, \tag{3.15}$$

$$\frac{d\,[\mathrm{IEP}]}{dt} = k_9 m\,[\mathrm{CycB}](1 - [\mathrm{IEP}]) - k_{10}\,[\mathrm{IEP}]\ . \tag{3.16}$$

For the above system we define the following variables,

$[\mathrm{Cdc20_T}]$: total concentration of active and inactive protein Cdc20,

[MAD] : toggle that is set to 1 if chromosome alignment is completed "on time" or set to a large number if not,

[IEP] : concentration of active hypothetical intermediary enzyme.

The [MAD] variable represents, in biological terms, a family of spindle checkpoint genes that inactivate Cdc20 if DNA synthesis and chromosome alignment is not completed on time (Tyson and Novak, 2001). A Hill function is used to

describe the activation of the transcription factor by CycB/Cdk for synthesis of Cdc20. As the cell grows, CycB/Cdk complexes increase and, in turn, synthesis of Cdc20 is switched on. During mitosis the activity of Cdc20 becomes highly important as it is used to activate the Cdh1/APC complex and consequently destroys the target protein cyclinB so the cell can successfully exit the M phase.

We implemented the above model using the mathematical software package Maple, version 11.0, with the equations and parameters published by the authors. The plot in Figure 3.2 shows the replication of the Tyson-Novak model and is in good agreement with the published results. We used the inbuilt 'dsolve' command to solve the system of ordinary differential equations. Under the 'dsolve' command we implemented the 'numeric' parameter to find a numerical solution and applied the classical fourth order Runge-Kutta method. The 'dsolve' command will allow the user to choose a particular numerical method to solve a system of ordinary differential equations.

The Maple code we used to generate Figure 3.2 can be viewed in Appendix A. Figure 3.2 reflects the cyclic nature of proteins during the division cycle and also shows a distinct contrast in the APC/Cdh1 complex with the cyclin B and associated Cdk complex.

We also considered some changes to the model using the Briggs-Haldane and Michaelis-Menten kinetics, as we discuss below. The equation that was of particular interest to our research was equation (3.11). The inactivation term in this equation is in the form of Michaelis-Menten kinetics where this inactivation refers to the S-G2-M phase of the cell cycle.

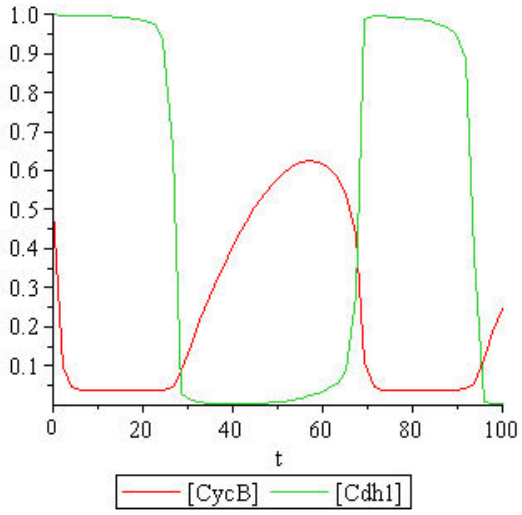

Figure 3.2: Tyson and Novak model for yeast cell cycle, where t is in minutes.

Table 3.1: Tyson and Novak vs Michaelis-Menten

Tyson and Novak	Michaelis-Menten
k_4	r
m[CycB]	b
J_4	$\frac{h}{k}$
$k_3' + k_3''$A	rb_1

We re-write equation (3.8) using Michaelis-Menten terminology and define the variables presented in Table 3.1.2. By doing this we can see how the Michaelis constant is derived, in a mathematical sense, and how any small changes may impact a mathematical modelling environment. During the S-G2-M phase of the cell cycle APC/Cdh1 activity is low, whereas cyclinB/CDK activity is high. Amongst the inactivitation of APC/Cdh1 Tyson and Novak are describing the total concentration of enzyme as being given by the product between the mass of the cell and concentration of cyclinB/CDK, hence there

is dependence on the mass of the cell.

We consider for manipulation equation (3.8) from the Tyson and Novak paper, (Tyson and Novak, 2001). We recall equation (3.8) for the convenience.

$$\frac{d\,[\text{Cdh1}]}{dt} = \frac{(k_3' + k_3'' A)(1 - [\text{Cdh1}])}{J_3 + 1 - [\text{Cdh1}]} - \frac{k_4 m\,[\text{Cdh1}]\,[\text{CycB}]}{J_4 + [\text{Cdh1}]}$$

The motivation for manipulating equation (3.8) is due to discovering through readings of biochemical literature (Alberts et al., 2008; Rawn, 1989; Nelson and Cox, 2005), that many biochemical processes follow the Briggs and Haldane kinetic model, not Michaelis and Menten. Briggs and Haldane, however, refined Michaelis and Menten's model by proposing that the complex formed during a reaction may not always be in equilibrium as Michaelis and Menten suggest. According to Laidler (Laidler, 1997), Briggs and Haldane propose that the complex forming is actually present in a steady state. Briggs and Haldane support their assumption with the use of a differential equation. Using the same terminology as in Chapter 2, Section 2.3.2, we write the differential equation as follows,

$$\frac{dx}{dt} = \frac{k_3 e(a - x)}{\frac{k_2 + k_3}{k_1} + a - x} \tag{3.17}$$

We now describe our manipulation of equation (3.8). We replace the Michaelis constant term in equation (3.8) with a term derived by Briggs and Haldane (Briggs and Haldane, 1925). We discuss both Michaelis-Menten and Briggs-Haldane kinetics in Chapter 2, however, we give a brief summary here with further discussion on the Briggs-Haldane kinetic modelling. Although, the ki-

netics for each are very similar it is interesting to see how small changes in constant terms impact on biological modelling, in particular, cell cycle modelling of yeast and mammals. Our analysis of this type of modelling follows.

In terms of Michaelis-Menten kinetics we would need to assign an enzyme, substrate and product and to also recognise the complexes being formed from the enzymetic reaction.

If we refer back to Chapter 2 where both Michaelis-Menten and Briggs-Haldane kinetic modelling were considered, we can recall the enzymetic equations representing substrate, enzyme and product. We present the equations below.

$$A + E \underset{k_2}{\overset{k_1}{\rightleftharpoons}} AE \xrightarrow{k_3} B + E \tag{3.18}$$

$$\tag{3.19}$$

where

A : is the concentration of the substrate at time t,

E : is the concentration of the enzyme at time t,

AE : complex forming A and E at time t,

B : is the concentration of product after time t,

k_1 : the reaction rate constant,

k_2 : the dissociation rate constant,

k_3 : the catalytic rate constant.

We will adopt a new nomenclature to represent the rate constants as well as new variable names to represent the substrate, enzyme and product from the Briggs-Haldane and Michaelis-Menten kinetics. The new variable assignment is listed below.

x : total concentration of enzyme, at time t,

y : average concentration of substrate, at time t,

z : average concentration of product, at time t,

h_a : the dissociation constant,

k_a : the reaction rate constant,

r_a : the catalytic rate constant.

We now display the set of rate equations that describe the kinetics with the new variable assignment. The new rate equations are displayed below.

$$\frac{dy}{dt} = \frac{-r_a z y}{\frac{h_a}{k_a} + y}, \tag{3.20}$$

$$\frac{dz}{dt} = \frac{r_a z y}{\frac{h_a}{k_a} + y}. \tag{3.21}$$

We consider two cases to highlight the significance of using differing constant terms with the Briggs-Haldane kinetics. At the end of our case study analysis we compare the two cases we present with Michaelis-Menten kinetics. The assumptions we make for equations (3.20) and (3.21) are that $r_a << h_a$ and that $k_a > 0$ for Case 1. We assume that $r_a >> h_a$ for Case 2 and as for Case 1 $k_a > 0$. The values we assign for Case 1 and 2 are listed in Table 3.1.2.

Table 3.2: Two cases for Briggs-Haldane kinetics in Tyson and Novak.

Constant Terms	Case 1	Case 2
h_a	100	0.1
r_a	35	35
k_a	2500	2.5

We can re-write equation (3.11) using the Briggs-Haldane kinetic principle. The equation will be much the same, however, constant variables J_3 and J_4 representing a Michaelis type constant, will be re-written in terms of Briggs-Haldane kinetics. The equation representing this follows,

$$\frac{d\,[\text{Cdh1}]}{dt} = \frac{k_4 b_1\,[\text{Cdh1}]_S}{\frac{h_a+k_4}{k_a} + [\text{Cdh1}]_S} - \frac{k_4 b_2\,[\text{Cdh1}]_S}{\frac{h_a+k_4}{k_a} + [\text{Cdh1}]_S}\,, \tag{3.22}$$

where,

$[\text{Cdh1}]_S$: substrate concentration of Cdh1 at time t,

b_1 : total concentration of enzyme at activation, time t,

b_2 : total concentration of enzyme at inactivation, time t.

The remaining variables have previously been defined above.

We can see from Figures 3.3 and 3.4 that small changes to equation (3.22), in terms of kinetics, can change the results significantly. This is an important outcome as it shows how sensitive biological modelling can be and how we need to consider this when using kinetics for mathematical modelling. Both the results plotted in Figures 3.3 and 3.4 are realistic in terms of modelling a division cycle in the life of a budding yeast cell. However, the result for case 2

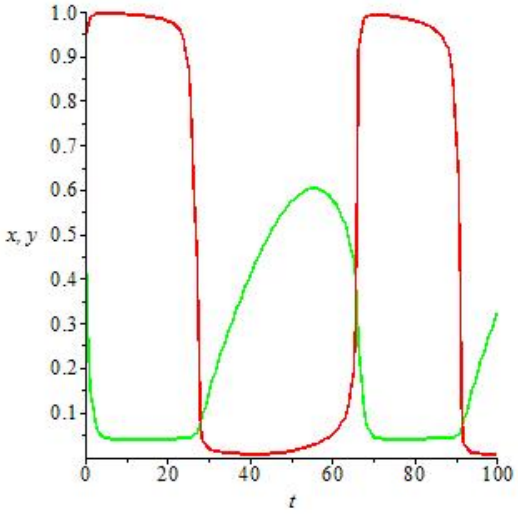

Figure 3.3: Case 1 for Tyson and Novak model in terms of Briggs-Haldane. The red line represents variable x, the green line represents variable y and time, t, is in minutes.

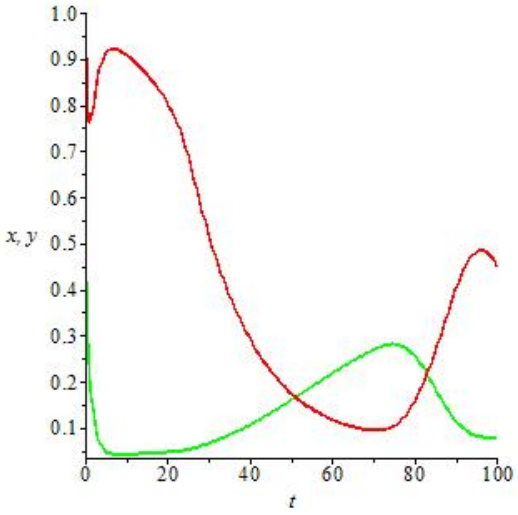

Figure 3.4: Case 2 for Tyson and Novak model in terms of Briggs-Haldane. The red line represents variable x, the green line represents variable y and time, t, is in minutes.

suggests that the cycle is incomplete or starts again with a half concentration in variable x, representing the concentration of [Cdh1].

In comparison with the Michaelis-Menten kinetics, the h_a/k_a term of the Briggs-Haldane model in equations (3.20) and (3.21) is described by a single constant value in the Michaelis-Menten model. Applying Cases 1 and 2 to the Michaelis-Menten model would consequently be redundant and the same result would be reached. This is a significant result in relation to the kinetic type modelling that has been applied to cell cycle models in this thesis.

In the literature reviewed it has been stated that the APC/C is an enzyme that targets particular proteins for destruction through its binding with proteins that are part of a particular complex, mainly with Cdh1 and Cdc20. A substrate of the APC/Cdh1 complex is cyclin B (Brown et al., 2007). Buschhorn and Peters also state that cyclin A is a substrate of the APC/Cdc20 complex (Buschhorn and Peters, 2006).

Tyson and Novak, in modelling the yeast cell cycle, also make use of a model developed by Goldbeter and Koshland (Goldbeter and Koshland, 1981). As previously described in Chapter 2, Goldbeter and Koshland use Michaelis-Menten type kinetics to describe a covalent reaction between modified and unmodified proteins. Tyson and Novak have used the Goldbeter and Koshland formulation to describe the reaction taking place in equation (3.8), the activation and inactivation of Cdh1. We give a detailed interpretation of how the Goldbeter and Koshland model is used. Below is the Goldbeter and Koshland equation that is under consideration and which was also presented

in Chapter 2.

$$\frac{dW^*}{dt} = \frac{V_2}{W_T}\left[\frac{(V_1/V_2)(1-W^*)}{K_1+1-W^*} - \frac{W^*}{K_2+W^*}\right].$$

Simplifying we have,

$$\frac{dW^*}{dt} = \frac{V_1(1-W^*)}{(K_1+1-W^*)W_T} - \frac{V_2W^*}{(K_2+W^*)W_T}, \tag{3.23}$$

where W_T is defined as being the total concentration of Cdh1. The authors assign a value of 1 for the total concentration of Cdh1. Hence, we substituting $W_T = 1$ into equation, (3.23), and we end up with the following,

$$\frac{dW^*}{dt} = \frac{V_1(1-W^*)}{K_1+1-W^*} - \frac{V_2W^*}{K_2+W^*}. \tag{3.24}$$

We interpret the unmodified protein, W, as Cdh1 and the modified protein, W^*, as the complexes formed with the APC/C, [Cdh1]. From Goldbeter and Koshland, we have $V_1 = k_1E_{1T}$ and $V_2 = k_2E_{2T}$, where k_1 and k_2 are catalytic rate constants for the product of modified and unmodified protein, respectively. E_{1T} and E_{2T} are the total concentrations of enzymes E_1 and E_2 respectively. Hence,

$$\frac{dW^*}{dt} = \frac{k_1E_{1T}(1-W^*)}{K_1+1-W^*} - \frac{k_2E_{2T}W^*}{K_2+W^*},$$

where

$$K_1 = \frac{d_1+k_1}{a_1W_T}, \quad K_2 = \frac{d_2+k_2}{a_2W_T}.$$

Due to $W_T = 1$, K_1 and K_2 are reduced to Michaelis constants. Using the Tyson and Novak notation, the Michaelis constants are J_3 and J_4.

In Chapter 5 we propose a model for melanoma growth which relies heavily on the kinetics we have discussed throughout Chapters 2 and 3. Our analysis here shows the versatility of kinetic modelling and how small changes can influence results, such as those seen in Figures 3.3 and 3.4. We consequently consider these results and how kinetics impact on biological modelling when building our own model for melanoma growth.

3.2 Mammalian Cell Cycle

Here we consider a model that describes the mammalian cell cycle for normal cell division. As well as producing yeast cell cycle models, Tyson and Novak produced a model for the mammalian cell cycle for non-cancerous cells (Novak and Tyson, 2004). The model incorporates comparisons to previous yeast cell cycle models and the use of a drug treatment, cycloheximide, as well as modelling its effects on the cell cycle and the time frame within which it needs to be administered.

Cycloheximide is an inhibitor of protein synthesis of eukaryotes at the beginning stages of the synthesis phase of the cell cycle (Paoletti et al., 2010). Cycloheximide is a drug that has commonly been used in experiments to detect at what point will cells stop dividing, once in a proliferating state.

The model revolves around the restriction point (R point) mentioned in earlier sections and chapters, where the cell must go through checkpoints before it can continue in the division process. There was some experimental

data published by Zetterberg and Larsson (Zetterberg and Larsson, 1995) to substantiate the model proposed in their paper, particularly in terms of the effects of the drug cycloheximide.

The restriction point mechanism of the model was based on comparisons with the biochemical circuitry network by Kohn (Kohn, 1999). Kohn's model is of a complex circuitry similar to that of an electrical circuit or an electrical network with switches and gates. They present several justifications for adopting a Kohn like model to represent what is essentially the cell cycle engine. They also incorporate early and delayed-response genes into the model to show the interactions that occur between the growth factors (GFs) and receptors that stimulate intracellular signal-transduction pathways (Novak and Tyson, 2004).

The retinoblastoma protein is an essential part of any cancer growth model. In particular, it is used to indicate the hypo and hyper-phosphorylation states of retinoblastoma protein and the interactions that may occur with other proteins in both an active or inactive state.

The model that describes the mammalian cell cycle consists of 18 ordinary differential equations and 4 steady-state relations. However, we only consider 4 of the 18 differential equations which are the most relevant to our research. To aid our later work in developing a model for melanoma growth, there are only certain aspects of the system that we are interested in analysing. The equations of most interest are those describing the activity of cyclin D and its forming of complexes with inhibitory protein Kip1. Another protein that we consider to be influential towards future work is a group of genes that codifies

a family of transcription factors, the E2F group. The equations are detailed below,

$$\frac{d\,[\text{CycD}]}{dt} = \varepsilon k_9\,[\text{DRG}] + V_6\,[\text{CycD: Kip1}] + k_{24r}\,[\text{CycD: Kip1}] - k_{24}\,[\text{CycD}]\,[\text{Kip1}] - k_{10}\,[\text{CycD}]\,, \tag{3.25}$$

$$\frac{d\,[\text{CycD: Kip1}]}{dt} = k_{24}\,[\text{CycD}]\,[\text{Kip1}] - k_{24r}\,[\text{CycD: Kip1}] - V_6\,[\text{CycD: Kip1}] - k_{10}\,[\text{CycD: Kip1}]\,, \tag{3.26}$$

$$\begin{aligned}\frac{d\,[\text{Kip1}]}{dt} = \varepsilon k_5 &- V_6\,[\text{Kip1}] - k_{24}\,[\text{CycD}]\,[\text{Kip1}] + k_{24r}\,[\text{CycD: Kip1}] \\ &+ k_{10}\,[\text{CycD: Kip1}] - k_{25}\,[\text{Kip1}]([\text{CycE}] + [\text{CycA}]) \\ &+ k_{25r}([\text{CycE: Kip1}] + [\text{CycA: Kip1}]) \\ &+ V_8\,[\text{CycE: Kip1}] + k_{30}\,[\text{Cdc20}]\,[\text{CycA: Kip1}]\,,\end{aligned} \tag{3.27}$$

$$\frac{d\,[\text{E2F}]}{dt} = k_{22}([\text{E2F}_\text{T}] - [\text{E2F}]) - (k'_{23} + k_{23}([\text{CycA}] + [\text{CycB}]))\,[\text{E2F}]\,, \tag{3.28}$$

where,

$$V_6 = k'_6 + k_6(\eta_E\,[\text{CycE}] + \eta_A\,[\text{CycA}] + \eta_B\,[\text{CycB}])\,, \tag{3.29}$$

$$V_8 = k'_8 \frac{k_8(\psi_E([\text{CycE}] + [\text{CycA}]) + \psi_B)}{J_8 + [\text{CycE}_\text{T}]} \tag{3.30}$$

and where the k_{ij}'s are rate constants, ε is a constant that toggles between 0 and 1, and η_A,η_B and η_E are dimensionless constant terms. The variables are detailed below,

[CycD] : concentration of cyclinD/Cdk complex,

[CycD: Kip1] : concentration of cyclinD/Cdk complexed with Kip1,

[Kip1] : concentration of protein Kip1,

[DRG] : concentration of delayed response gene products,

[CycE] : concentration of cyclinE/Cdk complex,

[CycA] : concentration of cyclinA/Cdk complex,

[CycE: Kip1] : concentration of cyclinE/Cdk complexed with Kip1,

[Cdc20] : concentration of protein Cdc20,

[CycA: Kip1] : concentration of cyclinA/Cdk complexed with Kip1,

[CycB] : concentration of cyclinB/Cdk complex,

[E2F] : total concentration of unphosphorylated [E2F],

[$E2F_T$] : concentration of all forms of [E2F] and has a constant value equal to 5.

Our work is mainly concerned with the choice of values for the model parameters and in the work presented above it is stated that some of these values were taken from experiments on yeast and frog egg models. However, there were some parameter values that were stated as being estimated using appropriate simulation modelling and by comparisons with experimental data published by Zetterberg and Larsson (Zetterberg and Larsson, 1995).

The authors explain the way in which they choose to name their independent variables according to the type of protein and the interactions that

particular proteins may encounter during the first phase of the cell cycle. For instance, [CycD] represents the concentration of the complex formed between cyclin D and its cyclin-dependent kinase Cdk4. The authors have also considered phosphorylation for E2F (transcription factor) and the retinoblastoma protein. For the retinoblastoma protein they have considered two forms of phosphorylation, one that is in an active state known as hypophosphorylation [Rb_{hypo}] and the other as an inactive state. The inactive state is given by [Rb_T]-[Rb_{hypo}], where [Rb_T] is the total concentration of Retinablastoma protein. Hyperphosphorylation is considered to be in equilibrium with the hypophosphorylation state which allows for neither a weak or elevated state of phosphorylation of Rb with other proteins.

3.3 A Model for Cancer Growth

An extended model of the Tyson and Novak system was developed by Alarcón et al (Alarcón et al., 2004a). This incorporates the division cycle for cancerous cells under hypoxic conditions. The extensions imply the interaction of the protein p27 with a generic cyclin-dependent kinase and its direct impact on the inhibition of this kinase. The authors show results for both normal and cancer cell division times for a generic cell. There is no indication as to whether the cell is a mammalian or yeast cell, so the assumption made for the purposes of our research is that a yeast cell cycle is being modelled, since the Tyson and Novak model was also based on a yeast cell cycle due to the "Start" and "Finish" stages described in the cell cycle. The Tyson and Novak model started with a eukaryote cell cycle but extended this to a yeast cell cycle. Alarcón et

al (Alarcón et al., 2004a) started with the initial model based on the eukaryotic cell cycle by Tyson and Novak (Tyson and Novak, 2001).

The cancer cell cycle is of particular interest to us and there are particular extensions that Alarcón et al applied to the Tyson-Novak model relating to a generic cancer cell cycle. The model by Alarcón et al is presented below,

$$\frac{dx}{d\tau} = \frac{(1+b_3u)(1-x)}{J_3+1-x} - \frac{b_4mxy}{J_4+x}, \tag{3.31}$$

$$\frac{dy}{d\tau} = a_4 - (a_1 + a_2x + a_3z)y, \tag{3.32}$$

$$\frac{dm}{d\tau} = \eta m\Big(1 - \frac{m}{m_*}\Big), \tag{3.33}$$

$$\frac{dz}{d\tau} = c_1 - c_2\frac{P}{B+P}z, \tag{3.34}$$

$$\frac{du}{d\tau} = d_1 - (d_2 + d_1y)u, \tag{3.35}$$

where,

x : average concentration of APC/Cdh1 complexes,

y : average concentration of generic Cyc/Cdk complexes,

m : mass of a cell as in the Tyson-Novak model,

z : average concentration of protein p27,

u : average concentration of non-phosphorylated pRb,

J_i : Michaelis constants for $i = 3, 4$,

B : constant term,

η : growth rate constant associated with cell mass,

P : oxygen tension,

m_* : maximum mass of a cell.

The rate constants in the above system are represented by a_1 to a_4, b_3, b_4, c_1, c_2, d_1 and d_2. The rate constants a_1, a_2, a_4, b_3, b_4, η, m_*, J_3 and J_4 are taken from Tyson and Novak (Tyson and Novak, 2001). The remaining rate constants a_3, c_1, c_2, B, d_1 and d_2 are estimations from literature by Deutsch and Dormann (Dormann and Deutsch, 2002).

The inhibition of CDK is shown through the inclusion of the variable y in equation (3.32), it also reveals the interaction occurring between protein p27 and the generic CDK activity. It is assumed in the model that the CDK is not specific to any cyclin and that the complex formed between the CDK and it's cyclin partner is also generic. The generic parameter from equation (3.11) is replaced with non-phosphorylating retinoblastoma (pRb), u.

According to the Alarcón et al the protein p27 is shown to be up-regulated under hypoxic conditions. Hence, P, the oxygen tension, is associated with the rate equation for p27, as experimental data referenced in the article has shown (Gardner et al., 2001). The value of the constant P can be chosen by the user in computer run simulations to show the effect of a change in oxygen tension.

Alarcón et al published a later paper (Alarcón et al., 2005), where equations (3.31) to (3.35) are presented with the addition of an algebraic equation for phosphorylated Rb. The basis of the dynamics is still essentially the same here as in the paper published in 2004 (Alarcón et al., 2004a). However, the model has a significant extension in now being a multiscale model. The model

considers differing time and length scales and looks at each layer of growth simultaneously. They achieve this through a system of ordinary differential equations with the addition of a site variable, $\mathbf{r}$. The variable $\mathbf{r}$ accounts for the location of a cell and the type of cell at that location, a cancer cell or a normal cell. The model is, consequently, successful at accounting for the competition between normal and cancer cells. This is done by analysing neighbouring cells and assigning appropriate parameter values.

The system of equations describing the G1/S transition phase of the cell cycle from (Alarcón et al., 2005) are given below,

$$\frac{dx(\boldsymbol{r})}{dt} = \frac{(k_3' + k_3'' u(\boldsymbol{r}))(1 - x(\boldsymbol{r}))}{J_3 + 1 - x(\boldsymbol{r})} - \frac{k_4 m(\boldsymbol{r}) y(\boldsymbol{r}) x(\boldsymbol{r})}{J_4 + x(\boldsymbol{r})} \tag{3.36}$$

$$\frac{dy(\boldsymbol{r})}{dt} = k_1 - (k_2' + k_2'' x(\boldsymbol{r}) + k_2''' z(\boldsymbol{r})) y(\boldsymbol{r}) \tag{3.37}$$

$$\frac{dm(\boldsymbol{r})}{dt} = \mu\Big(\frac{y(\boldsymbol{r})}{y(\boldsymbol{r}) + y_0}\Big) m(\boldsymbol{r}) \Big(1 - \frac{m(\boldsymbol{r})}{m_*}\Big) \tag{3.38}$$

$$\frac{dz(\boldsymbol{r})}{dt} = \chi\Big(m, \boldsymbol{r}\Big) - k_5' \frac{P(\boldsymbol{r})}{B + P(\boldsymbol{r})} z(\boldsymbol{r}) \tag{3.39}$$

$$\frac{du(\boldsymbol{r})}{dt} = k_6' - (k_6' + k_6 y(\boldsymbol{r})) u(\boldsymbol{r}) \tag{3.40}$$

$$v = 1 - u, \tag{3.41}$$

where,

x : average concentration of APC/Cdh1 complexes,

y : average concentration of generic Cyc/Cdk complexes,

m : mass of a cell as in the Tyson-Novak model,

z : average concentration of protein p27,

u : average concentration of non-phosphorylated pRb,

v : average concentration of phosphorylated pRb,

y_0 : initial concentration of variable y,

J_i : Michaelis constants for $i = 3, 4$,

B : constant term,

η : growth rate constant associated with cell mass,

m_* : maximum mass of a cell,

P : oxygen tension.

k_i : rate constants, for $i = 1$ to 6,

k_i' : rate constants relating to respective k_i's, for $i = 2$ to 6,

k_i'' : rate constants relating to respective k_i''s, for $i = 2$ and 3,

k_i''' : rate constant relating to respective k_i'', for $i = 2$.

The function $\chi\Big(x, \boldsymbol{r}\Big)$ is defined below,

$$\begin{cases} k_5 & \text{if } s_1(\boldsymbol{r}) = 1\,, \\ k_5\Big(1 - \frac{m_{\boldsymbol{r}}}{m_*}\Big) & \text{if } s_1(\boldsymbol{r}) = 2\,, \\ 0 & \text{otherwise.} \end{cases}$$

If $s_1(\boldsymbol{r}) = 1$ then there is a cancer cell located at $\boldsymbol{r}$. Similarly, if $s_1(\boldsymbol{r}) = 2$ then there is a normal cell located at $\boldsymbol{r}$. Including the location variable $\boldsymbol{r}$ gives the model the unique feature of being multiscale. This also allows for

the competition between cancer and normal cells to be modelled with differing time and length scales.

The initial conditions for the above system are as follows,

$$x_0 = 0.9, \quad y_0 = 0.001, \quad m_0 = 5, \quad z_0 = 0, \quad u_0 = 0\,.$$

There were also slight changes in a few of the other parameter values but this could be accounted for by the use of new experimental data or simply represent incremental improvements in the model itself.

In the model by Alarcón et al (Alarcón et al., 2004a) non-phosphorylated Rb is described as having an association with the APC/Cdh1 complex during the G_1 phase of the cell cycle. To our understanding, this does not agree with the actual biological process in a cell cycle. Rb is actually hypo-phosphorylated during this phase of the cell cycle and is only dephosphorylated at the transition point from the M phase to the G_1 phase. As cells pass through the R point, Rb becomes hyper-phosphorylated and remains this way until entering mitosis. In the original model developed by Tyson and Novak (Tyson and Novak, 2001) the equation describing the activity of the APC/Cdh1 complex housed a generic activator which was later replaced by a protein found in yeast, Cdc20. The replacement here with non-phosphorylated Rb does not make much biological sense, but since the model is generic and is not based on a particular type of cancer it is difficult to see how the protein from the Tyson and Novak model could be replaced.

There is also no account of hypo- or hyper-phosphorylated Rb in the model by Alarcón et al (Alarcón et al., 2004a). Tyson and Novak in a later

article (Novak and Tyson, 2004), discussed in Section 3.2, describe a model for the mammalian cell cycle and account for the hypo-phosphorylation of Rb. From a biological perspective, Weinberg in his book (Weinberg, 2007) explicitly describes the different phosphorylation states of Rb and how this can influence the cell cycle and, in particular, cancer growth. From a mathematical perspective, if there is no account for the different phosphorylation states of Rb then the mathematical model would not be accurately reflecting the growth of the cell cycle. This could consequently also affect any later extensions to the model. Extensions may include treatment scheduling and the addition of new biological research such as new protein mutations involved with cancer growth.

We attempted to replicate the results published by Alarcón et al (Alarcón et al., 2004a) with some difficulty. This is primarily due to incorrectly published parameter values and a misinterpretation of the variable, u, representing non-phosphorylated Rb. Several attempts were made in contacting the authors regarding the issues mentioned and to seek clarification, however, only limited information was given. We give a full discussion of this in Chapter 4.

3.4 Conclusion

In this chapter we have presented an analytical view on the mathematical research into cell cycle modelling. Specifically, we analyse and give background into both yeast and mammalian cell cycle modelling. We highlight several features pertaining to this type of modelling. In particular, the kinetics involved in cell cycle modelling and how interactions between proteins are described

using mathematics. We also apply the kinetic modelling of Briggs and Haldane (Briggs and Haldane, 1925) to the yeast cell cycle model published by Tyson and Novak in 2001 (Tyson and Novak, 2001).

We also review two mathematical models for a cancerous cell cycle. Both models are published by the same group of authors, Alarcón et al (Alarcón et al., 2004a, 2005). The cancer cell cycle models are based on the work published by Tyson and Novak (Tyson and Novak, 2001). We note the differences between the yeast cell cycle model and the cancer cell cycle model from both a mathematical and a biological point of view.

Chapter 4

Model for Parameter Selection

Optimal parameter selection is a method in dynamic optimisation that allows particular parameters in a dynamic system to be chosen in order to optimise a given objective. We detailed the background into Optimal Parameter Selection methodology and its formulation in terms of several different objective functions previously in Chapter 1. In this chapter we apply Optimal Parameter Selection techniques to two models relating to cell cycle growth. One model describes cancer cell growth and the other represents the growth of a non-cancerous cell cycle. We optimise parameters for both the non-cancerous and cancer cell models and solve the optimal parameter selection problem using the software package MISER3.3 (Jennings et al., 2004). Our results for both cancer and non-cancerous models are then discussed. Much of the optimal parameter selection methodology is based on the book by Teo, Goh and Wong (Teo et al., 1991).

4.1 Mathematical Model for Cancer Cells

Previously in Chapter 3 we discussed a model developed by Alarcón and associates (Alarcón et al., 2004a), which is an extension of a model developed by Tyson and Novak (Tyson and Novak, 2001). Here we describe the results of our attempts to implement the model and suggest improvements to refine the model.

As mentioned in Chapter 3, the model describes the influence that protein p27 has on cancer growth, in particular, its role in aiding cancer cells in avoiding the effects of hypoxia (oxygen starvation). We attempt to duplicate the results published by Alarcón et al (Alarcón et al., 2004a) as it is simplistic in nature and they are among the first to mathematically model a cancerous cell cycle that incorporates the activities occurring inside a cancer cell. The model is also widely cited and it would be an appropriate choice to base our own mathematical model for melanoma on. The dynamics of the model are presented below,

$$\frac{dx}{d\tau} = \frac{(1+b_3u)(1-x)}{J_3+1-x} - \frac{b_4mxy}{J_4+x}, \tag{4.1}$$

$$\frac{dy}{d\tau} = a_4 - (a_1 + a_2x + a_3z)y, \tag{4.2}$$

$$\frac{dm}{d\tau} = \eta m\Big(1 - \frac{m}{m_*}\Big), \tag{4.3}$$

$$\frac{dz}{d\tau} = c_1 - c_2\frac{P}{B+P}z, \tag{4.4}$$

$$\frac{du}{d\tau} = d_1 - (d_2 + d_1y)u, \tag{4.5}$$

The associated initial conditions are as follows,

$$x(0) = 0.9,\ y(0) = 0.01,\ m(0) = 5.0,\ z(0) = 0,\ u(0) = 1.0 \qquad (4.6)$$

The variables and parameters are described in the previous chapter, however, we shall recall them here.

x : average concentration of APC/Cdh1 complexes,

m : maximum mass of a cell,

z : average concentration of the protein p27,

y : average concentration of complex formed from Cdk/Cyc complexes,

u : average concentration of non-phosphorylating retinoblastoma protein (Rb).

The rate constants are described by parameters a_1, a_2, a_3, a_4, b_3, b_4, c_1, c_2, d_1 and d_2, η is the growth rate of the mass of a cell, constants J_3 and J_4 are the respective Michaelis constants determined by a biological experimental process, and B is a rate constant relating to the oxygen tension, P. The parameter P has varying values and the results published by the authors correspond to 1.0, 0.1, and 0.001 to show the differences in the effects of hypoxia on normal and on cancer cells. We will use the authors' values of P in our numerical simulations. The variable τ is dimensionless time and is equal to $\tau = k_2'' t$ with $k_2'' = 1\,\mathrm{min}^{-1}$ as detailed in both Tyson and Novak (Tyson and Novak, 2001) and Alarcón and co-workers (Alarcón et al., 2004a).

Table 4.1: Table of parameter values by Alarcón et al.

Parameter	Published Alarcón	Revised Alarcón
a_1	0.4	0.04
a_2	1.0	1.0
a_3	0.25	0.25
a_4	0.04	0.04
b_3	10.0	10.0
b_4	35.0	3.5
η	0.01	0.01
J_3, J_4	0.04	0.04
c_1	0.007	0.007
c_2	0.01	0.01
B	0.01	0.01
d_1	0.01	0.01
d_2	0.1	0.1

Using the parameter values published by Alarcón et al (Alarcón et al., 2004a), we first endeavoured to replicate their results. This proved to be a difficult task and ultimately could not be achieved. We used MISER3.3 in an attempt to solve the system of equations. The software, after switching to stiff mode several times, would return a fail to integrate message, rendering the system unsolvable by this software. We also used a Runge-Kutta fourth order subroutine in an attempt to solve the system. Unfortunately, the system once again was not solvable. Parameters a_1 and b_4 were published incorrectly and we were able to obtain correct parameter values through correspondence with the authors (see Table 4.1). The "Published Alarcón" values in Table (4.1) are those that were published in the article (Alarcón et al., 2004a), whereas the "Revised Alarcón" values are those that were sent to us upon corresponding with the authors.

We then attempted to replicate the model by Alarcón et al (Alarcón et al., 2004a) using the revised parameter values from Table 4.1. We were able

to solve the system of equations 4.1 to 4.5 with the revised parameter values, however, the results we obtained differ significantly from those published by Alarcón et al.

We display the results we obtained from implementing the Alarcdón model in Figure 4.1. We used a Fortran90 program to implement the model which we compiled with a Sun Studio Fortran90 compiler from the Fortran tool suite for Oracle Solaris and Linux operating systems. A fourth order Runge-Kutta method was used for integrating the system where fixed step sizes were assumed. This method is known for its simplicity and high degree of accuracy. Computationally it is a straight forward explicit algorithm and is easily implemented. The simulations were run on a Sun Netra Carrier-Grade machine with a 64-bit processor by Oracle Solaris Studio and with a Linux operating system. We also used the same scheme to solve the system of equations (4.1) to (4.5) on a SGI (Silicon Graphics International) Altix 3700 Bx2 called Cognac, which houses 192 x 1.5 GHz Itanium2 CPU's. The results from running numerical simulations of the Alarcón model are presented in Figures 4.1 and 4.2. We use the same Fortran90 code and step size with the same fourth order Runge-Kutta scheme on the SGI machine. The results of running this are plotted in Figure 4.2. We run the simulation for one complete division cycle as can be seen in Figure 4.2.

The reason for running simulations on two different machines, with the same computational algorithm, was that the algorithm produced a significantly different result on the two machines. This raised our suspicions as there have been many difficulties in reproducing the results from the Alarcón paper (Alar-

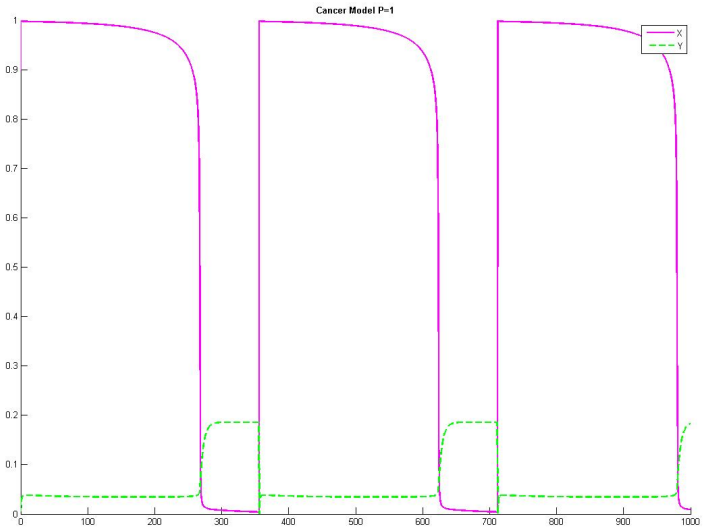

(a) Oxygen Tension, $P = 1.0$

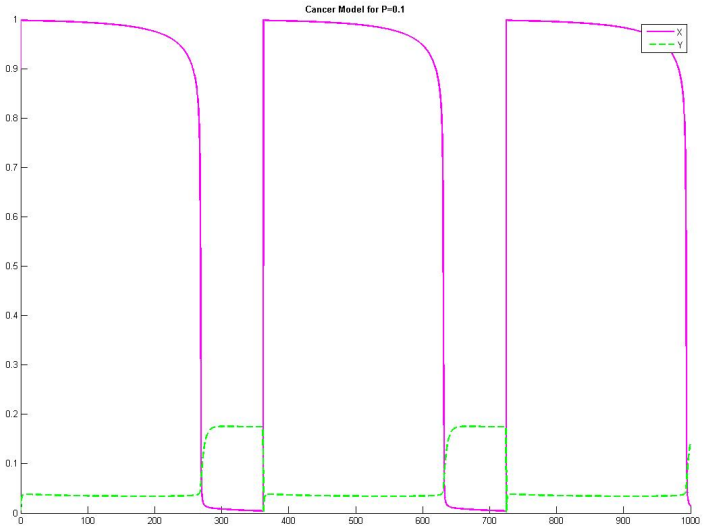

(b) Oxygen Tension, $P = 0.1$

Figure 4.1: The figures in (a) and (b) represent results for the oxygen tension $P = 1.0$ and $P = 0.1$, respectively.

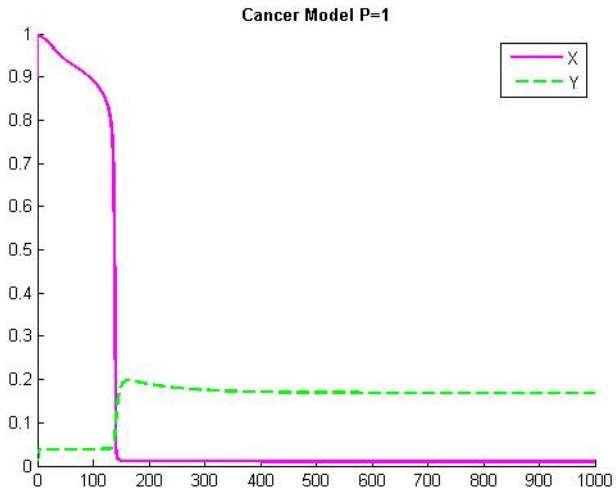

Figure 4.2: Plot produced by running equations (4.1) to (4.5) for variable representing APC/Cdh1 (x) and Cdk/Cyc (y) concentrations on a SGI machine.

cón et al., 2004a). The figure published by Alarcón et al, Figure 4.3, is plotted over a much longer time horizon than the figure we display for the same system of equations. Alarcón et al have a time horizon from 0 to 6000. In this time horizon almost 4 complete division cycles occur. In Figure 4.1(a) of our results, the time horizon is from 0 to 1000 and 3 complete division cycles occur in this time frame.

There are also some slight differences in the shape of each of the curves. Figure 4.3 descends more rapidly for variable x than the plot we produce for the corresponding variable. There is also a distinct difference toward the end of each cycle for variable y. Figure 4.1(a) of our results for variable y, is more elevated, closer to 0.2 units, than that of Figure 4.3. The most likely reasons for these differences include incorrectly published parameter values(beyond those clarified through correspondence), sensitivity of the model with respect

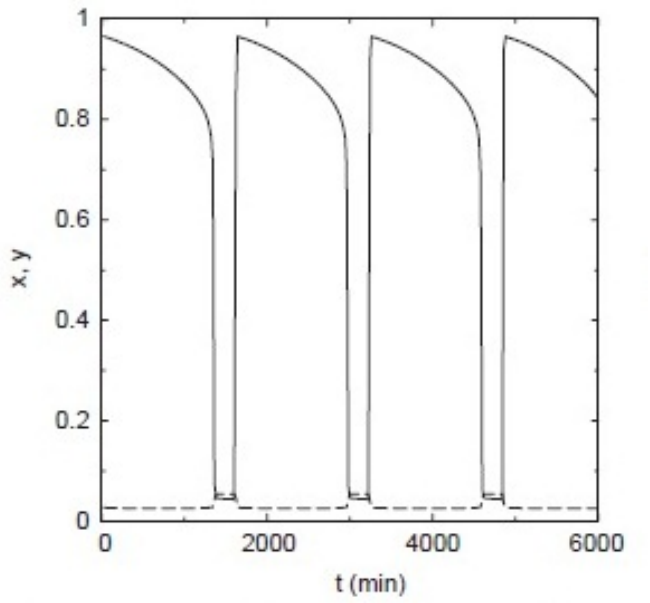

Figure 4.3: Figure 5(a) from Alarcón et al (Alarcón et al., 2004a) displaying results for a cancer cell cycle with $P = 1$.

to machine accuracy and a biological misinterpretation. We will elaborate on each of these possibilities later in this chapter.

Due to the variability in the results we obtained for the Alarcón model we aim to use optimal parameter selection techniques in an effort to establish correct parameter values and replicate the model Alarcón et al (Alarcón et al., 2004a) more precisely. As already shown in Chapter 3, we are able to reproduce the model by Tyson and Novak (Tyson and Novak, 2001) with great success. We will firstly apply optimal parameter selection techniques to the Tyson and Novak model where we use different start values for parameters than those published by Tyson and Novak. By using different start values we can show how MISER3.3 will return the optimal solution as the published parameter values by Tyson and Novak and thus confirm the applicability of this approach.

4.2 The Tyson and Novak Model as an Optimal Parameter Selection Problem

The Tyson-Novak model discussed previously in Chapter 3 described the cell cycle growth of eukaryotes with an emphasis on showing the steady states that exist in a normal eukaryote cell cycle and to describe the hysteresis loop at the core of the cell cycle and the antagonism that occurs between certain cyclin-dependent kinases and the APC. We present here a re-formulation into an Optimal Parameter Selection format. Our optimal parameter selection model for the T-N model is presented below,

$$\dot{x_1} = \zeta_1 - (\zeta_2 + \zeta_3 x_2)x_1 \,, \tag{4.7}$$

$$\dot{x_2} = \frac{\zeta_4 + \zeta_5 x_4)(1 - x_2)}{J_3 + 1 - x_2} - \frac{\zeta_6 x_6 x_2 x_1}{J_4 + x_2} \,, \tag{4.8}$$

$$\dot{x_3} = \zeta_7 + \frac{\zeta_8 (x_1 x_6 / J_5)^n}{1 + (x_1 x_6 / J_5)^n} - \zeta_9 x_3 \,, \tag{4.9}$$

$$\dot{x_4} = \frac{\zeta_{10} x_5 x_3 - x_4}{J_7 + x_3 - x_4} - \frac{\zeta_{11}[MAD] x_4}{J_8 + x_4} - \zeta_9 x_4 \,, \tag{4.10}$$

$$\dot{x_5} = \zeta_{12} x_6 x_1 (1 - x_5) - \zeta_{13} x_5 \,, \tag{4.11}$$

$$\dot{x_6} = \zeta_{14} x_6 \Big(1 - \frac{x_6}{m_*}\Big) \,. \tag{4.12}$$

The state variables are as follows,

x_1 : [CycB],

x_2 : [Cdh1],

x_3 : [$\mathrm{Cdc20_T}$],

x_4 : [$\mathrm{Cdc20_A}$],

x_5 : [IEP],

x_6 : m.

The parameter meanings are listed below,

ζ_1 : k_1,

ζ_2 : k_2',

ζ_3 : k_2'',

ζ_4 : k_3',

ζ_5 : k_3'',

ζ_6 : k_4,

ζ_7 : k_5',

ζ_8 : k_5'',

ζ_9 : k_6,

ζ_{10} : k_7,

ζ_{11} : k_8,

ζ_{12} : k_9,

ζ_{13} : k_{10},

ζ_{14} : μ.

The Michaelis constants J_3, J_4, J_5, J_7 and J_8 remain fixed constants in our formulation. The constant m_* is the maximum size of an adult cell as it was in the Alarcòn model, and therefore will also remain fixed throughout the formulation. [MAD] is a toggle and switches between 1 and a large number for completion of chromosome alignment. A value of 1 for "on time" completion and a large number for a completion not on time. We will assume that in our formulation that chromosome alignment is "on time" and hence, [MAD] is fixed to a value of 1. The coefficient n is a Hill coefficient and has a value of 4, as is published by Tyson and Novak (Alarcón et al., 2004a). The Hill coefficient represents the steepness of the relationship between concentration and response. As it is not closely related to the purpose of this research we will not give an in depth discussion relating to the Hill equation and its use in pharmacology.

We aim to minimise a particular objective function which we state as follows,

$$g_0(\boldsymbol{\zeta}) = \sum_{j=1}^{6} \sum_{i=1}^{7} \left(x_j(\tau_i|\boldsymbol{\zeta}) - x_j^*(\tau_i) \right)^2, \tag{4.13}$$

subject to the dynamical system described by equations (4.7) to (4.12) with initial conditions $[0.5, 1.0, 1.8, 1.3, 0.7, 0.6]^T$. The terminal time is denoted by T and for our formulation has a value of 60, where time t is in minutes. $x_j(t)$ are the theoretical values and $x_j^*(t)$ are the values we obtained from a successful implementation of Tyson and Novak's model and $\zeta = [\zeta_1, \ldots, \zeta_{14}]^\top$. We use all 6 state variables in the objective. We will use the method of Multiple Characteristic Time Points described in Chapter 1 for our numerical

Table 4.2: Starting values for computational work in MISER3.3

ζ	Start Values	Tyson
ζ_1	0.04	0.04
ζ_2	0.04	0.04
ζ_3	1.5	1.0
ζ_4	1.5	1.0
ζ_5	12.0	10.0
ζ_6	35.0	35.0
ζ_7	0.005	0.005
ζ_8	0.2	0.2
ζ_9	0.1	0.1
ζ_{10}	1.2	1.0
ζ_{11}	0.6	0.5
ζ_{12}	0.2	0.1
ζ_{13}	0.01	0.02
ζ_{14}	0.01	0.01

optimisation, with $M = 7$.

To test the applicability of the proposed formulation, we use perturbed versions of the parameter values published by Tyson and Novak as a starting point for our computations. The starting values that we used are chosen randomly for select parameters. The starting values we used and the published values by Tyson and Novak (Tyson and Novak, 2001) are displayed in Table 4.2.

We use MISER3.3 to minimise the objective function (4.13) over the stated time horizon, using multiple time points $\tau_1 = 0$, $\tau_2 = 10$, $\tau_3 = 20$, $\tau_4 = 30$, $\tau_5 = 40$, $\tau_6 = 50$ and $\tau_7 = 60$, where time is t minutes. The optimised parameters that MISER3.3 produced are presented in Table 4.3 alongside MISER3.3 rounded values and the published values by Tyson and Novak (Tyson and Novak, 2001). The results returned by MISER3.3 in Table 4.3 are to 6 significant figures. The rounded values show either an exact match

Table 4.3: Results from MISER3.3 for Multiple Characteristic Time points

$\boldsymbol{\zeta}$	MISER3.3	Rounded	Tyson
ζ_1	0.048528	0.05	0.04
ζ_2	0.0420341	0.04	0.04
ζ_3	1.00497	1.0	1.0
ζ_4	1.09633	1.1	1.0
ζ_5	9.74194	10.0	10.0
ζ_6	35.7286	36.0	35.0
ζ_7	0.00490765	0.005	0.005
ζ_8	0.199762	0.2	0.2
ζ_9	0.099762	0.1	0.1
ζ_{10}	1.00158	1.0	1.0
ζ_{11}	0.502537	0.5	0.5
ζ_{12}	0.101318	0.1	0.1
ζ_{13}	0.020161	0.02	0.02
ζ_{14}	0.009979	0.01	0.01

or very near match to those published by Tyson and Novak. The objective function value that MISER3.3 returned was 7.03004373. We would expect the objective function value to be equal to zero for an exact matching of parameter values. However, since the model is highly nonlinear, the objective value that has been returned is a reasonable result.

The parameter values returned by MISER3.3 were put back into the original model by Tyson and Novak for testing. We use the ode solver, ode45, in Matlab R2010b to the solve the system of equations with the optimised parameters. The results of this can be seen in Figure 4.4 for variables representing APC/Cdh1, x_2, and CycB/Cdk, x_1. The figure also shows how well MISER3.3 was able to reach the optimal solution and produce results that are in accordance with the published paper by Tyson and Novak (Tyson and Novak, 2001). We previously duplicated the figure by Tyson and Novak successfully in Chapter 3. We present Figure 4.5 from Chapter 3 here for comparison purposes.

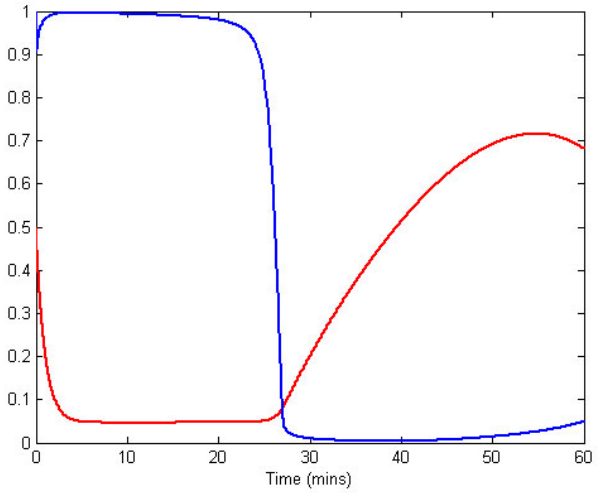

Figure 4.4: Results using optimal parameters from MISER3.3 for T-N model, showing variables representing APC/Cdh1, x_2, and CyclinB/Cdk concentration, x_1. Blue represents x_2 and red represents x_1.

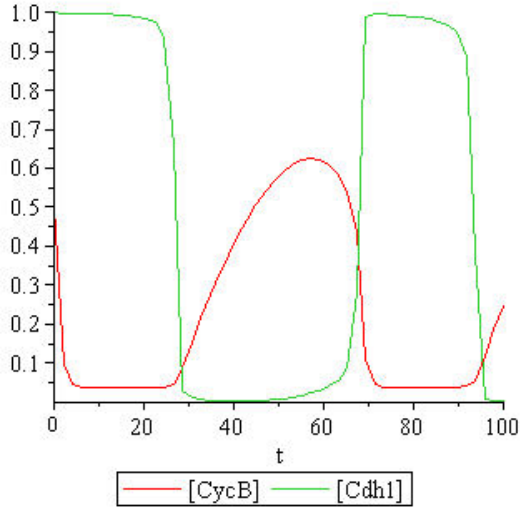

Figure 4.5: Successful duplication of the Tyson and Novak model for variables x_1, CyclinB/Cdk concentration and x_2, APC/Cdh1 concentration, t is in minutes.

Figures 4.4 and 4.5 are the same both quantitatively and qualitatively. They both show a division cycle for variables x_1 and x_2. We can see at the same points that both figures behave the same. This is a significant outcome and shows how well MISER3.3 is able to recover the correct model parameter values when starting with a set of perturbed ones.

4.3 Optimal Parameter Selection for the Alarcón Model

Part of our motivation behind using Optimal Parameter Selection techniques on the model by Alarcón et al (Alarcón et al., 2004a) was the absence of any optimisation techniques used in their model development. The model parameter values that were used by Alarcón et al were based either on values found in literature or on estimates based on values determined by Dormann and Deutsch (Dormann and Deutsch, 2002). It is not clear, however, if these parameters, either estimates or literature based, were optimised to ensure a good match between the model and experimental data. It is also not clear if the estimates taken from Dormann and Deutsch (Dormann and Deutsch, 2002) were optimised for model matching. Also, based in our discussion in Section 4.3, there is clearly some doubt as to whether parameter values were reported correctly in Alarcón et el.

We present the model from Alarcón et al (Alarcón et al., 2004a) in canonical optimal parameter selection form. Here, the vector $\boldsymbol{x} = [x_1, \ldots, x_n]^\top$ represents the state variables and vector $\boldsymbol{\zeta} = [\zeta_1, \ldots, \zeta s]^\top$ represents the parameters

we are optimising. The system is presented as follows,

$$\dot{x}_1 = \frac{(1+\zeta_5 x_5)(1-x_1)}{J_3+1-x_1} - \frac{\zeta_6 x_3 x_1 x_2}{J_4+x_1}, \tag{4.14}$$

$$\dot{x}_2 = \zeta_4 - (\zeta_1 + \zeta_2 x_1 + \zeta_3 x_4) x_2, \tag{4.15}$$

$$\dot{x}_3 = \zeta_7 x_3 \Big(1 - \frac{x_3}{m_*}\Big), \tag{4.16}$$

$$\dot{x}_4 = \zeta_8 - \zeta_9 \frac{P}{\zeta_{10}+P} x_4, \tag{4.17}$$

$$\dot{x}_5 = \zeta_{12} - (\zeta_{12} + \zeta_{11} x_2) x_5, \tag{4.18}$$

As in the model proposed by (Alarcón et al., 2004a) the constant terms J_3 and J_4 represent Michaelis constants determined by biological observation. The constant variable m_* still represents the maximum adult mass of a cell and constant P remains the oxygen tension. A description of both the state variables and parameters that are being optimised are given below.

x_1 : average concentration of complex formed APC/Cdh1,

x_2 : average concentration of complex forming CycB/Cdk,

x_3 : the maximum mass of the cell,

x_4 : average concentration of protein p27,

x_5 : average concentration of non-phosphorylated Rb.

The parameter descriptions will relate to the parameters used in the Alarcón model previously described in Section 4.3, and are listed below,

ζ_1 : a_1,

ζ_2 : a_2,

ζ_3 : a_3,

ζ_4 : a_4,

ζ_5 : b_3,

ζ_6 : b_4,

ζ_7 : η ,

ζ_8 : c_1,

ζ_9 : c_2,

ζ_{10} : B,

ζ_{11} : d_1,

ζ_{12} : d_2.

We have taken the model proposed by Alarcón and associates (Alarcón et al., 2004a) and re-written it in the form of an optimal parameter selection formulation as described in Chapter 1, except for the formulation of an objective function. Assuming all states can be observed experimentally over the entire time horizon, we choose the objective as minimising,

$$g_0(\boldsymbol{\zeta}) = \int_0^T \sum_{i=1}^{5} (x_i(t|\boldsymbol{\zeta}) - x_i^*(t))^2 \mathrm{d}t \,, \tag{4.19}$$

subject to equations 4.14 to 4.18 and with the initial conditions

$$\boldsymbol{x}(0) = [0.9,\, 0.01,\, 5.0,\, 0,\, 1.0]^\top . \tag{4.20}$$

The initial conditions we have chosen are based on the conditions given by Alarcón and associates (Alarcón et al., 2004a). Here, the theoretical states that arise from the model are denoted by $x_i(t)$ and the corresponding observed experimental values by $x_i^*(t)$, $i = 1, \ldots, 5$. The experimental values can, in principle, be taken from continual observations of biological experiments. However, obtaining continuous biological data of this nature is not always possible often due to the lack of observability of certain states and due to the cost of continual monitoring.

In an experimental situation it is unlikely that we can actually measure data across a continuous time frame. Since we are attempting to mimick an experimental situation as much as possible simply defining a set of discrete time point at which state values are to be matched makes more sense. The objective function we used in our numerical studies can thus be defined as follows,

$$g_0(\boldsymbol{\zeta}) = \sum_{j=1}^{2} \sum_{i=1}^{11} \left(x_j(\tau_i|\boldsymbol{\zeta}) - x_j^*(\tau_i) \right)^2 , \tag{4.21}$$

where τ_1 to τ_M where $M = 11$, for each state $\boldsymbol{x} = [x_1, x_2]^\top$ and $\boldsymbol{\zeta} = [\zeta_1, \zeta_2, \ldots, \zeta_{12}]^\top$. We aim to minimise the objective functional (4.21) subject to equations (4.14) to (4.18) with initial conditions (4.20). Note that this once again constitutes an optimal parameter selection problem with multiple characteristic times as

defined in Chapter 1.

We chose to only use states x_1 and x_2 in the objective as these two states are the most affected during the G1 phase of a cancer cell cycle, in particular, the G1 phase up to the restriction point. The activity of these complex forming proteins is significant as the complexes can form cancerous mutations, as previously mentioned in Chapter 2. The x_1 state is of particular interest, as the differential equation representing this state implements Michaelis-Menten type kinetics which can lead to varying results.

As we have no direct access to appropriate experimental data, we simply use the graphs in (Alarcón et al., 2004a) to generate the 'experimental' state values $x_j^*(\tau_i)$, $i = 1, 2, \ldots, 11$ and $j = 1, 2$. We chose to use 11 time points at which we 'measure' the states, x_1 and x_2, leading to 11 multiple characteristic times. These are listed in the Table 4.4. Although the optimal parameter selection model we present is based on published data rather than experimental data, we can still produce a model that closely resembles data published by Alarcón et al. Note that the same technique could be used if actual experimental data was available. We will use the parameter values that were sent to us by Alarcón and associates (Alarcón et al., 2004a) as our initial starting point for the optimal parameter selection technique (the revised values in Table 4.1). By optimising the parameters we are aiming to obtain a "better fit" that more accurately resembles the graphical data from Alarcón et al (Alarcón et al., 2004a).

The optimised parameter values that we obtained using MISER3.3 are listed in Table 4.5 alongside the revised values given to us by Alarcón et

Table 4.4: Table of τ_i values for characteristic time points.

τ_i	Times
τ_1	0
τ_2	142
τ_3	284
τ_4	426
τ_5	568
τ_6	710
τ_7	852
τ_8	994
τ_9	1136
τ_{10}	1278
τ_{11}	1420

(4.22)

al (Alarcón et al., 2004a). We have also included a column of MISER3.3 values rounded to highlight the discrepancies between those obtained from MISER3.3 and the revised values from Alarcón et al. As can been seen the only parameters which are close to the revised parameters by Alarcón et al are ζ_5 and ζ_6. Some of the parameter values used by Alarcón et al (Alarcón et al., 2004a) were taken from previously published work by Tyson and Novak (Tyson and Novak, 2001). We would expect that since the Tyson and Novak model was easily duplicated (see Chapter 3, Section 1) that the use, in part, of their parameter values by Alarcón et al would be reasonable. After performing optimal parameter selection on the chosen parameters we are able to then put the parameters returned by MISER3.3 back into the system and plot the result.

Figure 4.6 shows variables x_1 and x_2, relating to the APC/Cdh1 complex and the generic Cyclin/Cdk complex respectively, using the optimised parameter values MISER3.3 returned. The objective function value returned by MISER3.3 was equal to $4.027395 * 10^6$. We expect this result as duplicating

Table 4.5: Table of simulated parameter values

ζ	MISER3.3	Rounded	Alarcón
ζ_1	0.00864931	0.009	0.04
ζ_2	0.990733	1.0	1.0
ζ_3	0.330044	0.33	0.25
ζ_4	0.0807658	0.08	0.04
ζ_5	10.0014	10.0	10.0
ζ_6	3.49825	3.5	3.5
ζ_7	0.0966571	0.1	0.01
ζ_8	0.07	0.07	0.007
ζ_9	0.0195864	0.02	0.01
ζ_{10}	0.00721735	0.007	0.01
ζ_{11}	0.000292239	0.0003	0.01
ζ_{12}	0.00494411	0.005	0.1

the original model was met with great difficulty. We have been able to highlight the difficulties with the model by Alarcón et al (Alarcón et al., 2004a) through the failed attempts to find suitable parameter values using optimal parameter selection techniques and as a result, not being able to successfully duplicate the model behaviour. In the following subsections we discuss some possible explanations as to why these discrepancies may have occurred.

4.3.1 Incorrect Parameter Values

Another paper published in 2005 by (Alarcón et al., 2005) also detailed the growth of cancer cells through a mathematical process, but dealt with multiple time scaling. One part of the time scale model had been adapted from the model on hypoxic cells as seen in (Alarcón et al., 2004a). Upon investigating the 2005 paper we noticed differences in the parameters, initial conditions and the equations themselves. The dynamics are primarily the same and we cannot see why the differences would be necessary. Due to the multiple time scaling

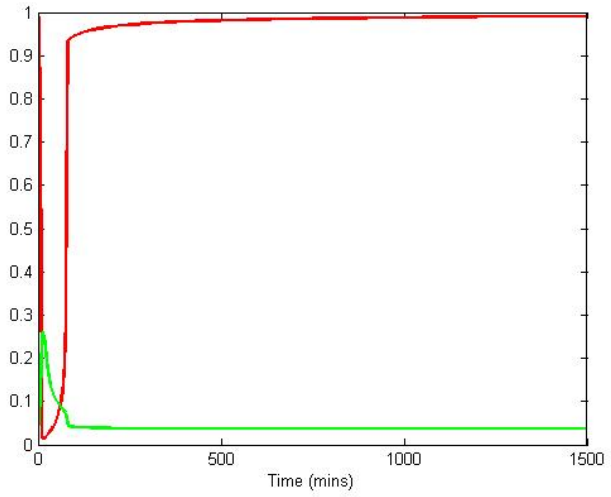

Figure 4.6: Plots representing results when optimised parameters from MISER3.3 were used in the Alarcón model. Variables plotted are x_1, red line, and x_2, green line.

the model had many different components and it was not possible for us to reproduce the results in the 2005 paper. We list the main part of the dynamics for the 2005 paper (Alarcón et al., 2005) in Chapter 3, but we recall them again here.

$$\frac{dx(\boldsymbol{r})}{dt} = \frac{(k_3' + k_3'' u(\boldsymbol{r}))(1 - x(\boldsymbol{r}))}{J_3 + 1 - x(\boldsymbol{r})} - \frac{k_4 m(\boldsymbol{r}) y(\boldsymbol{r}) x(\boldsymbol{r})}{J_4 + x(\boldsymbol{r})} \tag{4.23}$$

$$\frac{dy(\boldsymbol{r})}{dt} = k_1 - (k_2' + k_2'' x(\boldsymbol{r}) + k_2''' z(\boldsymbol{r})) y(\boldsymbol{r}) \tag{4.24}$$

$$\frac{dm(\boldsymbol{r})}{dt} = \mu\Big(\frac{y(\boldsymbol{r})}{y(\boldsymbol{r}) + y_0}\Big) m(\boldsymbol{r}) \Big(1 - \frac{m(\boldsymbol{r})}{m_*}\Big) \tag{4.25}$$

$$\frac{dz(\boldsymbol{r})}{dt} = \chi\Big(m, \boldsymbol{r}\Big) - k_5' \frac{P(\boldsymbol{r})}{B + P(\boldsymbol{r})} z(\boldsymbol{r}) \tag{4.26}$$

$$\frac{du(\boldsymbol{r})}{dt} = k_6' - (k_6' + k_6 y(\boldsymbol{r})) u(\boldsymbol{r}) \tag{4.27}$$

$$v = 1 - u, \tag{4.28}$$

where,

x : average concentration of APC/Cdh1 complexes,

y : average concentration of generic Cyc/Cdk complexes,

m : mass of a cell as in the Tyson-Novak model,

z : average concentration of protein p27,

u : average concentration of non-phosphorylated pRb,

v : average concentration of phosphorylated pRb,

y_0 : initial concentration of variable y.

J_i : Michaelis constants for $i = 3, 4$,

B : constant term,

η : growth rate constant associated with cell mass,

m_* : maximum mass of a cell,

P : oxygen tension.

k_i : rate constants, for $i = 1, \ldots, 6$,

k_i' : rate constants relating to respective k_i's, for $i = 2, \ldots, 6$,

k_i'' : rate constants relating to respective k_i''s, for $i = 2$ and 3,

k_i''' : rate constant relating to respective k_i'', for $i = 2$.

The function $\chi\Big(x, \boldsymbol{r}\Big)$ is defined below,

$$\begin{cases} k_5 & \text{if } s_1(\boldsymbol{r}) = 1\,, \\ k_5\Big(1 - \frac{m_{\boldsymbol{r}}}{m_*}\Big) & \text{if } s_1(\boldsymbol{r}) = 2\,, \\ 0 & \text{otherwise.} \end{cases}$$

If $s_1(\boldsymbol{r}) = 1$ then there is a cancer cell located at $\boldsymbol{r}$ and if $s_1(\boldsymbol{r}) = 2$ then there is a normal cell located at $\boldsymbol{r}$.

Parameter value c_1 in (Alarcón et al., 2004a), denoted by k_5 in (Alarcón et al., 2005), is equal to 0.007. However, in the 2005 paper the associated parameter, k_5, is equal to 0.002.

The initial conditions for the dynamics are as follows,

$$x_0 = 0.9, \quad y_0 = 0.001, \quad m_0 = 5, \quad z_0 = 0, \quad u_0 = 0\,. \tag{4.29}$$

The initial conditions for the 2005 paper presented in (4.29) differ from the 2004 paper (Alarcón et al., 2004a) in variables y and u. In the 2004 paper published by Alarcón et al, variables y and u have initial conditions of 0.01 and 1.0, respectively. In the paper published by Alarcón et al in 2005, the initial conditions for both y and u have changed to 0.001 and 0, respectively. Variable u's initial condition is the one that interests us the most as going from 1.0 to 0 is a significant change in relation to the biology that this variable represents. To recall, variable u represents the average concentration of the retinoblastoma protein. The initial condition from the 2005 paper is closer to the correct biological setting for this variable. We give a discussion on this variable and its representation in equation (4.1) in Section 4.3.3.

We applied a stability analysis using Maple v12.0 to acquire the Jacobian matrix about the initial conditions and to subsequently check if the steplength value we had chosen for our simulations was appropriate. Our analysis revealed that our steplength value was entirely appropriate for our computations corresponding to the initial conditions published by the authors (Alarcón et al., 2004a). For a detailed script of our analysis and the Maple output produced we refer the reader to Appendix C.

4.3.2 Machine Accuracy and integration sensitivity

We discuss issues that we encounter with machine accuracy while working on this project. We ran simulations on 3 different machines and acquired varying results on each for the equations (4.1) to (4.5) with initial conditions (4.6). The results from 2 machines have been presented in Figures 4.1 and 4.2. The results for the SGI machine are plotted in Figure 4.2 and represent one complete division cycle of the cell. In Figure 4.1 we are able to show the results from the Sun Netra Carrier-Grade machine when oxygen tension,P, is set to 1.0 and 0.1 for three complete division cycles of a cell. Appendix B shows the code for the Fortran90 program that was used to implement the model on both machines published in the paper (Alarcón et al., 2004a).

We also show the results that we obtained using the software package Matlab R2010b, using the ode15s in-built ordinary differential equation solver, on a Dell PC with Intel 64-bit processor. The Matlab ode solver, ode15s, is a multistep solver and uses the inbuilt Matlab numerical differentiation formulas to solve a given system of equations. Appendix B shows the Matlab code that

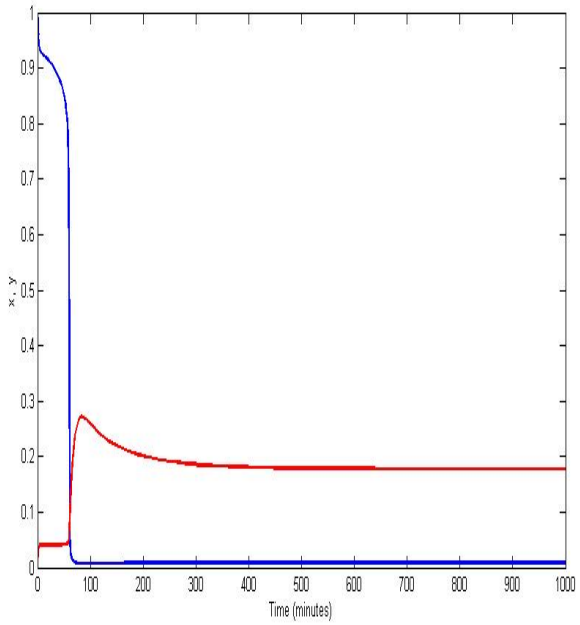

Figure 4.7: The above plot represents the average concentration of APC/Cdh1 (x) and generic Cyclin/Cdk complex (y) for an oxygen tension $P = 1.0$. Numerical simulations were performed using Matlab where x is the blue line and y is the red line.

was used to obtain our results. Our results are displayed in Figure 4.7.

We refer back to Section 4.3 where Figures 4.1 and 4.2 show different results for implementing the Alarcón model using the same algorithm on two different machines. We also have the results displayed for solving the Alarcón model in Matlab, as mentioned above, in Figure 4.7. All three figures display differing results in relation to the initial time steps for variable x. Although the results appear to be similar in their behaviour, the differences in their time horizon in a biological context is a significant factor. The initial phase of the cell cycle, the G1/S phase, in Figures 4.1, 4.2 and 4.7 are all significantly shorter than that of a typical cancer cell (Weinberg, 2007). A typical cell will

take approximately 6 to 8 hours to divide (Alberts et al., 2008). The time frame in Figure 4.7 is drastically shorter than the time frames in Figures 4.1 and 4.2. These differences lead us to discuss the sensitivity of the model and the numerical implications of this in the following paragraphs.

The equations (4.1) to (4.5), detailed in Section 4.3, represent a stiff system of equations and therefore need to be dealt with carefully. This appears to be an indication of the sensitivity of the model to numerical precision of the machine used. The nature of the equations presents problems numerically due to the varying timescales associated with modelling biological phenomena. For example, the interactions occurring among cells is on a different timescale to the protein interactions occurring inside the cell. In the paper (Alarcón et al., 2004a) the authors used a fourth order Runge-Kutta routine to solve the system in their computational procedure, as stated in their article. For a stiff system of equations the fourth order Runge-Kutta method is not the most suitable numerical method and there are more appropriate numerical procedures. Numerical methods that would be more suited would be a higher-order Runge-Kutta, such as a 6-order method, which will lead to a more accurate result. The method used should also be adaptive in nature so that the steplength can be adjusted as the integration proceeds.

The software package MISER3.3 (Jennings et al., 2004) is generally used to solve the optimal parameter selection problem. MISER3.3 uses a 6-order Runge-Kutta method to solve the numerical problem. The software package incorporates an ODE solver which will switch to a 'stiff' mode if necessary and output from the package indicates a high frequency of switches to this

stiff mode when solving the problem. The software encountered problems when using it's in-built integrator attempting to solve the problem. For the dynamics presented by (Alarcón et al., 2004a) the software would often switch to the in-built stiff integrator indicating that the system is a stiff system.

These differing results lead us to examine equations (4.1) to (4.5) which most of our analysis has primarily focussed on, with much more scrutiny. In particular due to some sensitivity relating to the kinetic dynamics that are embedded in the equations. Upon further investigation we discovered a misinterpretation with one of the equations, specifically equation (4.1), and how it relates to the variable representing the retinoblastoma protein in non-phosphorylated form.

4.3.3 Biological misinterpretation

We present equation (4.1) below, followed by a discussion that will examine the link between the biology and the mathematics of this particular equation. We also include a discussion on the representation of the retinoblastoma protein in this equation.

$$\frac{dx}{d\tau} = \frac{(1 + b_3 u)(1 - x)}{J_3 + 1 - x} - \frac{b_4 m x y}{J_4 + x},$$

where the variable u stands for non-phosphorylated Rb and its occurrence in the model where it is suppose to mimic the behaviour of non-phosphorylated Rb on Cdk activity (Alarcón et al., 2004a). Hypo-phosphorylation occurs during the G1 phase of the cell cycle up until the restriction point. After

this, it enters into a hyper-phosphorylation state. To state that during G1 phase of the cell cycle Rb is non-phosphorylated indicates that Rb is in an unphosphorylated form which only occurs at the M/G1 transition of the cell cycle (Weinberg, 2007). As previously mentioned, the above equation was originally developed by Tyson and Novak (Tyson and Novak, 2001).

The variable u in equation (4.1) above is replacing a generic activator in the model by Tyson and Novak (Tyson and Novak, 2001). This generic activator in the budding yeast cell cycle is the protein Cdc20. It has been found that a corresponding protein exists for the mammalian cell cycle, p55cdc, which exhibits many similarities to that of Cdc20 in yeast (Weinstein et al., 1994). Consequently, replacing protein activator Cdc20 with unphosphorylated Rb is not a reasonable choice. It would be more appropriate to make a direct replacement of Cdc20 with p55cdc. Protein p55cdc could be modelled similarly to Cdc20 which Tyson and Novak have described in both their 2001 and 2004 papers (Tyson and Novak, 2001; Novak and Tyson, 2004). This would still be an appropriate choice given that the model by Alarcón et al is based on a cancer cell cycle.

Having reviewed the papers by Tyson and Novak that effectively model the mammalian cell cycle, we are able to see the activity of protein Cdc20, although their modelling still refers to the cell division cycle protein as Cdc20 instead of its mammalian counterpart p55cdc. For a normal mammalian cell cycle Cdc20 initiates activity of APC/C during mitosis. More specifically during metaphase (third subphase of mitosis) Cdc20 forms a complex with MAD2 and the APC/C. Cdc20 becomes active with complex forming Cdc20-

APC/C during anaphase (Alberts et al., 2008).

The authors also explain the significance of protein Cdc20 in the division process and how its activation can be altered when a mutation is present (Novak and Tyson, 2004). We present the equation that Tyson and Novak developed in their 2004 paper below and will adopt their nomenclature. The equation is also presented earlier in Chapter 3.

$$\frac{d\,[\mathrm{Cdc20}]}{dt} = k_{13}\,[\mathrm{IEP}]\,\frac{[\mathrm{Cdc20_T}] - [\mathrm{Cdc20}]}{J_{13} + [\mathrm{Cdc20_T}] - [\mathrm{Cdc20}]} - k_{14}\frac{[\mathrm{Cdc20}]}{J_4 + [\mathrm{Cdc20}]} - k_{12}\,[\mathrm{Cdc20}]\,.$$

We have mentioned above how Cdc20 will form a complex with MAD2 and APC/C. The cell cycle, however, can be disrupted during mitosis when a cancerous mutation can occur. There has been research into the inactivation of MAD2 during mitosis of prostate epithelial cells (To-Ho et al., 2008). It has been reported by To-Ho et al (To-Ho et al., 2008) that the mitotic checkpoint during the cell cycle of the epithelial cells is disrupted due to this inactivation. This gives us an additional reason to believe that there is a biological mismodelling in relation to the APC and unphosphorylated Rb.

4.3.4 Uncertainty in Activity States of Proteins

In relation to Figure 4.6 from Section 4.3 there was a considerable difference with our results compared with the results published by Alarcón et al in relation to the time steps. Our time steps are much less than the time steps published by Alarcón et al, by a factor of approximately 10.

The initial behaviour of the model displays a sharpness in the curve due to the dynamics relating to the Michaelis-Menten type equations. As we have already seen Michaelis-Menten type modelling often poses problems when implemented using typical mathematical software, as we have used here.

To recap, we previously mentioned in Chapter 2 that Michaelis-Menten kinetics model biochemical activity occurring between substrates and enzymes. Often complexes forming are in an active or inactive state depending on where they have formed in the cell cycle and also due to the nature of the proteins themselves (Weinberg, 2007). We can use Michaelis-Menten kinetics to model this situation and consequently, it is often implemented in a mathematical environment to model such occurrences.

Tyson and Novak in their 2004 paper (Novak and Tyson, 2004), successfully model proteins in their active state using Michaelis-Menten kinetics. This relates to the proteins being unphosphorylated and in non-complex form i.e. not binding with another protein. The proteins PP1 (type-1 protein phosphatase) and E2F (transcription factor activating adenovirus E2 gene) are modelled by Tyson and Novak in active and inactive form. The equations to describe PP1 and E2F in an active form are given as,

$$[\mathrm{PP1_A}] = \frac{[\mathrm{PP1_T}]}{1 + K_{21}(\phi_E([\mathrm{CycE}] + [\mathrm{CycA}]) + \phi_B\,[\mathrm{CycB}])}\,, \tag{4.30}$$

$$[\mathrm{E2F_A}] = \frac{([\mathrm{E2F_T}] - [\mathrm{E2F{:}\,Rb}])\,[\mathrm{E2F}]}{[\mathrm{E2F_T}]}\,, \tag{4.31}$$

where

$[\mathrm{PP1_A}]$: is the average concentration of active protein PP1,

$[\mathrm{E2F_A}]$: is the average concentration of active protein E2F,

$[\mathrm{PP1_T}]$: is the total concentration of protein PP1 and has a constant value,

$[\mathrm{E2F_T}]$: is the total concentration of protein E2F in

[E2F] : is the total concentration of inactive protein E2F,

[E2F: Rb] : is the average concentration of E2F complexed with Rb,

[CycA] : is the average concentration of CyclinA,

[CycB] : is the average concentration of CyclinB,

[CycE] : is the average concentration of CyclinE,

Φ_B : is a dimensionless rate constant for CyclinB,

Φ_E : is a dimensionless rate constant for CyclinE,

K_{21} : is a dimensionless rate constant.

In contrast, the less active form of protein PP1 and inactive E2F are described without the use of Michaelis-Menten kinetics and are given as follows,

$$\frac{d\,[\mathrm{E2F}]}{dt} = k_{22}([\mathrm{E2F_T}] - [\mathrm{E2F}]) - [\mathrm{E2F}](k'_{23} + k_{23}([\mathrm{CycA}] + [\mathrm{CycB}]))\,, \quad (4.32)$$

$$[\mathrm{PP1}] = [\mathrm{PP1_T}] - [\mathrm{PP1_A}]\,, \quad (4.33)$$

where,

[PP1] : is the average concentration of less active protein PP1,

k_{22} and k_{23} : are both time dependent rate constants,

k'_{23} : is a time dependent rate constant.

Alarcón et al (Alarcón et al., 2004a) have modelled the APC/Cdh1 complex in an active state but their generic Cyc/Cdk complex in an inactive state. This may not be an entirely appropriate assumption to make based on the biology of cancer growth during the G1/S phase of the cell cycle (Weinberg, 2007). The above representation by Tyson and Novak (Novak and Tyson, 2004) would be a good starting point to resolve some of the issues with the model by Alarcón et al relating to whether complexes and/or proteins are to be modelled in an active or inactive state.

4.4 Conclusion

In this chapter we have applied optimal parameter selection techniques to two known models in the field of cancer and normal cell cycle growth. The first model we applied these techniques to was based on a non-cancerous cell cycle published by Tyson and Novak (Tyson and Novak, 2001). We have been able to show how using optimal parameter selection techniques we are able to achieve an optimal solution for the proposed problem. The parameter values returned by MISER3.3 were in strong agreement to the parameter values published by Tyson and Novak (Tyson and Novak, 2001). This demonstrates the effectiveness of the optimal parameter selection methodology.

The second model we applied optimal parameter selection techniques to was a cancer cell cycle model published by Alarcón et al (Alarcón et al.,

2004a). Our results showed that some of the published model parameters were far from optimal when trying to replicate their numerical results. Despite this, we were unable to replicate their published results and we suggested a number of possible reasons for this discrepancy.

We have shown how dynamic cell cycle models can be effectively matched to experimental data by the use of an optimal parameter selection formulation and numerical optimisation tools. Existing papers on cell cycle models have not used this approach to date.

Chapter 5

Mathematical Model of Melanoma

In this chapter we briefly examine some existing literature on mathematical models of melanoma growth and use this as a catalyst to develop our own model for describing melanoma growth.

In Section 5.1 we discuss two simple mathematical models that describe melanoma growth. Each of these models have a treatment term for describing some immune type response to eradiate the tumour growth. The models are mathematically different in that one model uses ordinary differential equations and the other is described in terms of partial differential equations. This highlights the different time and spatial elements required for modelling complex biological phenomena. Due to the rarity of melanoma type modelling these reviews are essentially a summary of what has been achieved so far in this area. These reviews also show the differing approaches to melanoma modelling and how these approaches may influence a real world situation.

In Section 5.2, we detail some kinetic background which was previously outlined in Chapter 2, but is recalled here for the benefit of the reader.

In Section 5.3 we then present a mathematical model we developed to describe the growth of melanoma using a system of ordinary differential equations. We discuss the need to incorporate the mutated Braf protein in the model as well as using kinetics to describe the biological reactions occurring.

Finally, in Section 5.4 we summarise what we have developed by way of a new approach to mathematically model melanoma growth.

5.1 Motivation

The motivation behind developing a mathematical model to describe melanoma growth is that there appears to be very little applied mathematical modelling for this type of cancer. There is widespread statistical analysis on melanoma growth and there is also a large amount of medical research, as previously mentioned in Chapter 2.

There are two types of models that describe the effective treatment of melanoma growth, both modelling an immune-type therapy. One model purely concentrates on the modelling of the treatment while the other develops the model to firstly describe the growth of melanoma and to then build on top of that to incorporate a treatment plan. The latter of the models also accounts for an immune response treatment with and without surgery.

The first of the melanoma models is a simplistic model that describes the immunotherapy for patients with metastatic melanoma and renal cell cancer. The model is an extension of previous work done by Kirschner and associates (Kirschner and Panetta, 1998) on modelling tumour immunotherapy. The extension changes the treatment parameter to a function dependent on

the volume of effector cells and time t.

The Kirschner model is presented below for comparison purposes.

$$\frac{dx}{dt} = cy - \mu_2 x + \frac{p_1 xz}{g_1 + z} + s_1 \tag{5.1}$$

$$\frac{dy}{dt} = r_2 y(1 - by) - \frac{axy}{g_2 + y} \tag{5.2}$$

$$\frac{dz}{dt} = \frac{p_2 xy}{g_3 + y} - \mu_3 z + s_2\,, \tag{5.3}$$

where,

x : volume of effector cells,

y : volume of tumour cells,

z : concentration of interleukin-2 relevant to tumour site and compartment model,

c : antigenicity of tumour,

s_1 : treatment term (constant) describing immunotherapy,

s_2 : treatment term (constant) describing interleukin-2,

μ_2 : half-life of effector cells, constant term,

μ_3 : degradation of interleukin-2, constant,

p_1 : rate constant,

p_2 : rate constant,

g_1 : michaelis constant,

g_2 : michaelis constant,

g_3 : michaelis constant,

r_2 : growth rate (constant),

b : logistic growth rate (constant),

a : rate constant,

t : time in minutes.

In this particular model the effector cells are T-Lymphocytes which are apart of the immunological response in the human body (Usman and Cunningham, 2005). The model by Kirschner, equations (5.1) to (5.3), has been extended by Usman and Cunningham (Usman and Cunningham, 2005). A treatment function has been added to replace the constant treatment term s_2. The extended system is presented below,

$$\frac{dx}{dt} = cy - \mu_2 x + \frac{p_1 xz}{g_1 + z} + s_1 \tag{5.4}$$

$$\frac{dy}{dt} = r_2 y(1 - by) - \frac{axy}{g_2 + y} \tag{5.5}$$

$$\frac{dz}{dt} = \frac{p_2 xy}{g_3 + y} - \mu_3 z + treatment(x, t)\,, \tag{5.6}$$

The definition of variables for the extended system are as for the Kirschner model already presented, equations (5.1) to (5.3). The new treatment function is dependent on the effector cells and time, measured in minutes, allowing for a switching type environment from a modelling perspective. The function can

switch from "on" at the start of treatment and when treatment reaches a predetermined threshold value the function switches to "off". This is modelled by the function $treatment(x,t)$. The treatment function is dependent on time when the system is in a delayed state. This is to account for treatment not generally starting until a tumour has been discovered and by then has reached a particular size.

The disadvantage of this model is that there isn't a re-entry point for treatment scheduling and there is no discussion of the optimality of any treatment choice. They have, however, stated that the model is sensitive to a patients' individual treatment requirements. They are able to demonstrate this by using a threshold value that the treatment function can reach and can be re-adjusted to suit the individual patient. They provide evidence of their treatment function working and show their results through a series of figures, see Figure 5: (a) to (f) of Usman and Cunningham (Usman and Cunningham, 2005).

Overall, the model is simplistic but effective in showing how an immune type therapy can be used in a real world setting to treat patients with Metastatic Melanoma and Renal Cell Carcinoma.

More recently, a model was developed by Eikenberry et al (Eikenberry et al., 2009). A set of partial differential equations describes the growth of a metastatic melanoma and also incorporates a natural immune response treatment. The system of equations describing these events is quite complicated and we refer the interested reader to (Eikenberry et al., 2009). We will, however, give a brief analysis of the mathematical model used and the accompanying

published results.

The tumour cell population, the healthy cell population, the tumour angiogenic factor, the blood vessel endothelial cells, the necrotic debris and the basement membrane are all modelled as density functions. ρ and z are spatial, cylindrical co-ordinates relating to the geometry of the skin surface where the tumour has formed and time id denoted by t. All of the mentioned density functions are assumed to depend on ρ, z and t, the independent variables of the mathematical model. The partial pressure of oxygen is also considered and modelled as a function of ρ, z and t.

The model describing the melanoma growth is extended to incorporate a natural immune response and two new variables are added to account for this extension. m represents an aggregate of all cytotoxic cells that specifically target tumour cells, remembering that these cell will be naturally occurring cells. There is also an "attractor" like term to describe the cumulation of chemokines that attract immune type cells. There are two corresponding partial differential equations to describe the densities of each of these new variables with respect to the independent variables ρ, z and t.

The authors publish results for simulations on the basic model for several different biological situations. These results are for when there is no immune response, when an immune response has been added, surgery with no immune response and surgery with an immune response.

These reviews illustrate the rarity of melanoma type modelling so far. The models presented above differ in nature to the model we present in Section 5.3. The model we develop is based on a cell cycle of melanoma growth and we

also incorporate the effects of the mutant B-raf protein into our model. These reviews, however, show the differing approaches to melanoma modelling and how these approaches can help reflect a real world situation.

5.2 Review of Kinetics

Michaelis-Menten kinetics played a significant role in developing the models we used for our analysis on Melanoma growth. Here we present the basic kinetics that we used in developing our model (also presented in Chapter 2). The kinetics are as follows,

$$E + S \underset{k_2}{\overset{k_1}{\rightleftharpoons}} C \xrightarrow{k_3} P + E\,, \tag{5.7}$$

where,

E : total concentration of enzyme,

S : average concentration of substrate,

C : average concentration of complex forming,

P: average concentration of product,

k_1 : the association rate constant,

k_2 : the dissociation rate constant,

k_3 : the catalytic rate constant or the turnover number.

It is essential to use some form of kinetic modelling as we are not only modelling biological phenomena but we are also modelling at a protein based or kinetic level. We have incorporated the use of Michaelis-Menten type modelling in developing our model for melanoma growth due to the benefits it presents in biological modelling as previously mentioned.

5.3 The Melanoma Growth Model

The objective of this type of modelling is to effectively describe the cell cycle of melanoma growth through the use of mathematical models and numerical procedures involving computational analysis. We develop a system of ordinary differential equations that describe the cell division cycle that can occur in a melanoma type cancer. Some of the underlaying biological assumptions we model are protein interactions, protein based mutations, over-expression of particular complexes and protein degradation.

There are certain mathematical as well as biological assumptions that we need to make in the development of this model. We assume that all proteins and their associated complexes are in an active state and that in our system each ordinary differential equation represents a protein only. The mRNA's are assumed to be in steady state. These assumptions are necessary due to the complexity of modelling such biological phenomena and we don't want the model to become too complex at this stage.

A strong biological knowledge is also required to effectively model the growth of melanoma through the cell cycle mechanics. Many of the proteins mentioned in this chapter have been discussed in Chapter 2. However, some

repetition may occur here due to the significance of some of the proteins used for the modelling that we describe.

We require a transformation of the biological aspects that describe cell cycle growth of melanoma to a system of mathematical equations. This will enable us to effectively show the growth of melanoma through the cell cycle. An important aspect of this modelling is understanding the strong influence that a particular protein has on melanoma growth. The Cdk inhibitor $p16^{INK4a}$ inihibits the complex forming CyclinD/Cdk4,6 during the G1 phase of the cell cycle and has been shown, through biological experimentation, to play a significant role in the growth of melanoma. Proteins that share a similar role but will not be considered in a modelling sense in this work are $p15^{INK4b}$, $p18^{INK4c}$ and $p19^{INK4d}$. The disruption of the $p16^{INK4a}$/pRb pathway, largely due to an overexpression of CycD/Cdk4,6 complexes, is one of the main factors that cause a melanoma growth to start. The $p16^{INK4a}$ protein can be deactivated by cancer cells, in particular by melanocytes from melanoma.

To successfully model the influence that this protein has on melanoma growth we need to understand how it works in a biological sense and then work out how to mimic this behaviour in a modelling sense. As a result we consider several key biological events to model which we will briefly describe here.

The cyclins in the equations we have used are considered as the substrates, whereas the Cdk's are considered as enzymes but they are catalysed with the help of the cyclins to form cyclin/Cdk complexes.

We treat the rate of production of cyclinD as if cyclinD were a substrate for the complex forming between itself and Cdk4 and Cdk6. In reality, there

are other substrates that influence the complex forming CycD/Cdk4 and CycD/Cdk6 (Matsushime et al., 1994) but this would make the modelling process much more complicated and we only wish to give, at this stage, a simplified version. Below is a simple 'word' type equation describing the rate of production of cyclinD as a substrate. A formal set of ordinary differential equations will follow the word equation and this is merely to show the modelling process that we follow in relation to the biological aspects of this work.

$$\begin{aligned}\frac{d\,[\text{CycD}]}{dt} = &\,\text{mitogens} - \text{receptors} \\ &+ \text{kinases (binding and unbinding of Cdk's - forming complexes)} \\ &+ \text{growth factors} - \text{degradation} + \text{synthesis} \pm \text{inhibitors}\end{aligned}$$

We also wish to describe the complex forming CycD/Cdk4,6 due to the impact this complex has on melanoma growth. A simple word equation is below describing the rate of production of the complex forming CycD/Cdk4,6,

$$\begin{aligned}\frac{d\,[\text{CycD: Cdk}]}{dt} = &\,\text{synthesis} + \text{inactivation (p21 and p27)} \\ &+ \text{extracellular signalling (Ras-Raf-Erk pathway, E2F1)} \\ &+ \text{pRb interaction}\end{aligned}$$

The terms [CycD] and [CycD: Cdk] describe production of cyclin D and the complex forming CycD/Cdk4,6.

What accounts for this over-expression (protein levels at higher than normal levels (Weinberg, 2007)) of complex forming CycD/Cdk4,6? The shut-

down of the tumour suppressor gene $p16^{INK4a}$ leads to the over-expression of the complex and over-expression of cyclin D occurs due to the altering of the upstream signalling pathway. The E2F1 transcription factor is included here as it binds with pRb in an unphosphorylated or hypophosphorylated state.

In cancer cells, particularly in cancerous melanoma cells, pRb is inactivated abnormally by the CycD/Cdk4,6 complex. We need to account for this abnormal inactivation in our modelling by assigning an interaction expression between pRb and CycD/Cdk4,6.

One aspect that needs refining in this type of modelling is the incorporation of the protein $p16^{INK4a}$. We include this protein, and some of the associated interactions, into the ordinary differential system of equations we present. We firstly need to understand how the protein $p16^{INK4a}$ works in the cell cycle of melanoma growth and then how to define the growth rate of the protein in mathematical modelling terms.

Research has suggested that protein $p16^{INK4a}$ is activated at particular stages of melanoma growth (Rizos et al., 1999). Rizos et al propose in their 1999 paper, that primary melanoma cells would not be able to recognise a cell mutation when mutated $p16^{INK4a}$ was present. Hence, the cell would not undergo apoptosis after the G1 checkpoint, instead the cell would stay in the cell cycle leading to unbounded cell proliferation (Rizos et al., 1999).

Another article by Sharpless and Chin, see (Sharpless and Chin, 2003), also suggests that the mutated $p16^{INK4a}$ protein influences a melanoma cell to stay in the cell cycle after the G1 phase. They also suggest that the inactivation of this protein, in melanoma, is a result of activity occurring in the pathway

associated with Rb, see Chapter 2, Section 2.2.2.

The system of ordinary differential equations below describe the kinetics occurring between CyclinD and its kinase Cdk4,6 (we have combined Cdk4 and Cdk6 due to their similar properties). We also include interaction with the protein p16^{INK4a}. The system is presented as follows,

$$\frac{dx}{dt} = -a_1xy + d_1z\,, \tag{5.8}$$

$$\frac{dy}{dt} = -a_1xy + (d_1 + k_1)z\,, \tag{5.9}$$

$$\frac{dz}{dt} = a_1xy - (d_1 + k_1)z - b_1u\,, \tag{5.10}$$

where,

x : concentration of cyclin D,

y : concentration of Cdk4,6,

z : complex CycD/Cdk4,6 in active state,

u : concentration of p16$^{\mathrm{INK4a}}$.

The rate constants are given as a_1, d_1, k_1 and b_1, and are described by Michaelis-Menten kinetics.

Michaelis-menten kinetics are used to establish the first equations that describe the rates of formation for the complexes of CycD/Cdk4,6 and CycE/Cdk2 which both influence the G1 phase of the cell cycle of melanoma growth (Bandyopadhyay et al., 2001). In particular, upon entering the R point in the cell cycle, where a cell gets the ultimate say on its future - stay in a quiescent state, either return to the cycle or go through programmed cell death (apoptosis).

The model we develop will only incorporate the CycD/Cdk4,6 complex, but we discuss later in Chapter 6 the inclusion of complex CycE/Cdk2 in our future work.

We can assign parameter values to represent the over-expression of cyclin D and the complexes the cyclins form with its associated Cdk's (4 and 6). An inhibition in the tumour suppressor protein pRb will also need to be shown here as the over-expression in cyclin D will also contribute to this protein being shutdown.

The time scale, t, for complexes, binding of proteins, signalling pathways, etc is measured in minutes. Length and size scales are not considered here and as a result the system is a set of ordinary differential equations rather than a set of partial differential equations. Cell mass is ignored at early stages of modelling but may be incorporated later on. Exit from mitosis is not considered here, hence we will not consider interaction with APC/Cdh1 or APC/Cdc20 complexes. The mammalian cell cycle will be assumed but some features may relate to the yeast cell cycle depending on research and data that is attainable. No control mechanism is incorporated at this stage of the research but an extension to the model would be a control mechanism in the form of a drug treatment. We consider hypophosphorylation of pRb as we are only concentrating on the G1 phase of the cell cycle at present. With these considerations in mind, we have the following model,

$$\frac{dv}{dt} = \frac{K_{max}v}{K_n + v} + \frac{k_7}{k_8 + u} + k_9 w - v_{deg} v \,, \tag{5.11}$$

$$\frac{dw}{dt} = k_5 v w + k_6 v - w_{deg} w \,, \tag{5.12}$$

$$\frac{du}{dt} = k_3 v + k_4 v u - u_{deg} u \,, \tag{5.13}$$

$$\frac{df}{dt} = \frac{f^2}{{K_f}^2} \frac{K_n}{K_n + p} - k_{10} p + k_{11} w f \,, \tag{5.14}$$

where,

u : the concentration of $\mathrm{p16^{INK4a}}$,

v : the concentration of Braf,

w : the concentration of MEK,

f : the concentration of E2F1,

K_n : Michaelis constant,

K_{max} : catalytic rate constant,

v_{deg} : the degradation term for Braf,

w_{deg} : the degradation term for MEK,

u_{deg} : the degradation term for $\mathrm{p16^{INK4a}}$,

k_3 to k_{11} : rate constants.

The variable u represents the average concentration of $\mathrm{p16^{INK4a}}$ as before. Equation (5.14) is based on work by Swat et al (Swat et al., 2004) and our own understanding of the transcription factor E2F1 in relation to melanoma growth. We have used an adapted version of the Hill equation from biochemistry in equation (5.14). The Hill coefficient is equal to 2 here (>1) due to

E2F1 being treated as an activator of protein regulation and it is known to regulate cell cycle progression (Wenzel et al., 2011).

We extend the equation to describe the rate of production of the CyclinD/Cdk4,6 complex, variable z, which is given below,

$$\begin{aligned}\frac{dz}{dt} = a_1xy - (d_1z + k_1)z + \\ z_{ovr}z - b_1u + k_2zu\,,\end{aligned} \tag{5.15}$$

where,

k_1 : rate constant,

d_1 : rate constant,

z_{ovr} : a term to define the over-expression of the complex.

We chose to model from the start of the G1 phase of the cell cycle to the restriction point, as this is when cyclinD/CDK4,6 complexes are most active (Weinberg, 2007). CyclinD1 only influences G1 phase of the cell cycle as it is exported to the cytoplasm after G1/S transition. Also during the G1 phase of the cell cycle is when extracellular signals influence cell cycle progression the most. These signals communicate with the D-type cyclins and their forming complexes to aid cycle progression. The complex forming CyclinD/Cdk4,6 is said to go into a hyperactive state (rate of formation increased) which leads to inappropriate inactivation of pRb for tumour cells (Weinberg, 2007).

The rate of formation of cyclin D will depend, initially, on extracellular signalling as cyclin D communicates with the cell cycle clock and alerts it to

any extracellular activity. This is in order for the cell cycle clock to make appropriate updates to the cycle progression (Weinberg, 2007).

We now present the complete system for our melanoma model below,

$$\frac{dx}{dt} = -a_1 xy + d_1 z\,, \tag{5.16}$$

$$\frac{dy}{dt} = -a_1 xy + (d_1 + k_1) z\,, \tag{5.17}$$

$$\frac{dv}{dt} = \frac{K_{max} v}{K_n + v} + \frac{k_7}{k_8 + u} + k_9 w - v_{deg} v\,, \tag{5.18}$$

$$\frac{dw}{dt} = k_5 vw + k_6 v - w_{deg} w\,, \tag{5.19}$$

$$\frac{du}{dt} = k_3 v + k_4 vu - u_{deg} u\,, \tag{5.20}$$

$$\frac{df}{dt} = \frac{f^2}{{K_f}^2} \frac{K_n}{K_n + p} - k_{10} p + k_{11} wf\,, \tag{5.21}$$

$$\frac{dz}{dt} = a_1 xy - (d_1 + k_1) z + z_{ovr} z - b_1 u + k_2 zu\,, \tag{5.22}$$

$$p = k_{12} pz - p_{deg}\,, \tag{5.23}$$

where,

x : concentration of cyclin D,

y : concentration of Cdk4,6,

z : complex CycD/Cdk4,6 in active state,

u : concentration of $\mathrm{p16^{INK4a}}$,

v : concentration of Braf,

w : concentration of MEK,

f : concentration of E2F1,

p : concentration of pRb,

K_n : Michaelis constant,

K_{max} : catalytic rate constant,

K_f : Michaelis constant for Hill equation,

v_{deg} : degradation term for Braf,

u_{deg} : degradation term for $p16^{INK4a}$,

w_{deg} : degradation term for MEK,

p_{deg} : degradation term for pRb,

k_1 to k_{12} : rate constants,

a_1 : rate constant,

b_1 : rate constant,

d_1 : rate constant,

z_{ovr} : a term to define the over-expression of the complex.

Due to the requirement of extensive biological experimentation and no access to appropriate data, we are unable to determine parameter estimations for our model at present. However, were such data available, the techniques presented in Chapter 4 could be readily used to determine optimal parameter values.

5.4 Discussion

In this chapter we have given a brief overview of the existing mathematical modelling of melanoma growth and a review on the kinetics required to model such a growth.

We have then developed a theoretical model for melanoma growth with explanations linking the biology and mathematics of this particular cancer growth together.

In the future we will extend the model presented in Chapter 5 to include protein interactions occurring between MEK and E2F1. We will also include pRb phosphorylation for the G1 phase of the cell cycle and the interaction occurring between pRb with both cyclinD and E2F1. We also require simulations on the theoretical model and parameter optimisation on both the simple model presented here and future extended models.

The model we present also did not consider exit from mitosis. Hence, interactions among certain protein complexes, such as CyclinB and CDC2 (Weinberg, 2007), were not incorporated in the model. Further development of the model would see this feature included making it more inline with a real-world scenario.

The model presented here has not been developed in this form anywhere else, as far as we are aware. Due to the lack of biological data available for the Braf protein, in particular, when the protein is mutated, we have been unable to perform computational simulations on the model we developed in Section 5.3. From our investigations we could not find a mathematical model like the one we have presented that has modelled this particular protein, mak-

ing it difficult to accurately attain parameter estimations. In general, fitting appropriate parameter values to the model we have developed is currently not achievable due to time restrictions and the need to find adequate biological data. In principle the parameter fitting methods discussed would be used to fit the model once experimental data was obtained. In this sense, our work also gives valuable guidance to biologists in terms of the kind of experiments and experimental data that are needed in the future to make progress in this area.

Chapter 6

Conclusion and Future Work

We have presented work throughout this thesis that both challenges and provides insight into the mathematical modelling of cancer growth using optimisation techniques.

We introduced the theory and background into optimal control theory and optimal parameter selection in Chapter 1. We provided the basic theorems and concepts in this area of optimisation most relevant to our research and how we intended to apply them. We also gave insight into how optimisation techniques can be used in the biological arena. We presented some reviews on optimal control and how it can be applied to treatment scheduling of cancer growth.

In Chapter 2 we gave a detailed background into cell cycle and cancerous growth due to the biological nature of this research. We firstly gave an overview of each phase of the cell cycle, G1 through to M. We also gave our own interpretation of the RAS signalling pathway which relates to the model we developed in Chapter 5. A detailed discussion is given on cancer, how it grows

and spreads, and the many proteins associated with its development. We also gave a summary relating to particular proteins and the specific cancers they are connected with. The chapter finishes with a review on the biochemical kinetics that relate to our research.

We provided a literature review and background in Chapter 3 on the mathematical modelling of cell growth for both cancer and non-cancerous cell cycles. Our initial discussion was on the yeast cell cycle models published by Tyson and Novak (Tyson et al., 1995; Novak et al., 1998b; Tyson and Novak, 2001). We also gave a review on a mammalian cell cycle model by Tyson and Novak (Novak and Tyson, 2004). This model showed the mathematical complexities in modelling a mammalian cell cycle and was done through the use of a system of ordinary differential equations. We then give a detailed discussion of a model by Alarcón et al who describe a generic cell cycle model for cancer growth. We also highlight some important focal points with the model as we use this model in Chapter 4 for our optimal parameter selection problem.

In Chapter 3 we also provide a kinetic analysis applied to the model by Tyson and Novak (Tyson and Novak, 2001). This aids the work we present in Chapter 4 by revealing the nature of kinetics and the impact kinetic type equations can have on a mathematical system describing biological occurrences.

The main focus of our research we presented in Chapter 4. We were able to show the effectiveness of using optimal parameter selection techniques on both cancer and non-cancerous cell cycle models. We show how well the optimisation software we used is able to produce optimised parameters that

give a near match for the non-cancerous model when duplicated. This is an important result as it shows how well the software is able to obtain a match with different starting guesses for the parameters.

We then discuss the results we were able to duplicate for the cancer based model and the difficulties that we encountered trying to achieve this. We detailed our motivation for using optimal parameter selection techniques with some numerical discussion relating to the published work on the cancer based model. Our model development is then presented along with implementation using Multiple Characteristic Time points for the cancer model. There is a discussion on our results and how optimising the model parameters still led to differing results to those published. We then give an analysis of several possible reasons for this mismatch. In particular we identify a possible error in the mathematical representation of a particular protein in the cancer based model and present a possible solution.

Chapter 5 introduces our own theoretical model for melanoma growth. As there is very little modelling seen in this field we gave a brief review of two fundamentally different models we know to exist. A review of the kinetics from Chapter 2 is then given. We present a new model, in the form of a set of ordinary differential equations, for melanoma growth. In particular, we place emphasis on the modelling of the Braf protein which to our knowledge has yet to be mathematically modelled. The complete system is presented at the end of the Chapter with a discussion on what we have achieved and what can be achieved in the future.

6.1 Future Work

The main focus of this research has been optimising parameters for the mathematical modelling of cancer growth, with this in mind we need to consider how we can extend this work. We recall that a biological misinterpretation was discovered in the system of equations by Alarcón et al (Alarcón et al., 2004a) that we presented in Chapter 4. The first step in our future work would be to make appropriate changes to the particular equations to better represent the biological setting being modelled. As already outlined in Chapter 4 a good starting point would be to consider the model by Tyson and Novak who successfully model the G1/S phase of the yeast cell cycle (Tyson and Novak, 2001).

For the model we present in Chapter 5 on melanoma growth the next step forward would be to incorporate a control function in the model that would represent a treatment for a particular type of cancer. Since the latter part of this research has focussed around melanoma growth then a treatment for this type of cancer would be the most suitable option.

We would ideally like to stop the mutation from occurring at the G1/S phase of the cell cycle by manipulating that phase of the cycle using an appropriate control such as a targeted drug treatment. As a control function we could model a drug that inhibits or minimises hypoxia in cancer growth which may lead to a halt in cancer growth or at least a slower rate of growth. Considering a control function to represent a particular treatment by ways of representing a new treatment that is being used in clinical trials, can help ascertain its outcome on patient survival. The use of a control function in this

environment would also help with the effectiveness of treatment and could help plan for optimal treatment scheduling.

We also need to consider minimising cancer cells while maximising the survival of normal cells as patients are undergoing specific treatment. Ideally it would be beneficial to find a treatment by way of a drug or alternative medicine that minimises the effects of certain proteins that may harvest mutations which lead to cancerous growth. For example, in melanoma the proteins to consider would be pRb, p15, p16 and of course the mutant Braf gene which appears quite prevalent in many melanoma cases, see references (Cui and Guadagno, 2008; Davies et al., 2002; Michaloglou et al., 2005, 2008; Libra et al., 2005).

Incorporating a treatment expression is the final step to this modelling process. We would use optimal control theory and optimal parameter selection techniques to enable the model to be used in real-life settings. The ability to model using optimal control or optimal parameter selection in relation to a melanoma growth is something that would be of great benefit. A control mechanism to describe treatment scheduling of melanoma, with either pre-existing treatments or by analysing the effectiveness of using optimal control strategies of a new treatment.

In our research we have found that most proteins are prevalent in many different cancers. The question we ask is, what links these proteins together and how can we effectively use mathematics to describe this relationship? We have shown that mathematics is a tool that can be used successfully to answer such questions. We have also shown through the use of mathematical optimisation how these cancers grow and more importantly, how we may better understand and model them in the future.

Appendix A

Implementation of the Tyson-Novak model

Below is the code that was used to implement the model published by Tyson and Novak describing the cell division cycle of a budding yeast cell Tyson and Novak (2001). The model was implemented using MapleV11.0, classical worksheet environment, on a Dell with Intel©Core2Duo processor.

```
> restart;
```

```
> with(plots);
```

[*animate*, *animate3d*, *animatecurve*, *arrow*, *changecoords*, *complexplot*, *complexplot3d*, *conformal*, *conformal3d*, *contourplot*, *contourplot3d*, *coordplot*, *coordplot3d*, *densityplot*, *display*, *fieldplot*, *fieldplot3d*, *gradplot*, *gradplot3d*, *graphplot3d*, *implicitplot*, *implicitplot3d*, *inequal*, *interactive*, *interactiveparams*, *intersectplot*, *listcontplot*, *listcontplot3d*, *listdensityplot*, *listplot*, *listplot3d*, *loglogplot*, *logplot*, *matrixplot*, *multiple*, *odeplot*, *pareto*, *plotcompare*, *pointplot*, *pointplot3d*, *polarplot*, *polygonplot*, *polygonplot3d*, *polyhedra_supported*, *polyhedraplot*, *rootlocus*, *semilogplot*, *setcolors*, *setoptions*, *setoptions3d*, *spacecurve*, *sparsematrixplot*, *surfdata*, *textplot*, *textplot3d*, *tubeplot*]

Var's: x(t) = [CycB], y(t) = [Cdh1], v(t) = [Cdcd20T], u(t) = [Cdc20A], w(t) = [IEP], m(t) = m.

```
> sys2:=
> {diff(x(t),t)=k1-(k2p+k2pp*y(t))*x(t),diff(y(t),t)=(k3p+k3pp*u(t))*(1
> -y(t))/(J3+1-y(t))-k4*m(t)*x(t)*y(t)/(J4+y(t)),diff(v(t),t)=k5p+k5pp*(
> x(t)*m(t)/J5)^n/(1+(x(t)*m(t)/J5)^n)-k6*v(t),diff(u(t),t)=k7*w(t)*(v(t
> )-u(t))/(J7+v(t)-u(t))-k8*MAD*u(t)/(J8+u(t))-k6*u(t),diff(w(t),t)=k9*m
> (t)*x(t)*(1-w(t))-k10*w(t),diff(m(t),t)=mu*m(t)*(1-m(t)/mstar)};
```

$$sys2 := \left\{ \frac{d}{dt}\,\mathrm{x}(t) = k1 - (k2p + k2pp\,\mathrm{y}(t))\,\mathrm{x}(t),\right.$$

$$\frac{d}{dt}\,\mathrm{y}(t) = \frac{(k3p + k3pp\,\mathrm{u}(t))\,(1 - \mathrm{y}(t))}{J3 + 1 - \mathrm{y}(t)} - \frac{k4\,\mathrm{m}(t)\,\mathrm{x}(t)\,\mathrm{y}(t)}{J4 + \mathrm{y}(t)},$$

$$\frac{d}{dt}\,\mathrm{v}(t) = k5p + \frac{k5pp\,(\frac{\mathrm{x}(t)\,\mathrm{m}(t)}{J5})^n}{1 + (\frac{\mathrm{x}(t)\,\mathrm{m}(t)}{J5})^n} - k6\,\mathrm{v}(t),$$

$$\frac{d}{dt}\,\mathrm{u}(t) = \frac{k7\,\mathrm{w}(t)\,(\mathrm{v}(t) - \mathrm{u}(t))}{J7 + \mathrm{v}(t) - \mathrm{u}(t)} - \frac{k8\ MAD\,\mathrm{u}(t)}{J8 + \mathrm{u}(t)} - k6\,\mathrm{u}(t),$$

$$\left.\frac{d}{dt}\,\mathrm{w}(t) = k9\,\mathrm{m}(t)\,\mathrm{x}(t)\,(1 - \mathrm{w}(t)) - k10\,\mathrm{w}(t),\ \frac{d}{dt}\,\mathrm{m}(t) = \mu\,\mathrm{m}(t)\,(1 - \frac{\mathrm{m}(t)}{mstar})\right\}$$

Parameter values.

```
> k1:=0.04;k2p:=0.04;k2pp:=1.0;k3p:=1.0;k3pp:=10;k4:=35;k5p:=0.005;k5pp
> :=0.2;k6:=0.1;k7:=1.0;k8:=0.5;k9:=0.1;k10:=0.02;J3:=0.04;J4:=0.04;J5:=
> 0.3;J7:=10^(-3);J8:=10^(-3);MAD:=1.0;n:=4;mu:=0.01;mstar:=10;
```

$$k1 := 0.04$$

$$k2p := 0.04$$

$$k2pp := 1.0$$

$$k3p := 1.0$$

$$k3pp := 10$$

$$k4 := 35$$

$$k5p := 0.005$$

$$k5pp := 0.2$$

$$k6 := 0.1$$

$$k7 := 1.0$$

$$k8 := 0.5$$

$$k9 := 0.1$$

$$k10 := 0.02$$

$$J3 := 0.04$$

$$J4 := 0.04$$

$$J5 := 0.3$$

$$J7 := \frac{1}{1000}$$

$$J8 := \frac{1}{1000}$$

$$MAD := 1.0$$

$$n := 4$$

$$\mu := 0.01$$

$$mstar := 10$$

```
> init2:={x(0)=0.5,y(0)=1.0,v(0)=1.8,u(0)=1.3,w(0)=0.7,m(0)=0.6};
```

$$init2 := \{\mathrm{x}(0) = 0.5,\ \mathrm{y}(0) = 1.0,\ \mathrm{u}(0) = 1.3,\ \mathrm{w}(0) = 0.7,\ \mathrm{m}(0) = 0.6,\ \mathrm{v}(0) = 1.8\}$$

```
> sol2:=dsolve(sys2 union
> init2,numeric,method=classical[rk4]);
```

$$sol2 := \mathbf{proc}(x\_classical) \ldots \mathbf{end\ proc}$$

```
> odeplot(sol2,[[t,x(t)],[t,y(t)]],0..100);
```

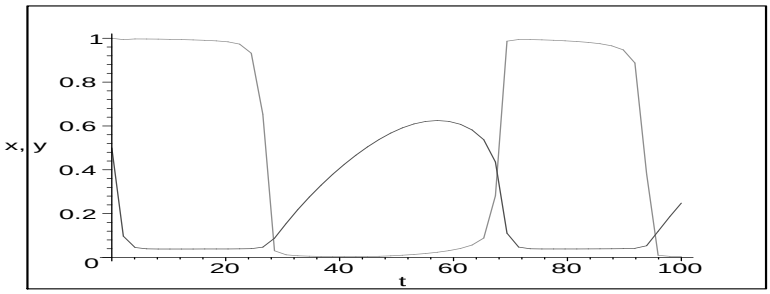


```
> odeplot(sol2,[[t,v(t)],[t,u(t)]],0..100);
```

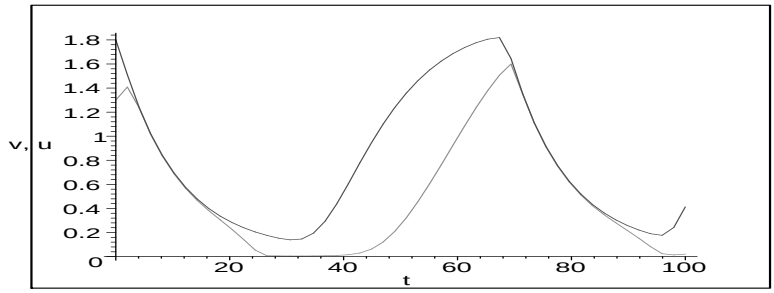


```
> odeplot(sol2,[t,m(t)],0..70);
```

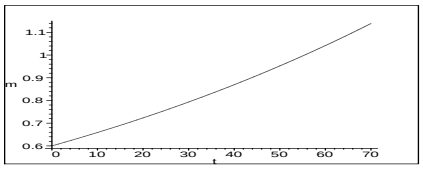

Appendix B

Matlab and Fortran90 code

Below is the Fortran90 code that produced Figure 4.1(a) and Figure 4.1(b) from Chapter 4 implemented on a Silicon Graphics Machine, Sunsparc Netra.

```
!!!!!!!!!!!!!!!!!!!!!!!!!!!!!!!!!!!!!!!!!!!!!!!!!!!!!!!!!!!!!!!!!!!!!!!!!
!This program uses a runge-kutta order 4 subroutine to solve a system!
!of ODE's that describe the cell cycle for a  cancer cell              !
! depending on set parameter values and the equation describing the   !
!concentration of p27.  Filename: cancerrk4.f90                        !
```

```
!
    !
!
    !!!!!!!!!!!!!!!!!!!!!!!!!!!!!!!!!!!!!!!!!!!!!!!!!!!!!!!!!!!!!!!!!!!!!!!

MODULE CONST
  IMPLICIT NONE
  INTEGER,PARAMETER::range=SELECTED_REAL_KIND(30)
END MODULE CONST

PROGRAM cancerrk4
  USE CONST
  IMPLICIT NONE

!
    !!!!!!!!!!!!!!!!!!!!!!!!!!!!!!!!!!!!!!!!!!!!!!!!!!!!!!!!!!!!!!!!!!!!!!!
!Define global variables, TO is the initial value of
    time T.                 !
!H is the value of step size h.
                                                            !
```

```
!TEND is the final value of time T.
                                                                !
!X(5) holds the values of the functions x(t), y(t), m(t)
    , z(t) and u(t)!
!F is the array that holds the values of the derivatives
     i.e                !
!dx/dt, dy/dt, dm/dt, dz/dt and du/dt.
                                                            !
!XWRK is the array that stores the value at each step of
     the                !
!runge-kutta algorithm.
                                                                              !

    !
!N is the number of equations to be solved.
                                                      !
!

    !
!
    !!!!!!!!!!!!!!!!!!!!!!!!!!!!!!!!!!!!!!!!!!!!!!!!!!!!!!!!!!!!!!!!!!!!!!!!!


REAL(KIND=range) :: TO,H,TEND,T
```

```
32 REAL(KIND=range) ::F(5),XEND(5),X(5)
33 REAL,PARAMETER::m_star = 10.0,XTHR = 0.004,YTHR=0.05
34 INTEGER::N,M,K
35
36 !Set values for TO, TEND and H.
37
38   OPEN(10,FILE='cancera_p1.out')
39
40   TO = 0.0
41   TEND = 1000.0
42   H = 0.001
43
44   N = 5
45   M = INT((TEND-TO)/H)
46
47 ! Initial values for the array X(5) i.e x(0),y(0),m(0),z
       (0) and u(0)
48
49   X(1) = 0.9_range
50   X(2) = 0.001_range
51   X(3) = m_star/2.0_range
52   X(4) = 0.0_range
53   X(5) = 1.0_range
54
```

```
55    WRITE(10,15)TO,X(1:N)
56
57  !This loop will solve the system of equations to find
        solutions for
58  !X(5), for M iterations.
59
60    DO K = 1,1
61
62    CALL RKSYST(TO,H,X,XEND,m_star,F,N)
63    TO = TO + H
64    WRITE(10,15)TO,XEND(1:N)
65     15 FORMAT(1X,F8.3,1X,5F13.9)
66
67  ! Checking to see if x(t) and y(t) have met threshold
        values and if so
68  ! XEND(:) will return to initial states.  Else will keep
        looping.
69
70    IF  (XEND(1)<XTHR.AND.XEND(2)>YTHR) THEN
71       XEND(3) = m_star/2.0_range
72       XEND(4) = 0.0_range
73       XEND(1) = 0.9_range
74       XEND(2) = 0.001_range
75       XEND(5) = 1.0_range
```

```
  ENDIF
  X(:) = XEND(:)

 ENDDO

 CLOSE(10)

END PROGRAM cancerrk4

!!!!!!!!!!!!!!!!!!!!!!!!!!!!!!!!!!!!!!!!!!!!!!!!!!!!!!!!!!!!!!!
! This subroutine establishes the derivatives to be           !
! used in the runge-kutta subroutine to solve for             !
! x(t), y(t), m(t), z(t) and u(t)                             !
!!!!!!!!!!!!!!!!!!!!!!!!!!!!!!!!!!!!!!!!!!!!!!!!!!!!!!!!!!!!!!!

SUBROUTINE DERIVS(X,T,m_star,F)

 USE CONST
 IMPLICIT NONE

 ! Declare variables

 REAL(KIND=range),INTENT(IN)::X(5),T,m_star
 REAL(KIND=range),INTENT(OUT)::F(5)
```

```
100   ! INTEGER,INTENT(IN) :: N
101
102   ! Parameter values for system of ODE's given. Local
          parameters.
103
104   REAL,PARAMETER:: a_4 = 0.04, a_1 = 0.04, a_2 = 1.0, a_3
          = 0.25,&
105                    b_3 = 10, b_4 = 3.5, eta = 0.01, J_3 =
                           0.04,&
106                    J_4 = 0.04, c_1 = 0.007, c_2 = 0.01, B
                           = 0.01,&
107                    d_1 = 0.01, d_2 = 0.1, P = 1.0
108
109   ! Derivative equations defined.
110
111   F(1) = (1 + b_3*X(5))*(1 - X(1))/(J_3 + 1 - X(1)) - &
112            (b_4*X(3)*X(1)*X(2))/(J_4 + X(1))
113   F(2) = a_4 - (a_1 + a_2*X(1) + a_3*X(4))*X(2)
114   F(3) = eta*X(3)*(1 - (X(3)/m_star))
115   F(4) = c_1 - (c_2*P*X(4))/(B + P)
116   F(5) = d_1 - (d_2 + d_1*X(2))*X(5)
117
118 END SUBROUTINE DERIVS
119
```

```
!!!!!!!!!!!!!!!!!!!!!!!!!!!!!!!!!!!!!!!!!!!!!!!!!!!!!!!!
! This subroutine solves for x(t),y(t),m(t),z(t) and  !
! u(t) using the subroutine DERIVS and the 4th order  !
! runge-kutta numerical technique. It is called       !
! through the main program.                           !
!!!!!!!!!!!!!!!!!!!!!!!!!!!!!!!!!!!!!!!!!!!!!!!!!!!!!!!!

SUBROUTINE RKSYST(TO,H,X,XEND,m_star,F,N)

  USE CONST
  IMPLICIT NONE

  ! Declare global variables

  REAL(KIND=range),INTENT(INOUT)::X(5),TO,XEND(5),F(5)
  REAL(KIND=range),INTENT(IN)::H,m_star
  INTEGER,INTENT(IN)::N

  ! Declare any local variables, such as the increment count.

  INTEGER::I
  REAL(KIND=range)::XWRK(4,5)

```

```
143   ! Calculate the first estimates K1.
144
145   XWRK(1:4,1:5)=0.0
146
147   CALL DERIVS(X,TO,m_star,F)
148
149   DO I=1,N
150      XWRK(1,I) = H*F(I)
151      XEND(I) = X(I) + XWRK(1,I)/2.0_range
152      WRITE(10,*) XEND(I)
153   ENDDO
154
155   ! Calculate the second estimates K2.
156
157   CALL DERIVS(XEND,TO+H/2.0,m_star,F)
158
159   DO I=1,N
160      XWRK(2,I) = H*F(I)
161      XEND(I) = X(I) + XWRK(2,I)/2.0_range
162      WRITE(10,*) XEND(I)
163   ENDDO
164
165   ! Calculate the third estimates K3.
166
```

```
167   CALL DERIVS(XEND,TO+H/2.0,m_star,F)
168
169   DO I=1,N
170      XWRK(3,I) = H*F(I)
171      XEND(I) = X(I) + XWRK(3,I)
172      WRITE(10,*) XEND(I)
173   ENDDO
174
175    ! Final estimate K4.
176
177   CALL DERIVS(XEND,TO+H,m_star,F)
178
179   DO I=1,N
180      XWRK(4,I) = H*F(I)
181      WRITE(10,*) XWRK(4,I)
182   ENDDO
183
184    ! Compute the values for each of x(t), y(t), m(t), z(t
          ) and u(t) in
185    ! array X at the end of each time step.
186
187   DO I=1,N
188    XEND(I) = X(I) + (XWRK(1,I) + 2.0*XWRK(2,I) &
189  + 2.0*XWRK(3,I) + XWRK(4,I))/6.0_range
```

```
190     WRITE(10,*) XEND(I)
191     ENDDO
192
193     RETURN
194
195 END SUBROUTINE RKSYST
```

The code below is an M-file created and used in Matlab R2010b to produce Figure 4.2 from Chapter 4. The Matlab function solver **ode15s** was used in conjunction with the M-file below to generate data for plotting.

```
1 function dx=alarcon(t,x)
2     dx=zeros(5,1);
3     P=1.0;
4     dx(1)=(1+10*x(5))*(1-x(1))/(0.04+1-x(1))-35*x(3)*x(1)*
          x(2)/(0.04+x(1));
5     dx(2)=0.04-(0.04+1.0*x(1)+0.25*x(4))*x(2);
6     dx(3)=0.01*x(3)*(1-x(3)/10);
7     dx(4)=0.007-0.01*P*x(4)/(0.01+P);
8     dx(5)=0.1-(0.1+0.01*x(2))*x(5);
```

Appendix C

Stability Analysis

In this appendix we attach the Maple output for the stability analysis that was conducted on the model published by Alarcón et al (Alarcón et al., 2004a).

For a stability analysis of a non-linear first-order differential system we must first write the system in the form of a vector.

$$\begin{aligned}
\frac{dx}{d\tau} &= \frac{(1+b_3)(1-x)}{J_3+1-x} - \frac{b_4 m x y}{J_4+x}, \\
\frac{dy}{d\tau} &= a_4 - (a_1 + a_2 x + a_3 z)y, \\
\frac{dm}{d\tau} &= \eta m\Big(1 - \frac{m}{m_*}\Big), \\
\frac{dz}{d\tau} &= c_1 - c_2 \frac{P}{B+P} z, \\
\frac{du}{d\tau} &= d_1 - (d_2 + d_1 y)u,
\end{aligned}$$

We can re-write the above system in vector form as follows.

Let

$$\boldsymbol{x} = [x_1, x_2, x_3, x_4, x_5]^\top, \tag{C.1}$$

where,

x : x_1,

y : x_2,

m : x_3,

z : x_4

u : x_5.

The matrix for calculating the Jacobian is as follows,

$$\boldsymbol{f}(\boldsymbol{y}) = \begin{bmatrix} f_1(x_1, \ldots, x_5) \\ f_2(x_1, \ldots, x_5) \\ f_3(x_1, \ldots, x_5) \\ f_4(x_1, \ldots, x5) \\ f_5(x_1, \ldots, x_5) \end{bmatrix}$$

where, $\dfrac{d\boldsymbol{y}}{dt} = \boldsymbol{f}(\boldsymbol{y})$.

The Maple code is as follows,

```
> restart:
> b3:=10;b4:=35;m1:=10;eta:=0.01;J3:=0.04;J4:=0.04;a4:=0.04;a1:=0.5;a2:
> =1;a3:=0.25;c1:=0.1;c2:=0.01;B:=0.01;d1:=0.01;d2:=0.1;P:=1;
```

$$b3 := 10$$

$$b4 := 35$$

$$m1 := 10$$

$$\eta := 0.01$$

$$J3 := 0.04$$

$$J4 := 0.04$$

$$a4 := 0.04$$

$$a1 := 0.5$$

$$a2 := 1$$

$$a3 := 0.25$$

$$c1 := 0.1$$

$$c2 := 0.01$$

$$B := 0.01$$

$$d1 := 0.01$$

$$d2 := 0.1$$

$$P := 1$$

```
> dx:=(1+b3*u)*(1-x)/(J3+1-x)-(b4*m*x*y)/(J4+x);dy:=a4-(a1+a2*x+a3*z)*y
> ;dm:=eta*m*(1-m/m1);dz:=c1*(1-m/m1)-c2*(P/(B+P))*z;du:=d1-(d2+d1*y)*u;
```

$$dx := \frac{(1+10\,u)\,(1-x)}{1.04-x} - \frac{35\,m\,x\,y}{0.04+x}$$

$$dy := 0.04 - (0.5 + x + 0.25\,z)\,y$$

$$dm := 0.01\,m\,(1 - \frac{m}{10})$$

$$dz := 0.1 - 0.01000000000\,m - 0.009900990099\,z$$

$$du := 0.01 - (0.1 + 0.01\,y)\,u$$

```
> dfx:=diff(dx,x);
```

$$dfx := -\frac{1+10\,u}{1.04-x} + \frac{(1+10\,u)\,(1-x)}{(1.04-x)^2} - \frac{35\,m\,y}{0.04+x} + \frac{35\,m\,x\,y}{(0.04+x)^2}$$

```
> dfxu:=diff(du,x);
```

$$dfxu := 0$$

```
> dfxm:=diff(dm,x);
```

$$dfxm := 0$$

```
> dfxy:=diff(dy,x);
```

$$dfxy := -y$$

```
> dfx1:=subs({u=dfxu,m=dfxm,y=dfxy},dfx);
```

$$dfx1 := -\frac{1}{1.04 - x} + \frac{1 - x}{(1.04 - x)^2}$$

```
> xzero:=subs(x=0.9,dfx1);
```

$$xzero := -2.040816327$$

```
> exp(1)/xzero;
```

$$-0.4899999999\, e$$

```
> evalf(%);
```

$$-1.331958095$$

```
> dfy:=diff(dy,y);
```

$$dfy := -0.5 - x - 0.25\, z$$

```
> dfyx:=diff(dx,y);
```

$$dfyx := -\frac{35\, m\, x}{0.04 + x}$$

```
> dfyz:=diff(dz,y);
```

$$dfyz := 0$$

```
> dfy1:=subs({x=dfyx,z=dfyz},dfy);
```

$$dfy1 := -0.5 + \frac{35\, m\, x}{0.04 + x}$$

```
> yzero:=subs({x=0.9,m=m1/2},dfy1);
```

$$yzero := 167.0531915$$

```
> evalf(exp(1)/yzero);
```

$$0.01627195388$$

```
> dfm:=diff(dm,m);
```

$$dfm := 0.01 - 0.002000000000\, m$$

```
> mzero:=subs(m=m1/2,dfm);
```

$$mzero := 0.$$

```
> dfz:=diff(dz,z);
```

$$dfz := -0.009900990099$$

```
> evalf(exp(1)/dfz);
```

$$-274.5464646$$

```
> dfu:=diff(du,u);
```

$$dfu := -0.1 - 0.01\, y$$

```
> dfuy:=diff(du,y);
```

$$dfuy := -0.01\, u$$

```
> dfu1:=subs(y=dfuy,dfu);
```

$$dfu1 := -0.1 + 0.0001\, u$$

```
> uzero:=subs(u=1.0,dfu1);
```

$$uzero := -0.09990$$

```
> evalf(exp(1)/uzero);
```

$$-27.21002831$$

References

Alarcón, T., Byrne, H. M., and Maini, P. K. 2003. A cellular automaton model of tumour growth in inhomogeneous environmnent. *Journal of Theoretical Biology*, 225(2):257–274.

Alarcón, T., Byrne, H. M., and Maini, P. K. 2004a. A mathematical model of the effects of hypoxia on the cell-cycle of normal and cancer cells. *Journal of Theoretical Biology*, 229(3):397–411.

Alarcón, T., Byrne, H. M., and Maini, P. K. 2004b. Towards whole-organ modelling of tumour growth. *Progress in Biophysics and Molecular Biology*, 85(2-3):451–472.

Alarcón, T., Byrne, H. M., and Maini, P. K. 2005. A multiple scale model for tumour growth. *Multiscale Modelling and Simulation*, 3(2):440–475.

Alarcón, T., Owen, M. R., Byrne, H. M., and Maini, P. K. 2006. Multiscale modelling of tumour growth and therapy:the influence of vessel normalisation on chemotherapy. *Computational and Mathematical Methods in Medicine*, 7(2-3):85–119.

Alberts, B., Johnson, A., Lewis, J., Raff, M., Roberts, K., and Walter, P. 2008. *Molecular Biology of the Cell*. Garland Science, New York, fifth edition.

Anderson, A. R. A. 2005. A hybrid mathematical model of solid tumour invasion: the importance of cell adhesion. *Mathematical Medicine and Biology*, 22(2):163–186.

Araujo, R. P. and McElwain, D. L. S. 2004. A history of the study of solid tumour growth: The contribution of mathematical modelling. *Bulletin of Mathematical Biology*, 66:1039–1091.

Arnold, C. N., Goel, A., and Boland, C. R. 2003. Role of hmlh1 promoter hypermethylation in drug resistance to 5-fluorouracil in colorectal cancer cell lines. *International Journal of Cancer*, 106(1):66–73.

Ayati, B. P., Webb, G. F., and Anderson, A. R. A. 2006. Computational methods and results for structured multiscale models of tumor invasion. *Multiscale Modelling and Simulation*, 5(1):1–20.

Bandyopadhyay, D., Timchenko, N., Suwa, T., Hornsby, P. J., Campisi, J., and Medrano, E. E. 2001. The human melanocyte: a model system to study the complexity of cellular aging and transformation in non-fibroblastic cells. *Experimental Gerontology*, 36:1265–1275.

Bandyopadhyay, S., yuan Chiang, C., Srivastava, J., Gersten, M., White, S., Bell, R., Kurschner, C., Martin, C. H., Smoot, M., Sahasrabudhe, S., Barber, D. L., Chanda, S. K., and Ideker, T. 2010. A human map kinase interactome. *Nature Methods*, 7(10):801–807.

Bennett, D. C. 2007. How to make a melanoma: what do we know of the primary clonal events? *Pigment Cell and Melanoma Research*, 21:27–38.

Betteridge, R., Owen, M. R., Byrne, H. M., Alarcón, T., and Maini, P. K. 2006. The impact of cell crowding and active cell movement on vascular tumour growth. *Networks and Heterogeneous Media*, 1(4):515–535.

Briggs, G. E. and Haldane, J. B. S. 1925. A note on the kinetics of enzyme action. *Biochemical Journal*, 19(2):338–339.

Brown, N. R., Lowe, E. D., Petri, E., Skamnaki, V., Antrobus, R., and Johnson, L. N. 2007. Cyclin b and cyclin a confer different substrate recognition properties on cdk2. *Cell Cycle*, 6(11):1350–1359.

Buschhorn, B. A. and Peters, J.-M. 2006. How apc/c orders destruction. *Nature Cell Biology*, 8(3):209–211.

Cancer Council Australia 2012. Skin cancer facts and figures. Electronically on World Wide Web. accessed on 6/2/2012.

Cancer Council Australia 2013. Facts and figures. Electronically on World Wide Web. accessed on 29/10/2013.

Cecconi, F. and Gruss, P. 2001. Apaf1 in developmental apoptosis and cancer: how many ways to die? *Cellular and Molecular Life Sciences*, 58(11):1688–1697.

Chaudhary, P. M., Eby, M. T., Jasmin, A., Kumar, A., Liu, L., and Hood, L. 2000. Activation of the nf-kb pathway by caspase 8 and its homologs. *Oncogene*, 19:4451–4460.

Chen, S. P., Wu, C. C., Lin, S. Z., Kang, J. C., Su, C. C., Chen, Y. L., Lin, P. C., Chiu, S. C., Pang, C. Y., and Harn, H. J. 2009. Prognostic significance of interaction between somatic apc mutations and 5-fluorouracil adjuvant chemotherapy in taiwanese colorectal cancer subjects. *American Journal of Clinical Oncology*, 32(2):122–126.

Cui, Y. and Guadagno, T. M. 2008. B-rafv600e signaling deregulates the mitotic spindle checkpoint through stabilizing mps1 levels in melanoma cells. *Oncogene*, 27(22):3122–3133.

Davies, H., Bignell, G. R., Cox, C., Stephens, P., Edkins, S., Clegg, S., Teague, J., Woffendin, H., Garnett, M. J., Bottomley, W., Davis, N., Dicks, E., Ewing, R., Floyd, Y., Gray, K., Hall, S., Hawes, R., Hughes, J., Kosmidou, V., Menzies, A., Mould, C., Parker, A., Stevens, C., Watt, S., Hooper, S., Wilson, R., Jayatilake, H., Gusterson, B. A., Cooper, C., Shipley, J., Hargrave, D., Pritchard-Jones, K., Maitland, N., Chenevix-Trench, G., Riggins, G. J., Bigner, D. D., Palmieri, G., Cossu, A., Flanagan, A., Nicholson, A., Ho, J. W. C., Leung, S. Y., Yuen, S. T., Weber, B. L., Seigler, H. F., Darrow, T. L., Paterson, H., Marais, R., Marshall, C. J., Wooster, R., Stratton, M. R., and Futreal, P. A. 2002. Mutations of the braf gene in human cancer. *Nature*, 417:949–954.

d'Onofrio, A., Ledzewicz, U., Maurer, H., and Schättler, H. 2009. On optimal delivery of combination therapy for tumors. *Mathematical Biosciences*, 222:13–26.

Dormann, S. and Deutsch, A. 2002. Modeling of self-organized avascular tumor growth with a hybrid cellular automaton. *In Silico Biology*, 2:393–406.

Drost, M., Zonneveld, J. B., van Dijk, L., Morreau, H., Tops, C. M., Vasen, H. F., Wijnen, J. T., and de Wind, N. 2010. A cell-free assay for the functional analysis of variants of the mismatch repair protein mlh1. *Human Mutation*, 31(3):247–253.

Eikenberry, S., Thalhauser, C., and Kuang, Y. 2009. Tumor-immune interaction, surgical treatment, and cancer recurrence in a mathematical model of melanoma. *PLoS Computational Biology*, 5(4):1–18.

Franks, S. J., Byrne, H. M., and Lewis, J. C. E. U. C. E. 2005. Biological inferences from a mathematical model of comedo ductal carcinoma in situ of the breast. *Journal of Theoretical Biology*, 232:523–543.

Fu, W.-N., Bertoni, F., Kelsey, S. M., McElwaine, S. M., Cotter, F. E., Newland, A. C., and Jia, L. 2003. Role of dna methylation in the suppression of apaf-1 protein in human leukaemia. *Oncogene*, 22:451–455.

Gardner, L. B., Li, Q., Parks, M. S., Flanagan, W. M., Semenza, G. L., and Dang, C. V. 2001. Hypoxia inhibits g_1/s transition through regulation of p27 expression. *The Journal of Biological Chemistry*, 276:7919–7926.

Gerstein, A. V., Almeida, T. A., Zhao, G., Chess, E., Shih, I. M., Buhler, K., Pienta, K., Rubin, M. A., Vessella, R., and Papadopoulos, N. 2002. Apc/ctnnb1 (beta-catenin) pathway alterations in human prostate cancers. *Genes, Chromosomes and Cancer*, 34(1):9–16.

Globocan 2010. Globocan 2008 fast stats. Electronically on World Wide Web. accessed on 29/10/2013.

Goldbeter, A. and Koshland, D. E. 1981. An amplified sensitivity arising from covalent modification in biological systems. *Proceedings of the National Academy of Sciences*, 78(11):6840–6844.

Graham, T. A. and Leedham, S. J. 2010. Field defects in dna repair: is loss of mgmt an initial event in colorectal carcinogenesis? *Gut*, 59(11):1452–1453.

Grau, E., Martinez, F., Orellana, C., Canete, A., Yañez, Y., Oltra, S., Noguera, R., Hernandez, M., Bermúdez, J., and Castel, V. 2011. Hypermethylation of apoptotic genes as independent prognostic factor in neuroblastoma disease. *Molecular Carcinogenesis*, 50(3):153–162.

Ha, L., Ichikawa, T., Anver, M., Dickins, R., Lowe, S., Sharpless, N. E., Krimpenfort, P., DePinho, R. A., Bennett, D. C., Sviderskaya, E. V., and Merlino, G. 2007. Arf functions as a melanoma tumor suppressor by inducing p53-independent senescence. *Proceedings of the National Academy of Sciences*, 104(26):10968–10973.

Hoebeeck, J., Michels, E., Pattyn, F., Combaret, V., Vermeulen, J., Yigit, N., Hoyoux, C., Laureys, G., Paepe, A. D., Speleman, F., and Vandesompele, J. 2009. Aberrant methylation of candidate tumor suppressor genes in neuroblastoma. *Cancer Letters*, 273(2):336–346.

Holum, J. R. 1998. *Fundamentals of general, organic, and biological chemistry*. Wiley, New York, USA.

Ilyas, M., Efstathiou, J. A., Straub, J., Kim, H. C., and Bodmer, W. F. 1999. Transforming growth factor β stimulation of colorectal cancer cell lines: Type ii receptor bypass and changes in adhesion molecule expression. *Proceedings of the National Academy of Sciences USA*, 96(6):3087–3091.

Jennings, L. S., Fisher, M. E., Teo, K. L., , and Goh, C. J. 2004. *MISER3 Optimal Control Software: Theory and User Manual. Version 3.* The Department of Mathematics, The University of Western Australia, Nedlands, Western Australia.

Jiang, Y., Pjesivac, J., Cantrell, C., and Freyer, J. P. 2005. A multiscale model for avascular tumor growth. *Biophysical Journal*, 89(6):3884–3894.

Jones, P. A. 2001. Death and methylation. *Nature*, 409:141–144.

Kastritis, E., Murray, S., Kyriakou, F., Horti, M., Tamvakis, N., Kavantzas, N., Patsouris, E., Noni, A., Legaki, S., Dimopoulos, M. A., and Bamias, A. 2009. Somatic mutations of adenomatous polyposis coli gene and nuclear b-catenin accumulation have prognostic significance in invasive urothelial carcinomas: evidence for wnt pathway implication. *International Journal of Cancer*, 124(1):103–108.

Kirschner, D. and Panetta, J. C. 1998. Modeling immunotherapy of the tumor ï£¡ immune interaction. *Journal of Mathematical Biology*, 37(1):235–252.

Kohn, K. W. 1999. Molecular interaction map of the mammalian cell cycle control and dna repair systems. *Molecular Biology of the Cell*, 10:2703–2734.

Lachowicz, M. 2005. Micro and meso scales of description corresponding to a model of tissue invasion by solid tumours. *Mathematical Models and Methods in Applied Sciences*, 15(11):1667–1683.

Laidler, K. J. 1997. *A Brief History of Enzyme Kinetics*, pages 127–133. Cornish-Bowden.

Lázcoz, P., Muñoz, J., Nistal, M., Pestaña, A., Encío, I., and Castresana, J. S. 2006. Frequent promoter hypermethylation of rassf1a and casp8 in neuroblastoma. *BMC Cancer*, 6:254.

Ledzewicz, U., Marriott, J., Maurer, H., and Schättler, H. 2008. The scheduling of angiogenic inhibitors minimizing tumor volume. *Medical Informatics and Technologies Journal*, 12:23–28.

Ledzewicz, U., Maurer, H., and Schättler, H. 2009. Bang-bang and singular controls in a mathematical model for combined anti-angiogenic and chemotherapy treatments. In *Joint 48th IEEE Conference on Decision and Control and 28th Chinese Control Conference*, pages 2280–2285, Shanghai, P. R. China.

Ledzewicz, U., Maurer, H., and Schättler, H. 2010. Minimizing tumor volume for a mathematical model of anti-angiogenesis with linear pharmacokinetics. In *Recent Advances in Optimization and its Applications in Engineering*, pages 267–276. Springer Verlag, Dordreht.

Ledzewicz, U., Maurer, H., and Schättler, H. 2011. Optimal and suboptimal protocols for a mathematical model for tumor anti-angiogenesis in com-

bination with chemotherapy. *Mathematical Biosciences and Engineering*, 8(2):307–323.

Libra, M., Malaponte, G., Navolanic, P. M., Gangemi, P., Bevelacqua, V., Proietti, L., Bruni, B., Stivala, F., Mazzarino, M. C., Travali, S., and McCubrey, J. A. 2005. Analysis of braf mutation in primary and metastatic melanoma. *Cell Cycle*, 4(10):1382–1384.

Ling, A. Q., Tanaka, A., Li, P., Nakayama, T., Fujiyama, Y., Hattori, T., and Sugihara, H. 2010. Microsatellite instability with promoter methylation and silencing of hmlh1 can regionally occur during progression of gastric carcinoma. *Cancer Letters*, 297(2):244–251.

Loxton, R., Teo, K., and Rehbock, V. 2008. Optimal control problems with multiple characteristic time points in the objective and constraints. *Automatica*, 44(11):2923–2929.

Markowitz, S. D. and Bertagnolli, M. M. 2009. Molecular origins of cancer: Molecular basis of colorectal cancer. *The New England Journal of Medicine*, 361(25):2449ï£¡2460.

Martin, R. and Teo, K. L. 1994. *Optimal control of drug administration in cancer chemotherapy*. World Scientific Publishing Company Pte. Ltd., Singapore.

Martin, R. B. 1992. Optimal control drug scheduling of cancer chemotherapy. *Automatica*, 28(6):1113–1123.

Matsushime, H., Quelle, D. E., Shurtleff, S. A., Shibuya, M., Sherr, C. J., , and Kato, J.-Y. 1994. D-type cyclin-dependent kinase activity in mammalian cells. *Molecular And Cellular Biology*, 14(3):2066–2076.

McKee, A. E. and c. J. Thiele 2006. Targeting caspase 8 to reduce the formation of metastases in neuroblastoma. *Expert Opinion on Therapeutic Targets*, 10(5):703–708.

Michaloglou, C., Vredeveld, L. C. W., Mooi, W. J., and Peeper, D. S. 2008. Brafe600 in benign and malignant human tumours. *Oncogene*, 27:877–895.

Michaloglou, C., Vredeveld, L. C. W., Soengas, M. S., Denoyelle, C., Kuilman, T., van der Horst, C. M. A. M., Majoor, D. M., Shay, J. W., Mooi, W. J., and Peeper, D. S. 2005. Brafe600-associated senescence-like cell cycle arrest of human naevi. *Nature*, 436:720–724.

Murray, A. and Hunt, T. 1993. *The Cell Cycle: an introduction*. Oxford University Press, New York.

Nasmyth, K. 1995. Evolution of the cell cycle. *Philosophical transactions: biological sciences*, 349(1329):271–281.

Nasmyth, K. 1996. At the heart of the budding yeast cell cycle. *Trends in Genetics*, 12(10):405–412.

Neel, N. F., Martin, T. D., Stratford, J. K., Zand, T. P., Reiner, D. J., and Der, C. J. 2011. The ralgef-ral effector signaling network: The road less traveled for anti-ras drug discovery. *Genes and Cancer*, 2(3):275–287.

Nelson, D. L. and Cox, M. M. 2005. *Lehninger Principles of Biochemistry*. W. H. Freeman and Company, New York, fourth edition.

Niv, Y. 2007. Microsatellite instability and mlh1 promoter hypermethylation in colorectal cancer. *World Journal of Gastroenterology*, 13(12):1767–1769.

Novak, B., Csikasz-Nagy, A., Gyorffy, B., Chen, K., and Tyson, J. J. 1998a. Mathematical model of the fission yeast cell cycle with checkpoint controls at the g1/s, g2/m and metaphase/anaphase transitions. *Biophysical Chemistry*, 72:185–200.

Novak, B., Csikasz-Nagy, A., Gyorffy, B., Nasymth, K., and Tyson, J. J. 1998b. Model scenarios for evolution of the eukaryotic cell cycle. *Philosophical transactions of the Royal Society of London. Series B, Biological Sciences*, 353:2063–2076.

Novak, B. and Tyson, J. J. 2004. A model for restriction point control of the mammalian cell cycle. *Journal of Theoretical Biology*, 230:563–579.

Obermair, A., Youlden, D. R., Young, J. P., Lindor, N. M., Baron, J. A., Newcomb, P., Parry, S., Hopper, J. L., Haile, R., and Jenkins, M. A. 2010. Risk of endometrial cancer for women diagnosed with hnpcc-related colorectal carcinoma. *International Journal of Cancer*, 127:2678ï£¡2684.

Okpanyi, V., Schneider, D. T., Zahn, S., Sievers, S., Calaminus, G., Nicholson, J. C., Palmer, R. D., Leuschner, I., Borkhardt, A., and Schï£¡nberger, S. 2011. Analysis of the adenomatous polyposis coli (apc) gene in childhood and adolescent germ cell tumors. *Pediatric Blood and Cancer*, 56(3):384–391.

Olasz, J., Juhász, A., Remenár, É., Engi, H., Bak, M., Csuka, O., and Kásler, M. 2007. Rarβ2 suppression in head and neck squamous cell carcinoma correlates with site, histology and age. *Oncology Reports*, 18:105–112.

Paoletti, F., Ainger, K., Donati, I., Scardigli, R., Vetere, A., Cattaneo, A., and Campa, C. 2010. Novel fluorescent cycloheximide derivatives for the imaging of protein synthesis. *Biochemical and Biophysical Research Communications*, 396(2):258–264.

Piperi, C., Themistocleous, M. S., Papavassiliou, G. A., Farmaki, E., Levidou, G., Korkolopoulou, P., Adamopoulos, C., and Papavassiliou, A. G. 2010. High incidence of mgmt and rar promoter methylation in primary glioblastomas: Association with histopathological characteristics, inflammatory mediators and clinical outcome. *Molecular Medicine*, 16:1–9.

Preziosi, L., editor 2003. *Cancer Modelling and Simulation.* Mathematical Biology and Medicine Series. Chapman and Hall/CRC, London.

Psofaki, V., Kalogera, C., Tzambouras, N., Stephanou, D., Tsianos, E., Seferiadis, K., and Kolios, G. 2010. Promoter methylation status of hmlh1, mgmt, and cdkn2a/p16 in colorectal adenomas. *World Journal of Gastroenterology*, 16(28):3553–3560.

Rawn, D. J. 1989. *Biochemistry.* N. Patterson Publishers, Burlington, N.C.

Ricciardiello, L., Goel, A., Mantovani, V., Fiorini, T., Fossi, S., Chang, D. K., Lunedei, V., Pozzato, P., Zagari, R. M., Luca, L. D., Fuccio, L., Martinelli, G. N., Roda, E., Boland, C. R., and Bazzoli, F. 2003. Frequent loss of

hmlh1 by promoter hypermethylation leads to microsatellite instability in adenomatous polyps of patients with a single first-degree member affected by colon cancer. *Cancer Research*, 63(4):787–792.

Rizos, H., Darmanian, A. P., Indsto, J. O., Shannon, J. A., Kefford, R. F., and Mann, G. J. 1999. Multiple abnormalities of the p16^{INK4A}-prb regulatory pathway in cultured melanoma cells. *Melanoma Research*, 9:10–19.

Rufini, A., Agostini, M., Grespi, F., Tomasini, R., Sayan, B. S., Niklison-Chirou, M. V., Conforti, F., Velletri, T., Mastino, A., Mak, T. W., Melino, G., and Knight, R. A. 2011. p73 in cancer. *Genes and Cancer*, June 1:1–12.

Salimath, B., Marmé, D., and Finkenzeller, G. 2000. Expression of the vascular endothelial growth factor gene is inhibited by p73. *Oncogene*, 19(31):3470–3476.

Sharpless, N. E. and Chin, L. 2003. The ink4a/arf locus and melanoma. *Oncogene*, 22:3092–3098.

Smalley 2007. Targeting braf/mek in melanoma: new hope or another false dawn? *Expert Review of Dermatology*, 2(2):179–190.

Smith, J. A. and Martin, L. 1973. Do cells cycle? *Proceedings of the National Academy of Sciences*, 70(4):1263–1267.

Soengas, M. S., Capodieci, P., Polsky, D., Mora, J., Esteller, M., Opitz-Araya, X., McCombie, R., Herman, J. G., Gerald, W. L., Lazebnik, Y. A., Cordon-Cardo, C., and Lowe, S. W. 2001. Inactivation of the apoptosis effector *Apaf-1* in malignant melanoma. *Nature*, 409:201–211.

Sun, B., Wingate, H., Swisher, S. G., Keyomarsi, K., and Hunt, K. K. 2010. Absence of prb facilitates e2f1-induced apoptosis in breast cancer cells. *Cell Cycle*, 9(6):1122–1130.

Suzuki, T., Nakada, M., Yoshida, Y., Nambu, E., Furuyama, N., Kita, D., Hayashi, Y., Hayashi, Y., and Hamada, J. 2010. The correlation between promoter methylation status and the expression level of o6-methylguanine-dna methyltransferase in recurrent glioma. *Japanese Journal of Clinical Oncology*, 41(2):190–196.

Svedlund, J., Aurén, M., Sundström, M., Dralle, H., Akerström, G., Björklund, P., and Westin, G. 2010. Aberrant wnt/β-catenin signaling in parathyroid carcinoma. *Molecular Cancer*, 15(9):294.

Swanson, K. R., Bridge, C., Murray, J. D., and Jnr, E. C. A. 2003. Virtual and real brain tumors: uisng mathematical modeling to quantify glioma growth and invasion. *Journal of the Neurological Sciences*, 216:1–10.

Swat, M., Kel, A., and Herzel, H. 2004. Bifurcation analysis of the regulatory modules of the mammalian g1/s transition. *Bioinformatics*, 20(10):1506–1511.

Teo, K. L., Goh, C. J., and Wong, K. H. 1991. *A Unified Computational Approach to Optimal Control Problems*. Longman Scientific & Technical, Essex, England.

To-Ho, K. W., Cheung, H. W., Ling, M.-T., Wong, Y. C., and Wang, X. 2008.

Mad2δc induces aneuploidy and promotes anchorage-independent growth in human prostate epithelial cells. *Oncogene*, 27:347–357.

Tyson, J. J. and Novak, B. 2001. Regulation of the eukaryotic cell cycle: Molecular antagonism, hysteresis, and irreversible transitions. *Journal of Theoretical Biology*, 210:249–263.

Tyson, J. J., Novak, B., Chen, K., and Val, J. 1995. Checkpoints in the cell cycle from a modeler's perspective. *Progress in Cell Cycle Research*, 1:1–8.

Usman, A. and Cunningham, C. 2005. Application of the mathematical model of tumor-immume interactions for il-2 adoptive immunotherapy to studies on patients with metastatic melanoma or renal cell cancer. *Rose-Hulman Institute of Technology: Undergraduate Math Journal*, 6(2):1–17.

Wang, J. C., Su, C. C., Xu, J. B., Chen, L. Z., Hu, X. H., Wang, G. Y., Bao, Y., Huang, Q., Fu, S. B., Li, P., Lu, C. Q., Zhang, R. M., and Luo, Z. W. 2007. Novel microdeletion in the transforming growth factor beta type ii receptor gene is associated with giant and large cell variants of nonsmall cell lung carcinoma. *Genes, Chromosomes and Cancer*, 46(2):192–201.

Waš̈ch, R. and Engelbert, D. 2005. Anaphase-promoting complex-dependent proteolysis of cell cycle regulators and genomic instability of cancer cells. *Oncogene*, 24:1–10.

Watanabe, T., Hirota, Y., Arakawa, Y., Fujisawa, H., Tachibana, O., Hasegawa, M., Yamashita, J., and Hayashi, Y. 2003. Frequent loh at chro-

mosome 12q22-23 and apaf-1 inactivation in glioblastoma. *Brain Pathology*, 13(4):431–439.

Weinberg, R. A. 1997. How cancer arises. In *What You Need to Know About Cancer*, pages 3–14. W. H. Freeman and Company, New York.

Weinberg, R. A. 2007. *The Biology of Cancer*. Garland Science, New York.

Weinstein, J., Jacobsen, F. W., Hsu-Chen, J., Wu, T., and Baum, L. G. 1994. A novel mammalian protein, p55cdc, present in dividing cells is associated with protein kinase activity and has homology to the *Saccharomyces cerevisiae* cell division cycle proteins cdc20 and cdc4. *Molecular and Cellular Biology*, 14(5):3350–3363.

Wenzel, P. L., Chong, J.-L., Sáenz-Robles, M. T., Ferrey, A., Hagan, J. P., Gomez, Y. M., Rajmohan, R., Sharma, N., Chen, H.-Z., Pipas, J. M., Robinson, M. L., and Leone, G. 2011. Cell proliferation in the absence of e2f1-3. *Developmental Biology*, 351:35–45.

World Health Organization 2013. World health statistics 2013.

Xu, J. B., Bao, Y., Liu, X., Liu, Y., Huang, S., and Wang, J. C. 2007. Defective expression of transforming growth factor beta type ii receptor (tgfbr2) in the large cell variant of non-small cell lung carcinoma. *Lung Cancer*, 58(1):36–43.

Yamamoto, H., Itoh, F., Nakamura, H., Fukushima, H., Sasaki, S., Perucho, M., and Imai, K. 2001. Genetic and clinical features of human pancreatic

ductal adenocarcinomas with widespread microsatellite instability. *Cancer Research*, 61:3139–3144.

Zetterberg, A. and Larsson, O. 1995. Cell cycle progression and growth in mammalian cells kinetic aspects of transition events. In Hutchison, C. and Glover, D. M., editors, *Cell Cycle Control*, pages 206–227. Oxford University Press.

Zhang, X.-P., Liu, F., and Wang, W. 2010. Coordination between cell cycle progression and cell fate decision by the p53 and e2f1 pathways in response to dna damage. *The Journal of Biological Chemistry*, 285(41):31571–31580.